Carina Koller, B.Sc.

# The impact of Eukaryotic Initiation Factors (eIF) on Colorectal Cancer

**MASTER'S THESIS**

to achieve the university degree of

Master of Science

Master's degree programme: Biochemistry and Molecular Biomedical Sciences

submitted to

**Graz University of Technology**

Supervisor

Assoz. Prof. Dr. Dr. Johannes Haybaeck

Institute of Pathology; Medical University of Graz

Graz, June 2015

## AFFIDAVIT

I declare that I have authored this thesis independently, that I have not used other than the declared sources/resources, and that I have explicitly indicated all material which has been quoted either literally or by content from the sources used. The text document uploaded to TUGRAZonline is identical to the present master‘s thesis dissertation.

Date

Signature

# Acknowledgement

First of all I would like to express my sincerest gratitude to my supervisor Johannes Haybaeck, for giving me the opportunity to work on this project. Thank you for always being reachable and your constant support.

Furthermore I would also like to express my great appreciation to the members of the Haybaeck group, especially to my friend Nicole Golob-Schwarzl. You came up with the idea of doing this thesis in the Haybaeck LAB. Thank you Nicole for introducing me to the LAB, for critical discussion of the results and for your encouraging words.

Special thanks also go to my family and my cohabitee Christopher. Without their support, this work would never have been begun and finished. Thank you for your constant support and understanding.

In addition, special thanks and the sincerest apology to the helping hands and names I missed mentioning here.

The research leading to these results has received support from the Innovative Medicines Initiative under grand agreement n° 115234 (OncoTrack), resources of which are composed of financial contribution from the European Union's Seventh Framework Programme (FP7/2007-2013) and EFPIA companies' in kind contribution.

# Abstract

**Background:**

With almost 1.4 million new cases per year, colorectal cancer (CRC) is the third most commonly diagnosed cancer type worldwide. However, treatment strategies for CRC still have to be improved. Therefore it is necessary to understand the etiology and pathogenesis of CRC. Different studies showed that mTOR activity is significantly increased in various human cancers types. Since eIFs are linked to mTOR signaling they also play a key role in carcinogenesis and tumor progression.

**Objective:**

The aim of this master project was to analyze various eIF subunits and important components of the mTOR pathway, to describe characteristic features of eIFs in CRC and show their contribution within the cancer related mTOR signaling pathway. This is necessary to develop new treatment strategies and find novel prognostic and predictive biomarkers for. Experiments were done using primary carcinoma samples and patient derived xenograft models (PDX) of CRC patients. Various subunits of eIFs were analyzed on protein level using Tissue Micro Arrays and Western Blot. In addition mRNA analysis was done with real-time PCR to show variations on mRNA level.

**Results and Conclusion:**

The obtained data display elevated protein expression of several eIF subunits and mTOR components in CRC. Western Blot analysis reveals an overexpression of AKT, eIF2α, eIF3A and eIF3D in colon cancer compared to healthy colon tissue. In comparison to healthy rectum tissue, protein expression mTOR, PTEN, 4E-BP1, eIF3I and eIF4E is increased in rectum cancer. In addition, compared to respectively healthy control tissue, elevated protein expression of eIF3B, eIF3M, eIF3B and eIF6 is visible in colon and rectum cancer. Obtained data reveal a significant difference in protein expression of eIF2α, eIF3A, eIF4B, PTEN, 4E-BP1 and eIF4E comparing colon and rectum cancer. Chemosensitivity testing of colorectal PDX models shows a high biological meaningful reduction of tumor growth under treatment with standard chemotherapeutic drugs. The results of this study indicate a major contribution of eIFs in the development and progression of CRC. Further experiments may be necessary to find novel treatment strategies and biomarkers.

# Zusammenfassung

**Hintergrund:**

Kolorektale Karzinome (CRC) zählen, mit einer Neuerkrankungsrate von 1.4 Millionen Fällen jährlich, zu den am Häufigsten vorkommenden Krebsarten weltweit. Hierbei ist es nach wie vor sehr wichtig, die bereits bekannten Therapiemodelle zu erweitern. Darum ist es von großer Bedeutung ein größeres Verständnis der Ätiologie und Pathogenese von CRC zu bekommen. Unterschiedliche Studien haben bereits gezeigt, dass die Aktivität des mTOR Signalweges in unterschiedlichen Krebsarten deutlich erhöht ist. Da eukaryotische Initiationsfaktoren (eIF) mit dem mTOR Signalweg verknüpft sind, geht man davon aus, dass auch sie eine wichtige Rolle in onkogenen Prozessen spielen.

**Ziel:**

Das Ziel dieses Masterprojekts war es, unterschiedliche eIF Untereinheiten sowie mTOR Komponenten zu analysieren, die charakteristischen Eigenschaften von eIFs in CRC zu beschreiben und ihre Verknüpfung zum mTOR Signalweg darzustellen. All das ist notwendig, um neue Therapie Strategien zu entwickeln und Biomarker zu identifizieren. Die Experimente wurden mit Primärkarzinomproben und Proben von behandelten Xenograft Modellen durchgeführt. Die unterschiedlichen eIF Untereinheiten wurden hierbei auf Proteinlevel mit Tissue Micro Arrays und Western Blot untersucht. Die Expressionsmuster von eIFs auf mRNA Level wurden mit Real-Time-PCR analysiert.

**Resultate und Aussage:**

Die erhaltenen Daten zeigen eine erhöhte Proteinexpression unterschiedlicher eIF Untereinheiten und mTOR Komponenten in CRC. Die Analyse mittels Western Blot weist, im Vergleich zu gesundem Kolongewebe, auf eine Überexpression von AKT, eIF2α, eIF3A und eIF3D in Kolonkarzinomen hin. Im Unterschied zu gesundem Rektumgewebe, ist die Proteinexpression von mTOR, PTEN, 4E-BP1, eIF3I und eIF4E in Rektumkarzinomen erhöht. Vergleicht man Kolon- und Rektumkarzinome, findet man signifikante Unterschiede in der Proteinexpression von eIF2α, eIF3A, eIF4B, PTEN, 4E-BP1 und eIF4E. Chemosensitivitätstests kolorektaler PDX Modelle zeigten die größte biologisch bedeutsame Verminderung der Tumorgröße unter Behandlung mit Standardchemotherapeutika. Die Ergebnisse dieser Studie geben einen wichtigen Hinweis auf eine Beteiligung von eIFs an der Entwicklung und Progression von CRC. Weitere Experimente sind notwendig um neuartige Therapiestrategien und Biomarker zu identifizieren.

# Table of Contents

# 1 Introduction

## 1.1 Colorectal Cancer

### 1.1.1 Overview

With almost 1.4 million new cases per year, colorectal cancer (CRC) is the third most commonly diagnosed cancer type and the third leading cause of cancer death worldwide [1]. About 600.000 deaths per year (i.e. 8% of all cancer deaths) are caused by CRC. A high incidence of CRC can be observed in populations with a Western type diet, which is characterized by highly caloric food, rich in animal fat combined with physical inactivity. Epidemiologic studies showed that meat consumption, smoking and alcohol abuse are risk factors in CRC development. In addition chronic inflammatory bowel diseases like Ulcerative Colitis and Crohn Disease increase the CRC risk [2]. The most important risk factor thus is increasing age, whereas 90% of all CRCs are diagnosed after an age of 50 years. In addition a personal history of CRC, high risk adenomas, or ovarian cancer also increase the risk [3]. CRC is defined as a malignant epithelial tumor of the colon or rectum, whereas only tumors penetrating through the muscularis mucosae into sub mucosal tissue are considered as malignant [2]. Colon and rectum are parts of the digestive systems and together they form the large intestine (see Figure 1) With a length of about 1.5 m and a diameter of about 5-7 cm the colon performs the vital task of absorbing water and vitamins while converting digested food into feces. It consists of 4 parts named the ascending-, the transverse-, the descending- and the sigmoid colon. While the ascending and transvers sections are collectively referred to as proximal colon, descending and sigmoid sections are described as distal colon. CRC shows genetic and immunological differences between the proximal (right-sided) colon and the distal (left-sided) colorectum. Although the majority of CRCs are located in the sigmoid colon and rectum, the number of proximal carcinomas increased in recent years [4]. The rectum, which is located within the pelvis, extends from the anal dentate line to the sigmoid colon at the peritoneal reflection. The rectum measures a length of 10-15 cm. Rectal tumor location is indicated by the distance between anal verge, dentate line, or anorectal ring and the lower tumor edge [5].

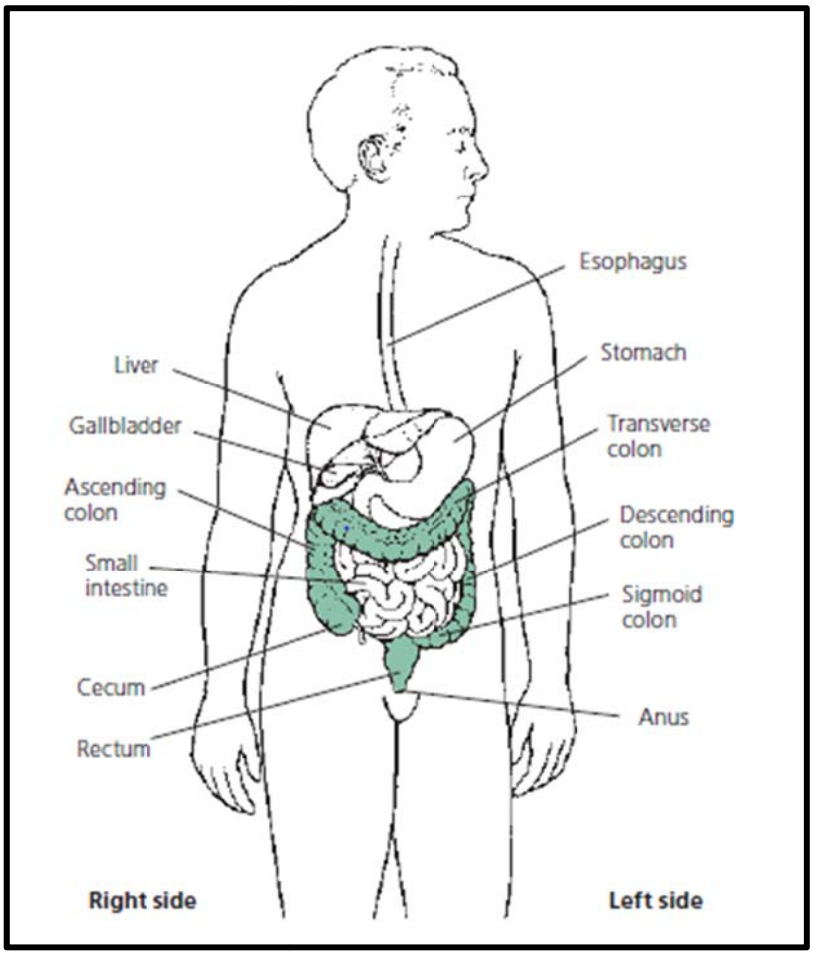


**Figure 1: Anatomy of Colon and Rectum;** adopted from "Colorectal Cancer Facts & Figures 2014-2016" [6].

### 1.1.2 Histology of healthy Colon and Rectum Tissue

All parts of the gastro intestinal (GI) - tract show a similar structure in layer formation. In general colon and rectum are composed of a tunica mucosa, a tela submucosa, a tunica muscularis propria (externa) and a tunica serosa.

The mucosa consists of the glandular epithelium, the lamina propria and the muscularis mucosae. In colon and rectum mucosa no plicae circulares and villi are visible as they end in the ileum. Instead of these, regular arranged deep crypts of Lieberkühn, increasing their depth in anal direction, are visible. The mono layered columnar epithelium contains a large number of goblet cells for mucus secretion. In addition enterocytes, undifferentiated cells and endocrine cells are present. The tall columnar cells are mainly present at the crypt surface, goblet cells are more concentrated at the base. There is only a small lamina propria which extends to a prominent muscularis mucosae.

The tela submucosa is wider than in the small intestine, comprises more fat cells and also lymph follicles. It also contains blood vessels, collagen and many lymphocytes and plasma cells.

The tunica muscularis shows an outer longitudinal and an inner circular musculature. The outer longitudinal musculature forms three separate bands called teniae coli [7][8].

The rectum is histologically similar to the colon, nevertheless there are some differences. Epithelial cells of the rectum have almost completely switched to goblet cells. In addition it contains plicae transversales, leading to permanent transverse folds of the rectum. Crypts of Lieberkühn are longer than in the colon and taenial structures change to complete investment of outer longitudinal and inner circular muscle fibres [9].

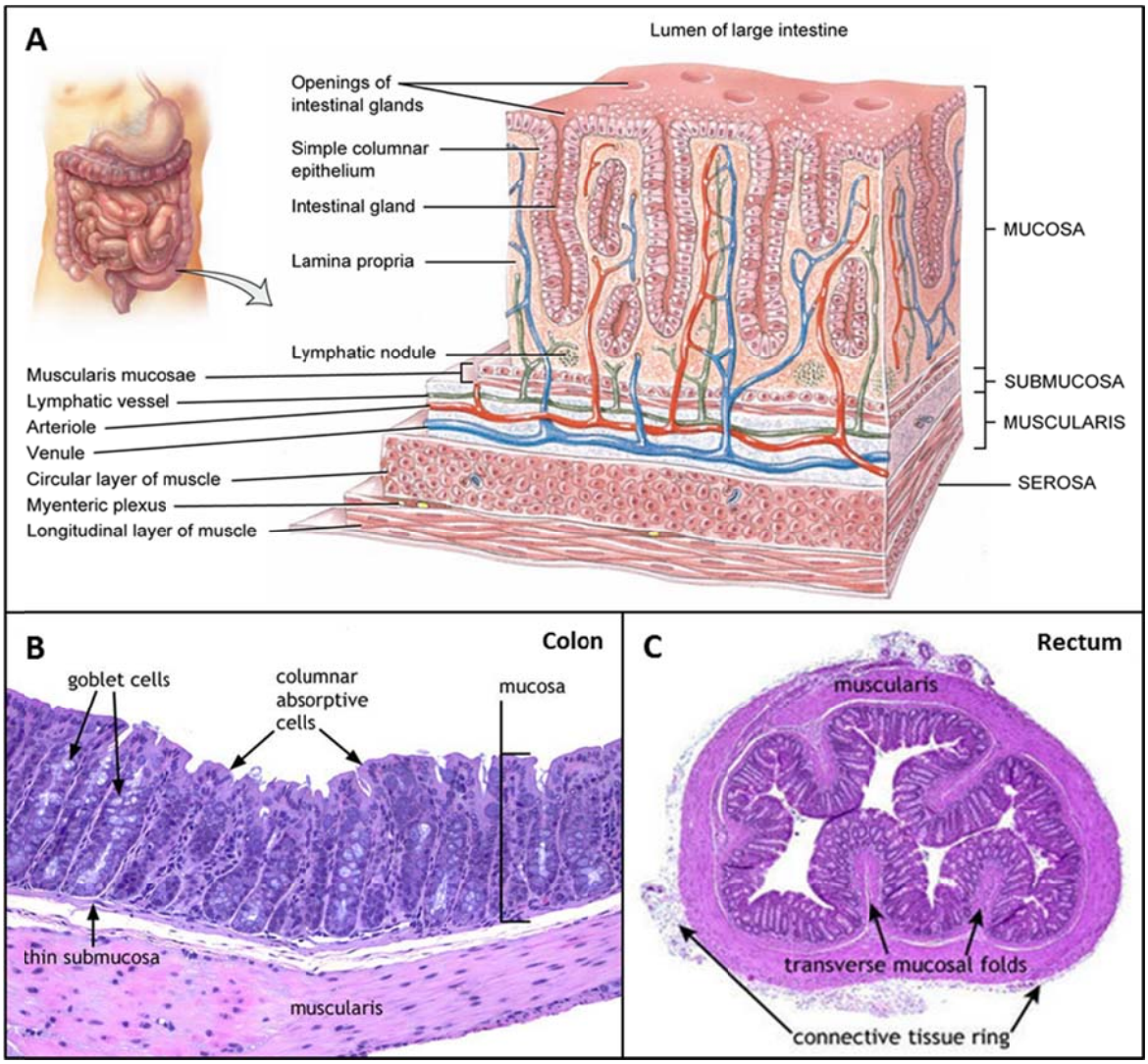


**Figure 2: Normal Colorectal Histology.** [A] Three dimensional view of the large intestine layers [10]; [B] Normal Histology of the Colon [11]; [C] Normal Histology of the Rectum [12].

### 1.1.3 Diagnosis and Histology of Colorectal Cancer

Different screening tools including Fecal Occult Blood Test, Sigmoidoscopy, Digital Rectal Exam and Colonoscopy reduce CRC mortality. In addition different blood test like Complete Blood Count (CBC) and measurement of liver enzymes and tumor markers are important diagnostic tools. If a polyp or a tumor is found during Sigmoidoscopy or Colonoscopy a biopsy or polypectomy is performed ending up in histological analysis to determine if cancer is present [13].

CRC usually develops over a long time period of 10 to 20 years and often primarily occurs as a noncancerous growth called polyp. The most common kind of polyp is called adenoma and develops on the inner lining of the colon or rectum. Adenomas arise from mucus producing glandular cells. One-third to one-half of affected individuals develop more than one adenoma, whereas fewer than 10% progress to an invasive carcinoma [6]. Over 90% of all CRCs are adenocarcinomas arising from the epithelial cells of the colorectal mucosa. Other rare types include neuroendocrine-, squamous cell-, adenosquamous-, spindle cell- and undifferentiated - carcinomas.

More than 95% of well differentiated conventional adenocarcinomas show glandular formation, which is important concerning histologic tumor grading. Glandular formation is also present in 50-95% of moderately differentiated and in < 50% of poorly differentiated adenocarcinomas. Over 70% of colorectal adenocarcinomas are diagnosed as moderately differentiated.

The key feature for defining a CRC histologically is invasion of cancer cells through the basal membrane into the muscularis mucosae and into the submucosa. Carcinomas are often located in close proximity to submucosal blood vessels. Lesions with morphologic characteristics of adenocarcinoma that do not invade the muscularis mucosae have virtually no risk of metastases. Well and moderately differentiated adenocarcinomas show large and tall epithelial cells. In addition the gland lumina often contain cellular debris. Another feature of invasive CRC is the presence of fibrous proliferation, termed desmoplasia [14].

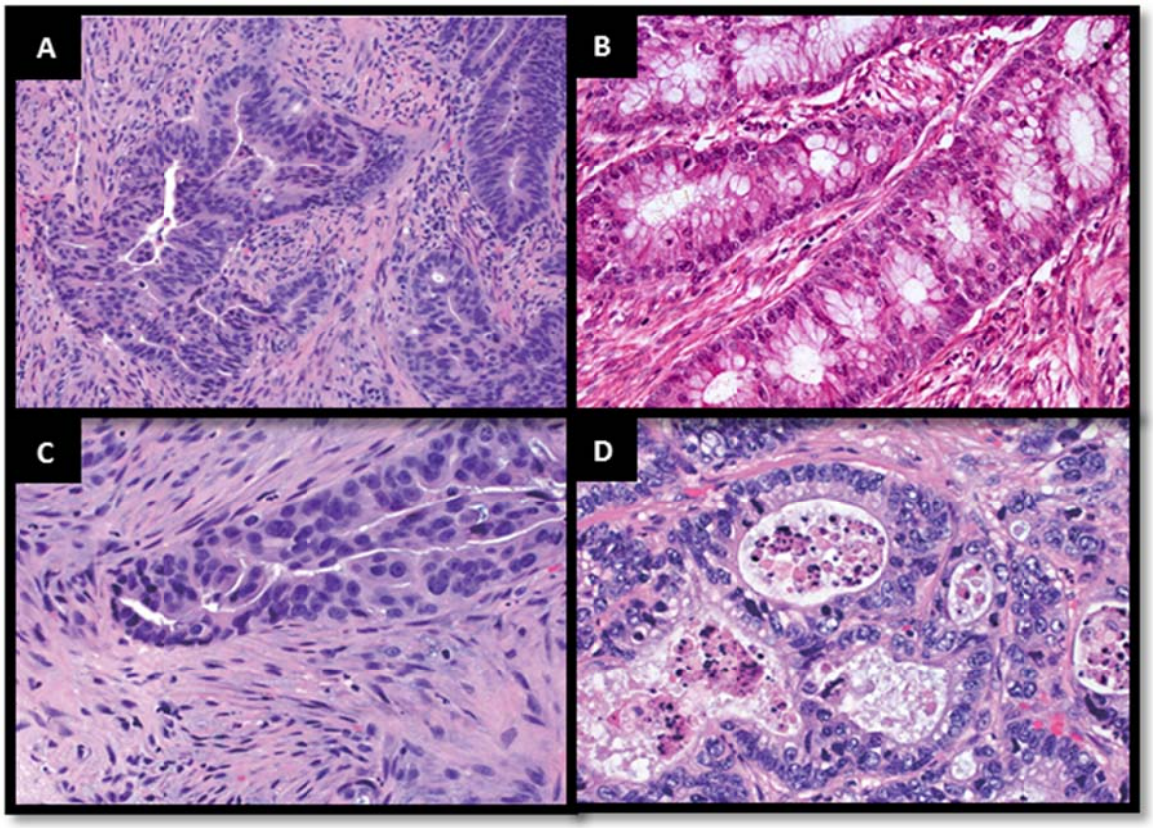


**Figure 3: Histological features of CRC.** [A] Moderately differentiated adenocarcinoma in a desmoplastic stroma (x 200); [B] Moderately differentiated adenocarcinoma; [C]; Desmoplastic reaction (x 400) [D] Necrotic debris within the lumina of adenocarcinomatous glands.(x 400) [14].

### 1.1.4 Staging of Colorectal Cancer

Staging is described as the extent to which cancer has spread at the time of diagnosis and is important in treatment and prognostic determination. The standard staging system for CRC which is recommended by the American Joint Committee on Cancer (AJCC) is called tumor, node, metastasis (TNM) staging. Histologic examination of surgically resected specimens gives information about depth of tumor invasion (T) and the extent of nodal metastasis (N). T describes the extent of primary tumor spread through colon and rectum layers. N characterizes the extent of spread to regional lymph nodes and M indicates metastatic spread to other orangs [15]. About 50% of all patients suffering from CRC develop hepatic metastasis [16] [17].

**TNM Staging:**

I. Primary Tumor (T)

- TX primary tumor cannot be assessed
- T0 no evidence of primary tumor
- Tis carcinoma in situ: intraepithelial or invasion of lamina propria
- T1 tumor invades submucosa
- T2 tumor invades muscularis propria
- T3 tumor invades through muscularis propria into subserosa
- T4 tumor directly invades other tissue or organs

II. Regional Lymph Nodes (N)

- NX regional lymph nodes cannot be assessed
- N0 no regional lymph node metastasis
- N1 metastasis in one to three regional lymph nodes
- N2 metastasis in four or more regional lymph nodes

III. Distant Metastases (M)

- MX distant metastasis cannot be assessed
- M0 no distant metastasis
- M1 distant metastasis [15]

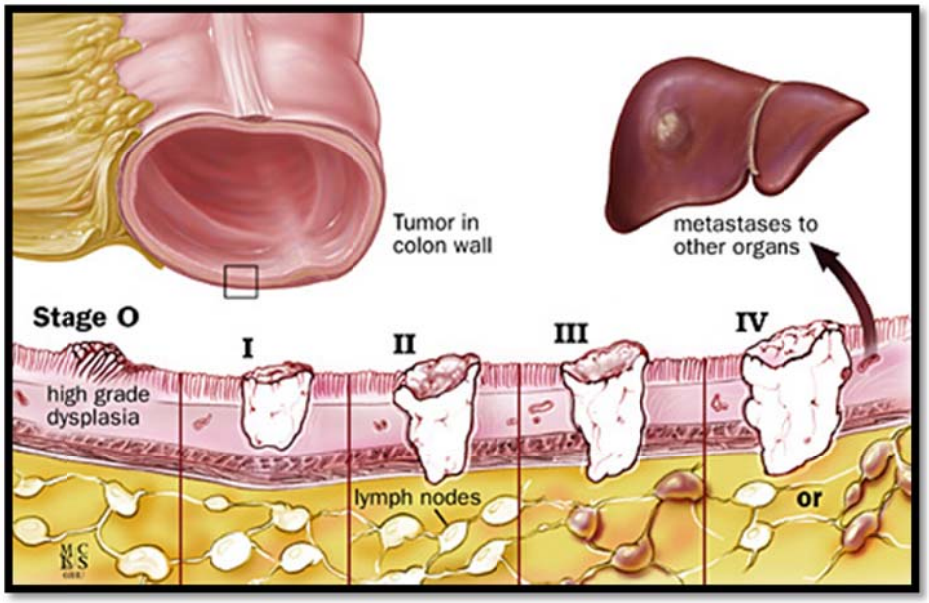


**Figure 4: TNM classification of colorectal cancer stages;** adopted from "TNM Classification for Colorectal Cancer" [18].

### 1.1.5 Molecular Background of CRC

Depending on environmental factors, about 75% of all CRC patients have a sporadic disease. The remaining 25% show a family history with a hereditary contribution. CRC development is associated with numerous molecular events [19]. Germline mutations lead to generation of hereditary CRC syndromes. A stepwise accumulation of genetic and epigenetic alterations is responsible for sporadic CRC development. CRC arises as a result of mutational oncogene activation combined with mutational tumor suppressor gene inactivation. Therefore a minimum of 4-5 mutations are required for cancer development. The accumulation of these mutational events is important for determining the biologic behavior of the tumor [20].

Three major molecular CRC pathways have been described. With 70%, the chromosomal instability (CIN) pathway is the most common. It defines the accumulation of numerical or structural chromosomal abnormalities which lead to karyotypic variations from cell to cell. CIN tumors comprise a loss-of-heterozygosis (LOH) at tumor suppressor gene loci, chromosomal rearrangements and accumulation of mutations in specific oncogenes (e.g. APC, KRAS, PIK3CA, BRAF, SMAD4, TP53, etc.) and tumor suppressor genes. This leads to an activation of pathways, critical for CRC tumorigenesis [21]. The second important pathway is the microsatellite instability (MSI) pathway which is caused by dysfunctions of DNA mismatch repair genes leading to an increased mutability. Microsatellites are prone to accumulation of mutations because DNA polymerase is not able to bind efficiently. The last pathway is defined as CpG Island Methylation Pathway (CIMP). CpG islands are cytosine-guanosine dinucleotide repeats that are present in human genes. Methylation of cytosine residues in promoter regions represses gene transcription [22].

Recent studies displayed the presence of molecular differences between proximal and distal colon cancer. Already in healthy colon tissue, a difference in gene expression is visible [23]. During life over 1000 different genes additional develop differences in expression relevant to major signaling pathways involved in pathogenesis of CRC [24]. Molecular analysis showed that about 70% of these genes are higher expressed in the distal colon and 30% in the proximal colon. In addition a higher transcriptional activity was detected in the distal colon [4].

### 1.1.6 Therapeutic Strategies

Depending on the TNM tumor stage different treatment options are used for colon cancer. The standard treatment option for stage 0-II is an open resection of the primary tumor and of regional lymph nodes [25]. Stage III colon cancer is treated by surgery in addition with adjuvant chemotherapy. Common treatment options for stage IV colon cancer are surgery, chemotherapy and targeted therapy. Liver metastases are treated by surgery, neoadjuvant chemotherapy, local ablation, adjuvant chemotherapy and intra-arterial chemotherapy [26] [27].
Due to the local recurrence risk and a poorer overall prognosis, the treatment management of rectum cancer is somewhat different to that of colon cancer [28]. Differences include the use of radiation, the surgical techniques and the chemotherapeutic treatment [29]. Stage 0 rectal cancer is treated by polypectomy or surgery. Surgery with or without chemo radiation therapy is the standard method for stage I. Stage II and stage III rectal cancer are treated by surgery, preoperative chemo radiation therapy, short-course preoperative radiation therapy and postoperative chemo radiation therapy. Treatment options for stage IV and recurrent rectal cancer includes surgery with or without chemotherapy or radiation therapy, first-line chemotherapy and targeted therapy, second-line chemotherapy and palliative therapy. Liver metastasis treatment consists of surgery, neoadjuvant chemotherapy, local ablation, adjuvant chemotherapy and intra-arterial chemotherapy [30].

Depending on cancer type and TNM stage of colon and rectal carcinomas different chemotherapy regimens, which are dose depending, are used for treatment:

* German AIO: folic acid, 5-FU, and irinotecan
* CAPOX: capecitabine and oxaliplatin
* Douillard: folic acid, 5-FU, and irinotecan
* FOLFIRI: leucovorin, 5-FU, and irinotecan
* FOLFOX4/6: oxaliplatin, LV, and 5-FU
* FOLFOXIRI: irinotecan, oxaliplatin, LV, 5-FU
* FUOX: 5-FU plus oxaliplatin
* IFL: irinotecan, 5-FU, and LV
* XELOX: capecitabine plus oxaliplatin [31]

| Drug | Subclass | Mode of Action |
|---|---|---|
| 5-Fluorouracil (5-FU, Adrucil®) | Antimetabolite (Pyrimidinantagonist) | Contact Inhibition: Incorporation of antimetabolites into the cellular metabolism stops cell division. |
| Folic acid | Vitamin B9 | Essential vitamin for red blood cell production. |
| Irinotecan (IFL, Camptosar®) | Topoismerase I Inhibitor | Prevention of DNA relegation by topoismerase I inhibition causes DNA double strand break and cell death. |
| Capecitapine | Antimetabolite | The prodrug capecitapine is enzymatically converted to fluorouracil in the tumor. |
| Oxaliplatin (Eloxatin®) | Alkylating agent | Leads to a cell cycle unspecific inhibition of DNA synthesis in cells due to cytotoxic effects. |
| Leucovorin (LV) | Reduced folic acid (folinic acid) | It is used as "chemoprotectant" in combination therapies. It allows the cell to do some normal DNA replication processes. |
| Cetuximab | epidermal growth factor receptor inhibitor | It is used for treatment of metastatic colorectal cancer. Leads inhibition of cell growth and apoptosis. |
| Avastin | Angiogenesis inhibitor | It blocks angiogenesis by inhibiting vascular endothelial growth factor A (VEGF-A) and is used treatment of metastatic colon cancer. |
| Regorafenib | Multi-kinase inhibitor | It targets angiogenic, stromal and oncogenic receptor tyrosine kinase (RTK) and is used treatment of metastatic colon cancer. |

**Table 1: Common chemotherapeutic drugs for CRC treatment [32].**

## 1.2 Eukaryotic Translation Initiation

### 1.2.1 Eukaryotic Translation Initiation

The regulation of eukaryotic gene expression mainly takes place at the level of transcription and mRNA translation. Translation is the process of converting mRNA, produced during transcription, into a polypeptide chain generating a protein. The translation process can be divided into4 parts named initiation, elongation, termination, and recycling. Translation is mainly regulated at the level of initiation, which is supported by 12 eukaryotic initiation factors (eIF) [33].

The classical process of eukaryotic translation initiation, which is also referred to as canonical translation initiation is divided into 9 stages (see Figure 5):

(1) As a first step separated 40S and 60S ribosomal subunits are captured by recycling of post-termination complexes.
(2) The so called 2 (eIF2)–GTP–Met-tRNA$^{Met}$ ternary complex is formed by the binding of Met-tRNA$^{Met}$ to the eIF2 GTP complex.
(3) Together the 40S subunit, eIF1, eIF1A, eIF3, eIF5 and the ternary complex build the 43S preinitiation complex.
(4) The mRNA cap-proximal region is unwound by the eIF4F complex (eIF4E, eIF4A, eIF4G) assisted by eIF4B, which leads to mRNA activation.
(5) Activated mRNA is attached to the 43S preinitiation complex.
(6) Scanning of the mRNAs 5' UTR by the 43S complex is performed.
(7) The recognition of the initiation codon and the following hydrolysis of eIF2 bound GTP (partial loss) leads to generation of the 48S initiation complex.
(8) The 48S initiation complex builds a connection with the 60S ribosomal subunit. eIF5B mediates the displacement of eIF2–GDP, eIF1, eIF3, eIF4B, eIF4F and eIF5.
(9) As a last step hydrolysis of eIF5B bound GTP leads to the release of eIF1A and GDP-bound eIF5B. 80S initiation complex is formed and elongation takes place. Elongation is followed by termination and recycling [34] [35] [36].

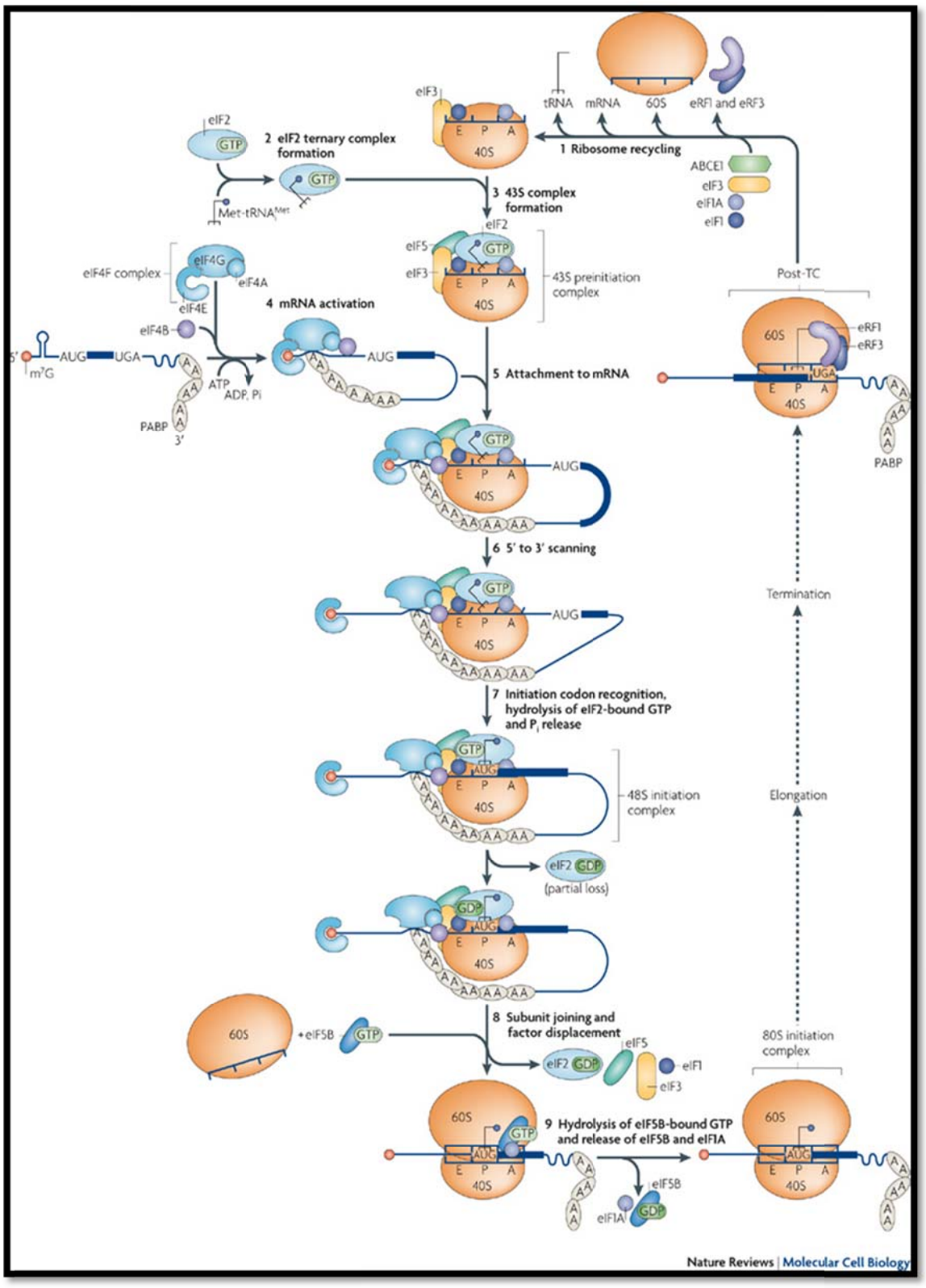


**Figure 5: The 9 steps of the canonical pathway of eukaryotic translation initiation**; adopted from Jackson et al. 2010. [35].

### 1.2.2 mTOR Signaling Pathway

An important pathway in eukaryotic translation initiation is the PI3K/AKT/mTOR (phosphatidylinositol-3-kinases/AKT/mammalian target of rapamycin) signaling pathway. It plays an important role in cell growth and metabolism control [37]. The mTOR pathway is deregulated in different diseases and in tumorigenesis [38]. mTOR interacts with different proteins, forming two major complexes called mTORC1 and mTORC2 [39]. mTORC1, which is inhibited by rapamycin, regulates translation due to phosphorylation of the downstream effectors S6 Kinase (S6K) and eIF4E binding proteins (4E-BP1) [40] [41]. mTORC1 is activated by the PI3K/AKT pathway. The PI3K/AKT pathway starts with the binding of a growth factor to the growth factor receptor leading to phosphorylation and therefore activation of PIP3. Phosphorylated PIP3 activates AKT by phosphorylation. AKT can be inhibited by the phosphatase and tensin homolog (PTEN). Active AKT phosphorylates and inhibits the TSC1/2 complex leading to activation of Rheb which activates mTOR. Active mTOR further phosphorylates its downstream targets S6K and 4E-BP1 [42]. The formation of the eIF4F complex is a rate limiting step in translation initiation, depending on eIF4E inhibitory proteins, called 4E-BP. 4E-BPs inhibit translation initiation by binding eIF4E and therefore preventing association of eIF4E with eIF4G [43]. Due to mitotic signals, 4E-BP is phosphorylated leading to dissociation from eIF4E and formation of the eIF4F complex. Therefore translation initiation is stimulated. The overall translation level is decreased when 4E-BP1 is activated which is regulated by mTOR depended phosphorylation. mTOR is upstream regulated by growth factors, amino acid availability and the energy status of the cell [44]. Decreased mTOR activation leads to 4E-BP1 hypophosphorylation and therefore allows 4E-BP1 efficiently to bind eIF4E and block translation initiation. When mTOR activity is high, 4EBP1 is phosphorylated which results in eIF4E release and increasing cap dependent translation [45].

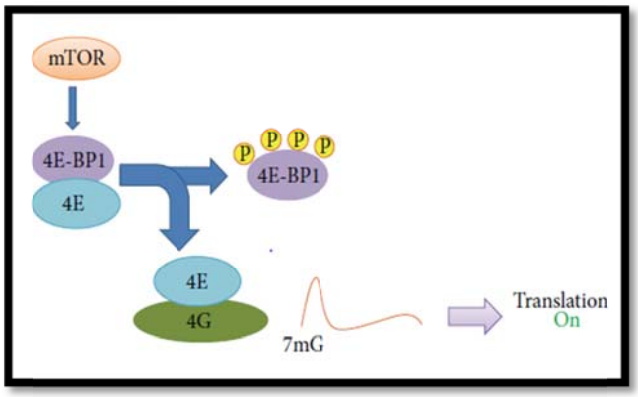


**Figure 6: Regulation of cap dependent translation [45].**

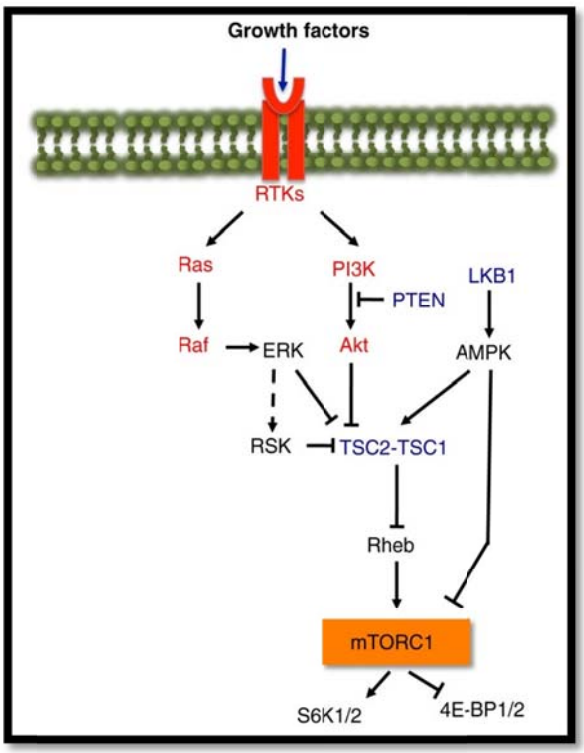


**Figure 7: Regulation of the mTORC1 pathway**; adopted from "Regulation of the mTORC1 pathway" [46].

### 1.2.3 Eukaryotic Initiation Factors and Cancer

Different CRC screening programs displayed the great importance of early treatment in CRC mortality. However, treatment strategies for CRC still have to be improved. Therefore it is necessary to better understand the etiology and pathogenesis of CRC. Deregulation of protein synthesis displayed as a major player in cancer development and progression [47] [48].

Different studies showed that mTOR activity is significantly increased in various human cancers types, but only a small number of mTOR gene mutations have been found [49] [50] [51]. This indicates that mTOR over activation arises due to signal defects upstream of mTOR in the phosphatidylinositol-3-kinase (PI3K)/Akt/mTOR pathway [52]. Since eIFs are linked to mTOR signaling they also play a key role in carcinogenesis and tumor progression. Various studies already displayed the involvement eIFs in different oncogenic processes and their contribution to onset and progression of cancer [33]. As translation initiation is highly critical phase of gene expression, cancer onset and cancer progression, it is of utmost interest for targeting cancer and in biomarker research [53].

Various studies show that eIFs display different roles in cell proliferation and tumorigenesis. While some eIFs act as tumor suppressors, others promote carcinogenesis and tumor progression by acting as proto-oncogenes [54] [55]. Like already mentioned, eIFs interact with the mTOR signaling pathway. In addition they are also implemented into other pathways like NF-κB signaling and cell cycle regulation. mTOR signals via 4E-BP1 and eIF4E or via the S6K. eIF4E is also a downstream target of the MAPK/ERK pathway and therefore interlinked with various tumor promoters like Raf, VEGF, Her2 and Ras. Different stress responsive kinases phosphorylate eIF2. Inhibition of this phosphorylation may lead to carcinogenesis. Up regulation of eIF1 can be induced by UV light driven tissue damage. Within the eIF3 complex, eIF3k induces apoptosis via caspase 3 and eIF3i represses transcription of TGFβ target genes.

An important event in tumor development is the inactivation of the adenomatous polyposis coli (APC) gene, which is suggested to play a major role in transcription regulation. The loss of wt APC leads to up regulation of c-myc expression. Myc triggers transcription of eIF4E [33] [34].

## 1.3 Oncotrack

Oncotrack is an international study group consisting of over 80 scientists that has the goal to develop and assess approaches for identification of new biomarkers and therapy strategies concerning CRC. Although the basic general mechanisms of CRC are already well known, most therapies only offer an interim solution and fail to stop the cancer spreading. Therefore specific research is necessary to enlarge the already available knowledge.

The Oncotrack project is based on a large scale deep sequencing program, combining specific selection of well-defined tissues with information of the tumor methylome and transcriptome, to provide a complete description of changes at the genetic and molecular level of colon cancer development and metastatic events.

All samples analyzed during this master thesis project and the funding were kindly provided by Oncotrack.

## 1.4 Aim of the Study

Altered translation initiation and therefore abnormal gene expression increases the risk of cancer development. Previous studies already showed, that deregulation along the eIF cascade is associated with malignant transformation and progression of cancer. More detailed research concerning this topic is necessary to get a better overview of CRC cancerogenesis. This might help to develop new treatment strategies and find novel prognostic and predictive biomarkers.

The aim of this master project was to analyze various eIF subunits and important components of the mTOR pathway, to describe characteristic features of eIFs in CRC and show their contribution within the cancer related mTOR signaling pathway. Analysis was done on protein level using Tissue Micro Arrays (TMA) and Western Blot. In addition mRNA analysis was done with real-time PCR to display variations on mRNA level.

# 2 Materials and Methods

## 2.1 Tissue Samples

### 2.1.1 Tumor and Control Samples

Formalin fixed paraffin embedded (FFPE) colorectal tissue samples and the corresponding clinical data were obtained from the archive of OncoTrack. This selection included tissue material of a total of 60 patients suffering from CRC. The collection contained tissue of primary carcinomas, metastases and the respectively healthy controls. The formalin fixed paraffin embedded tissue samples were used for generation of Tissue Microarrays (TMA).

Cryo samples were also provided by OncoTrack. Colorectal carcinoma tissue and respectively healthy controls were resected during surgery. The obtained material was divided into pieces of 3 to 4 mm. While one part of the cut tissue pieces was immediately shock frozen and stored at -80°C until further use, the other part was collected in cell culture medium for Xenograft generation.

### 2.1.2 Generation of Xenograft Models

5 primary carcinoma samples and 2 liver metastases samples of patients suffering from rectum cancer, as well as 4 primary carcinoma samples and 1 liver metastasis sample of patients suffering from colon cancer were sent to EPO Berlin-Buch GmbH (Berlin, Germany). The tissue samples were transplanted into 3 to 6 immunodeficient NOD/SCID mice. The tumor growth was monitored in a daily rhythm. At a size of about 1 $cm^3$, the tumors were removed and transferred to naive NMRI:nu/nu mice for chemosensitivity testing [56] [57] . Xenotransplanted carcinomas and metastases were treated with different standard and novel chemotherapeutic drugs (see Table 2). During chemosensitivity testing the tumor volume was measured regularly and used to generate growth curves. After a time period of 30-40 days the tumors were excised and analyzed by Western Blot and Real-Time-PCR. Chemosensitivity data were kindly provided by EPO Berlin-Buch GmbH. Tumor volume of treatment in comparison to control (T/C) was calculated in percent.

| Drug | Subclass |
|---|---|
| Oxaliplatin* | Alkylating agent |
| Irinotecan* | Topoismerase I Inhibitor |
| 5-FU* | Antimetabolite (Pyrimidinantagonist) |
| Cetuximab* | Epidermal growth factor receptor inhibitor |
| AZD8931 | Reversible inhibitor of signaling by epidermal growth factor receptor |
| AZD6244 | Mitogen-activated protein kinase kinase (MEK or MAPK/ERK kinases) 1 and 2 inhibitor |
| Afatinib | Tyrosine Kinase inhibitor |
| Avastin* | Angiogenesis inhibitor |
| Regorafenib* | Multi-kinase inhibitor |
| Nintedanib | Angiokinase inhibitor for VEGFR1/2/3, FGFR1/2/3 and PDGFRα/β |
| mTOR FR | mTOR inhibitor |
| IGF 1/2 mAB * | IGF-1/IGF-2 co-neutralizing monoclonal antibody |
| AZ1* | Aziridinylbenzoquinone |
| Volitinib* | c-Met inhibitor |

**Table 2: Chemotherapeutic drugs used for chemosensitivity testing.** Standard drugs for CRC treatment*; Novel drugs in preclinical testing*.

## 2.2 Tissue Micro Array (TMA)

### 2.2.1 Overview

The TMA technology is an important innovation in the field of pathology and offers the opportunity to assemble small representative tissue samples from hundreds of different cases on a single histologic slide, which allows a high throughput analysis. TMAs are paraffin blocks generated by extracting cylindrical tissue cones from donor paraffin blocks and embedding these into a single microarray block at defined array positions. Therefore simultaneous visual analysis of specific proteins can be done under identical and standardized conditions [58].

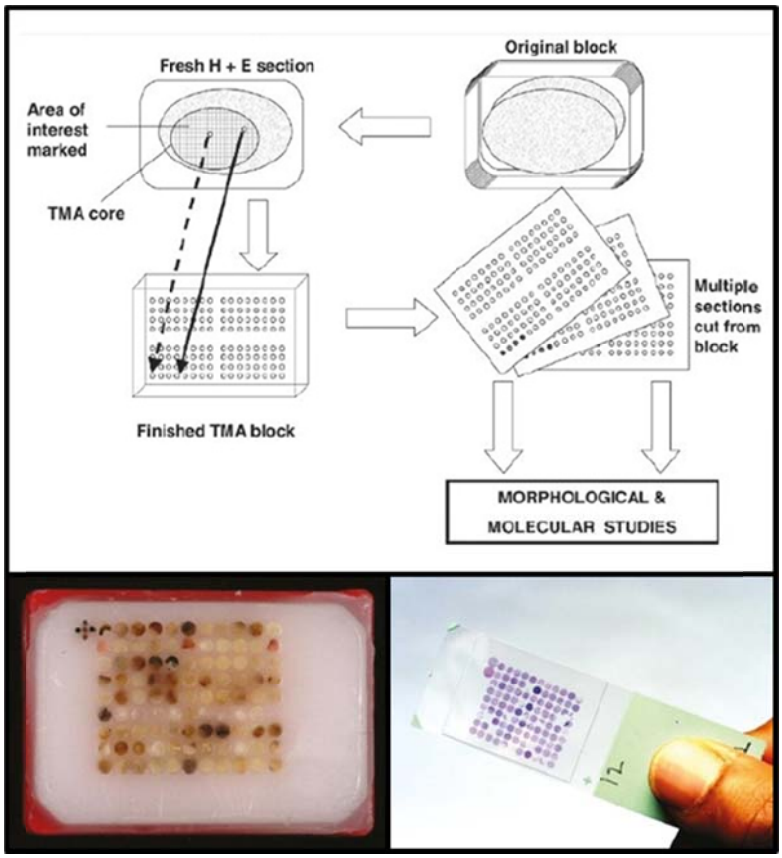


**Figure 8: Construction of a tissue microarray [58].**

### 2.2.2 Sample Preparation

FFPE samples of colorectal carcinoma tissue, liver metastases from CRC and respectively healthy control tissue from a total of 44 patients were collected and used to generate 2 TMAs.

As a first step, each sample was stained for Haemotoxylin/Eosin (HE) and examined by an experienced board certified pathologist, to find relevant tumor sides which were marked on the slide. Tissue cones of the chosen tumor regions were excised, assembled in an array structure and embedded into a fresh paraffin block. The specific position of each sample was carefully documented.

### 2.2.3 Immunohistochemistry (IHC)

Immunohistochemistry was used to analyze protein expression levels of eIFs in CRC tissue. Slices of 3 µm thickness were cut from the generated TMA blocks, mounted on glass slides and fixed at 65 °C for one hour. After the incubation step, slides were rinsed with tap water, dehydrated and covered with Entellan. All subsequent steps were

performed with the Ventana Immunostainer XT (Ventana Medical Systems, Tucson, USA). Counterstaining was performed with haemotoxylin and bluing reagent.

| Primary Antibody | Company | Dilution | Second Antibody |
|---|---|---|---|
| eIF4G | Cell Signaling (#2498) | 1:100 | Rabbit |
| eIF4E | Cell Signaling (#9742) | 1:100 | Rabbit |
| eIF2α (D7D3) XP | Cell Signaling (#5324) | 1:500 | Rabbit |
| eIF3P110 (B-6) | Santa Cruz (sc-74507) | 1:500 | Mouse |
| eIF6 | Gene Tex (GTX63642) | 1:200 | Rabbit |
| eIF3M (V-21) | Santa Cruz (sc-133541) | 1:50 | Rabbit |
| eIF1 | Sigma Aldrich (HPA043003) | 1:50 | Rabbit |
| eIF3A | Cell Signaling (#2538) | 1:50 | Rabbit |
| eIF3B (eIF3η D-9) | Santa Cruz (sc-137215) | 1:100 | Mouse |
| eIF3H (D9C1) XP | Cell Signaling (#3413) | 1:500 | Rabbit |

**Table 3: Primary antibodies for immunohistochemistry.**

### 2.2.4 TMA Evaluation

The intensity of IHC staining was evaluated by two independent assessors by light microscopy. Density and intensity of each TMA spot was scored in a semi-quantitative manner by differentiating nuclear and cytoplasmic staining. The Total Immunostaining Score (TIS) was calculated in percent. No staining was termed as 0, weak staining as 1, moderate staining as 2 and strong staining as 3.

## 2.3 Western Blot

### 2.3.1 Overview

Western blotting, also referred to as immunoblotting, is a major technique in cell and molecular biology. It is used to detect specific proteins in a complex mixture extracted from the cell. After total protein isolation, the protein mixture is separated by size using gel electrophoresis, followed by an efficient transfer of the separated proteins onto a solid support and the detection of the protein of interest by a specific antibody [59].

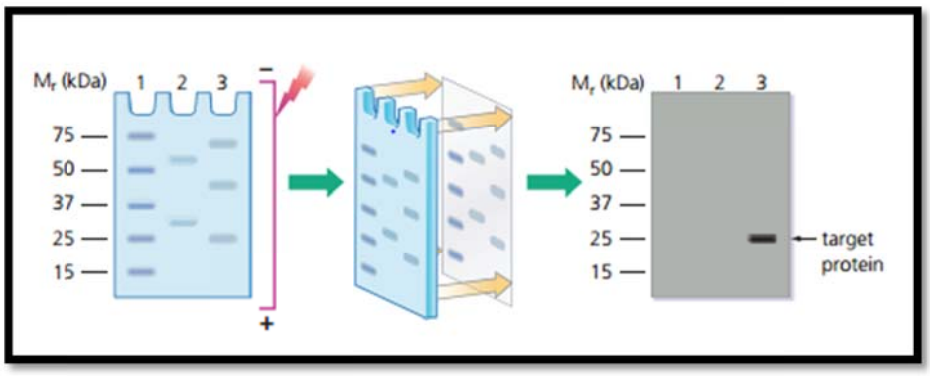


**Figure 9: Western Blot Technique.** A complex protein mixture is separated by gel electrophoresis, transferred onto a blotting membrane and detected by specific antibody binding [59].

### 2.3.2 Protein Isolation

Total protein was isolated from 5 rectum primary carcinoma samples, 5 healthy rectum controls, 5 colon primary carcinoma samples and 5 healthy colon controls. In addition total protein was isolated from 5 untreated and 70 treated rectum xenograft samples as well as from 6 untreated and 84 treated colon xenograft samples.

All steps during protein isolation were done on ice. 1 M DDT (dichlorodiphenyltrichloroethane, Sigma-Aldrich, St. Louis, USA) and 0,1 M Pefabloc (Merck, Darmstadt, Germany) were freshly added to 9 ml NP40 Lysis Buffer and mixed completely. 1 tablet of Phosphostop (Roche) and 1 tablet of cOmplete Mini protease inhibitor (Roche) were dissolved in 1 ml AD and added to the Lysis Buffer.

| Reagent | Final Concentration |
|---|---|
| Tris HCl (pH 7.5) | 50 mM |
| NaCl | 150 mM |
| NP-40 | 1% |

**Table 4: NP40 Lysis buffer.**

The tissue samples were homogenized with 300 µl of Lysis Buffer using MagNA Lyser Green Beads (Roche Diagnostics, Basel, Switzerland) for 30 seconds at 6500 rpm with the Magna Lyser Instrument (Roche Diagnostics). After homogenization the tubes were centrifuged for 10 min at 10 000 rpm and 4 °C. The supernatant was transferred into a fresh tube and immediately stored on ice.

### 2.3.3 Determination of the Protein Concentration

Protein concentration was determined by using the Bradford Protein Assay (Bio-Rad Laboratories, Hercules, USA).

The Bradford Solution was diluted 1:5 with AD. A BSA standard curve was generated with the BioSpectrometer (Eppendorf AG, Hamburg, Germany) using concentrations of 0.5, 1, 2, 4, 6, 8 and 10 µg/µl. For sample measurement 2 µl of 1:10 diluted protein sample was transferred into cuvettes and 998 µl of diluted Bradford Solution were added. After an incubation step of 15 min, samples were measured with the BioSpectrometer at a wavelength of 594 nm. When the absorbance of the sample exceeded 1, a further sample dilution was done. All samples were measured in triplicates whereat the mean of all three samples was used to determine the protein concentration and further dilute all samples to a final protein concentration of 3 µg/µl with 2x Laemlli Sample Buffer (Biorad, 5% β-mercaptoethanol freshly added) and 2x Lyses Buffer. All samples were stored at -80 °C until further use.

### 2.3.4 SDS Page and Western Blot

Sodium Dodecyl Sulfate Polyacrylamide Gel Electrophoresis (SDS-PAGE) is a widely used technique to separate proteins in accordance to their molecular mass. SDS is an anionic detergent added to the protein sample to linearize proteins and impart a negative charge to them.

Depending on the molecular mass of the proteins of interest, 8% or 12.5% polyacrylamide gels were casted using the four gel caster S235 (Hoefer Inc, Holliston, USA). Protein samples were heated for 5 min at 95 °C to ensure protein denaturation. A total amount of 30 µg protein was loaded onto the gel. As molecular weight marker the Novex Pre-Stained Protein Standard (Life Technologies, Carlsbad, USA) was used. Electrophoresis was performed for about 1.5 h at 120 V with the SE 250 Mini-Vertical Electrophoresis Chamber (Hoefer Inc) using a 1x SDS Running Buffer.

After electrophoreses the gel was blotted and immobilized onto a PVDF-membrane (Immobilin-P transfer membrane, Merck Millipore, Darmstadt, Germany) by using a Semi-Dry Blotting Unit (JH Bioinnovations, Bangalore, India). Due to immobilization proteins are accessible for specific antibody (AB) binding, which enables quantitative detection. The PVDF-membrane was activated with methanol (Sigma-Aldrich) for

15 sec, washed with AD for 2 min and incubated in Towbin Transfer Buffer for 5 min. During the semi-dry transfer, gel and membrane were sandwiched between two stacks of filter paper (Whatman Filter Paper, GE Healthcare, Chalfont, Great Britain) that were in direct contact with the plate electrodes. Transfer for two gels was performed for 1.5 h at 160 mA (1 mA/cm² membrane).

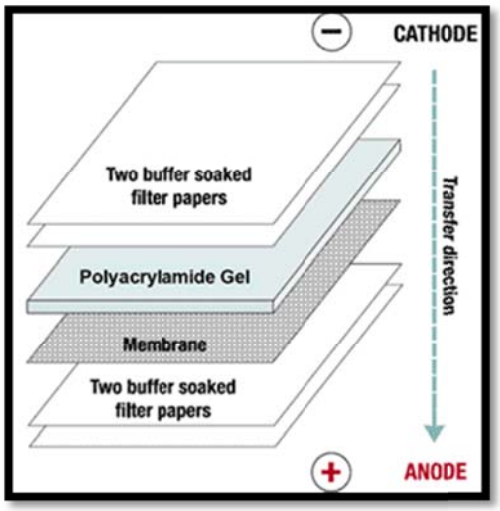


**Figure 10: Semi-Dry Western Blot transfer** (http://www.gibthai.com).

Successful protein transfer was confirmed by Ponceau-S-Staining (Ponceau S solution, Sigma-Aldrich). The membrane was washed 3 times for 5 min with 0.1% TBS-Tween buffer and blocked for 1 h with 5% non-fat milk (non-fat dried powder dissolved in 0.1% TBS-Tween buffer), to prevent non specific background binding of primary and secondary AB to the membrane. After incubation, the membrane was washed 3 times for 5 min with 0.1% TBS-Tween buffer and incubated with the primary AB overnight at 4 °C. All primary AB dilutions were done in 5% Bovine Serum Albumin (BSA) solution depending on the recommented concentration of the company. After 3 washing steps with 0.1% TBS Tween, the HRP (Horse radish peroxidase) - linked secondary AB was diluted in 5% non-fat milk and incubated with the membrane for 1.5 h.

Protein detection was done using the HRP compatible ECL Select Western Blot Detection Kit (GE Healthcare), followed by exposure to the MultiImageTM Light Cabinet (Alpha Innotech Corporation, San Leandro, USA). The camera of the MultiImageTM system detects chemiluminescence emanating from the membrane and transforms it into a digital image. Exposure time depended on the intensity of the chemliluminescent signal.

| Reagent | |
|---|---|
| AD | 3.1 ml |
| Tris 1.5 M pH 6.8 | 1.25 ml |
| Acrylamide | 0.5 ml |
| 10% SDS | 50 µl |
| APS (Ammonium Persulfate) | 25 µl |
| TEMED | 7.5 µl |

**Table 5: Stacking gel.**

| Reagent | 8% | 12.5% |
|---|---|---|
| AD | 4.6 ml | 3.3 ml |
| Tris 1.5 M pH 8.8 | 2.5 ml | 2.5 ml |
| Acrylamide | 2.7 ml | 4.0 ml |
| 10% SDS | 100 µl | 100 µl |
| APS (Ammonium Persulfate) | 100 µl | 100 µl |
| TEMED | 6.0 µl | 7.5 µl |

**Table 6: Separation gel.**

| Reagent | Final Concentration |
|---|---|
| TrisHCl (pH 8.4) | 250 mM |
| Glycine | 192 mM |
| SDS | 1% |

**Table 7: SDS Running buffer (10x).**

| Reagent | Final Concentration |
|---|---|
| Tris | 25 mM |
| Glycine | 190 mM |
| Methanol | 20% |

**Table 8: Towbin Transfer buffer (1x).**

| Reagent | Final Concentration |
|---|---|
| Tris | 0.2 M |
| NACL | 1.4 M |
| adjust to pH 7.6 with HCl | |

**Table 9: TBS buffer (10x). Add 0.1% Tween-20 to 1x TBS buffer.**

| Primary Antibody | Company | Dilution | Second Antibody |
|---|---|---|---|
| Phospho-mTOR | Cell Signaling (#5536) | 1:1000 | Rabbit |
| mTOR | Cell Signaling (#2983) | 1:1000 | Rabbit |
| Phospho-PTEN | Cell Signaling (#9551) | 1:1000 | Rabbit |
| PTEN | Cell Signaling (#9559) | 1:1000 | Rabbit |
| Phospho-P70S6K | Cell Signaling (#9204) | 1:1000 | Rabbit |
| P70S6K | Cell Signaling (#9202) | 1:1000 | Rabbit |
| Phospho Akt | Cell Signaling (#4058) | 1:1000 | Rabbit |
| Akt | Cell Signaling (#9272) | 1:1000 | Rabbit |
| GAPDH | Cell Signaling (#2118) | 1:3000 | Rabbit |
| Phospho 4E-BP1 | Cell Signaling (#9456) | 1:1000 | Rabbit |
| 4E-BP1 | Cell Signaling (#9452) | 1:1000 | Rabbit |
| Anti-Actin | Sigma (A2103) | 1:1000 | Rabbit |
| eIF1 | Sigma (HPA043003) | 1:500 | Rabbit |
| Phospho-eIF2α (Ser51)(D9G8) | Cell Signaling (#3398) | 1:1000 | Rabid |
| eIF2α (D7D3) XP | Cell Signaling (#5324) | 1:1000 | Rabbit |
| eIF3A | Cell Signaling (#2538) | 1:1000 | Rabbit |
| eIF3β (A-8) = eIF3I | Santa Cruz (sc-374155) | 1:1000 | Mouse |
| eIF3C | Cell Signaling (#2068) | 1:1000 | Rabbit |
| eIF3H (D9C1) XP | Cell Signaling (#3413) | 1:1000 | Rabbit |
| eIF3J | Cell Signaling (#3261) | 1:1000 | Rabbit |
| eIF3K (2313C2a) | Santa Cruz (sc-81262) | 1:1000 | Mouse |
| eIF3M (V-21) | Santa Cruz (sc-133541) | 1:500 | Rabbit |
| eIF3B = eIF3η D-9 | Santa Cruz (sc-137215) | 1:1000 | Mouse |
| eIF3P110 (B-6) | Santa Cruz (sc-74507) | 1:500 | Mouse |
| eIF3θ (H-300) | Santa Cruz (sc-30149) | 1:1000 | Rabbit |
| eIF3ζ (H-300) = eIF3D | Santa Cruz (sc-28856) | 1:1000 | Rabbit |
| Phospho eIF4b (Ser406) | Cell Signaling (#5399) | 1.1000 | Rabbit |
| eIF4B | Cell Signaling (#3592) | 1.1000 | Rabbit |
| eIF4E | Cell Signaling (#9742) | 1:1000 | Rabbit |
| eIF4G | Cell Signaling (#2498) | 1:1000 | Rabbit |
| eIF5 | GeneTex (GTX114923) | 1:500 | Rabbit |
| eIF6 | Gene Tex (GTX63642) | 1:1000 | Rabbit |

**Table 10: Primary antibodies for Western Blot.** Depending on the primary AB source, horseradish peroxidase (HRP) linked anti-rabbid (Dilution 1:5000; GE Healthcare) or anti-mouse (Dilution 1:300; GE Healthcare) AB was used.

### 2.3.5 Relative Quantification of Western Blots

Imaging of the blots was performed by using the ECL Select Western Blot Detection Reagents (GE Healthcare). ImageJ (National Institute of Health) was used to compare the density of each band on the western blot membrane. The aim of the analysis was to compare density of samples on multiple membranes and show differences between treatments in the experiments. Therefore the healthy control was always used as standard sample and GAPDH and Actin were applied as internal loading controls.

$$\textbf{Relative density}_{\textbf{sample HKG}} = {}^{\text{AUC}_{\,sample\ HKG}}\Big/_{AUC_{Control\ \ HKG}}$$

$$\textbf{Relative density}_{\textbf{sample POI}} = {}^{AUC_{\,sample\ POI}}\Big/_{AUC_{Control\ \ POI}}$$

$$\textbf{Adjusted density}_{\textbf{sample POI}} = {}^{Relative\ density_{\,sample\ POI}}\Big/_{Relative\ density_{\,sample\ HKG}}$$

**Figure 11: Relative Quantification of Western Blot Data.** "Area under the Curve" is defined as AUC, "Protein of Interest" as POI.

Vertical scatter plots were created using GraphPad Prism (Version 5.01), displaying the results for relative density and the mean. The p-value was calculated using a paired two-tailed t-test. The level of statistical significance was set at $p < 0.05$.

## 2.4 mRNA Analysis using Real-Time PCR

### 2.4.1 Overview

Quantitative real-time PCR (qRT-PCR) is a widely used technique based on polymerase chain reaction (PCR), to amplify and simultaneously detect and quantify a targeted DNA molecule. Common used methods for detection in qRT-PCR are: (1) non-specific fluorescent dyes, for example SYBR Green I, that intercalate with any double-stranded DNA and (2) sequence-specific DNA probes, for example TaqMan probes, that are labeled with a fluorescent reporter. The simplest quantification method is the use of SYBR Green, which is a fluorescent dye that intercalates with double-stranded DNA.

The intercalation leads to an increase in fluorescence which correlates with the increase of target DNA. Fluorescent intensity is measured at the end of elongation in each cycle within the exponential phase. qRT-PCR is a widely used technique for studying gene expression by relative quantification of mRNA levels. Relative quantification is a method that compares the gene expression of one sample to that of another. Therefore it can be used to display differences in mRNA expression of drug-treated samples and untreated control samples [60].

### 2.4.2 RNA Isolation

Total RNA was isolated from fresh-frozen tissue of colorectal carcinomas, healthy controls and untreated/treated xenograft samples using a Trizol based protocol. 50-120 mg of tissue was homogenized with MagNA Lyser Green Beads (Roche) by addition of 1 ml TRIzol reagent (Life Technologies) for 30 sec at 6500 rpm with the MagNA Lyser (Roche). The lysate was incubated for 10 minutes at room temperature (RT). 200 µl of chloroform was added to the vial, incubated for 3 min at RT and centrifuged for 15 min at 10 000 rpm and 4°C. The upper RNA containing phase was transferred to a fresh tube, mixed with 500 µl isopropanol and centrifuged for 20 min at 10 000 rpm and 4°C. After discarding the supernatant, the pellet was washed for 2 times with 1 ml of 80% ethanol and dried for 5 min at 37°C. Depending on the size of the pellet, it was dissolved in 100 – 200 µl RNase free water. After a 10 min incubation step at 58°C the RNA samples were stored at -80°C until further use.

### 2.4.3 cDNA synthesis

cDNA was synthetized from total mRNA with the High-Capacity cDNA Reverse Transcription Kit (Applied Biosystems). 20 µg of RNA were added to 10 µl of 2x RT master mix ending up in a final volume of 20 µl and PCR was performed using the PCR GeneAmp 9700 Thermocycler (Applied Biosystems).

| PCR Program | Step 1 | Step 2 | Step 3 | Step 4 |
|---|---|---|---|---|
| Temperature [°C] | 25 | 37 | 85 | 4 |
| Time | 10 min | 120 min | 5 min | ∞ |

**Table 11: PCR program used for cDNA synthesis.**

| 2x Reverse Transcriptase Master Mix | |
|---|---|
| **Component** | **Volume [µl]** |
| 10x RT Buffer | 2.0 µl |
| 25x dNTP Mix (100 mM) | 0.8 µl |
| 10x RT Random Primers | 2.0 µl |
| MultiScribe™ Reverse Transcriptase | 1.0 µl |
| RNase Inhibitor | 1.0 µl |
| Nuclease-free H2O | 3.2 µl |
| **Total per Reaction** | **10.0 µl** |

**Table 12: Components of the 2x Reverse Transcriptase Master Mix used for cDNA synthesis.**

### 2.4.4 Quantitative Real-Time PCR

qRT-PCR was performed using the Power SYBR Green PCR Master Mix Kit (Applied Biosystems). 5 µl of template cDNA were added to 25 µl of the RT PCR Master Mix and qRT-PCR was performed using the 7900HT Fast Real-Time PCR System (Applied Biosystems). Due to the fact that qRT PCR with SYBR Green does not enable the detection of unspecific side products or primer dimers, a dissociation curve was done after amplification. Therefore a rapid denaturation step to 95°C was followed by cooling the sample to 60°C and let the DNA double strands anneal. Subsequent the temperature was slowly increased by 0.2°C/sec and the fluorescent signal was plotted against the temperature. All qRT PCR primers were designed for specific mRNA detection of different human eIF subunits.

| Master Mix | |
|---|---|
| **Component** | **Volume [µl]** |
| Power SYBR Green PCR Master Mix (2x) | 15 µl |
| Forward Primer [10 pm] | 1 µl |
| Reversed Primer [10 pm] | 1 µl |
| Nuclease-free H2O | 8 µl |
| **Total per reaction** | **25 µl** |

**Table 13: SYBR Green I Master Mix used for Real-Time PCR.**

| Step | AmpliTaq Activation | PCR [40 cycles] | |
|---|---|---|---|
| | Hold | Denature | Anneal/Extent |
| Temperature [°C] | 95 | 95 | 60 |
| Time | 10 min | 20 sec | 2 min |

**Table 14: Real Time PCR program.**

| Gene | Primer Pair | Sequence (5'-3') | Length | Tm [°C] |
|---|---|---|---|---|
| **mTOR** | Fwd | ATGCTTGGAACCGGACCTG | 19 | 60 |
| | Rev | TCTTGACTCATCTCTCGGAGTT | 22 | 58 |
| **PTEN** | Fwd | TGGATTCGACTTAGACTTGACCT | 23 | 58 |
| | Rev | GGTGGGTTATGGTCTTCAAAAGG | 23 | 59 |
| **eIF2α** | Fwd | TGGTGAATGTCAGATCCATTGC | 22 | 60 |
| | Rev | TAGAACGGATACGCCTTCTGG | 21 | 61 |
| **eIF3A** | Fwd | GCCGGAAAATGCCCTCAAAC | 20 | 62 |
| | Rev | TGGTTCGTGTATCTTTTGCCAT | 22 | 60 |
| **eIF3B** | Fwd | GGACCCGACCGACTTGAGA | 19 | 63 |
| | Rev | TTGACCCGGAATGTGTGCTG | 20 | 63 |
| **eIF3J** | Fwd | GTCAAGGATAACTGGGATGACG | 22 | 60 |
| | Rev | CGAGGTCTGACTCTTCCTGTAA | 22 | 61 |
| **eIF4B** | Fwd | CCTCCCAGTCCACTCGAGCTG | 21 | 65 |
| | Rev | GCTTGGGTGTCTCTCCCGAGG | 21 | 65 |
| **eIF4G1** | Fwd | CCCGAAAAGAACCACGCAAG | 20 | 62 |
| | Rev | TTCCCCTCGATCCTTATCAGC | 21 | 61 |
| **eIF5** | Fwd | AGCGTGTCAGACCAGTTCTAT | 21 | 61 |
| | Rev | CTGTCTTGATTCCATTGCCTTTG | 23 | 60 |

**Table 15: Human Real-time PCR primer sets.**

### 2.4.5 Data Analysis

mRNA expression data were analyzed by relative quantification using the ΔΔCt (cycle threshold) method and normalized to GAPDH and Actin as internal housekeeping genes. The used housekeeping genes aimed to normalize possible variations during treatment, sample preparation, RNA isolation, reverse transcription and PCR set up.

The Ct-value, which indicates the cycle number at which fluorescence signal crosses threshold, of each carcinoma sample, was compared to the Ct-value of the healthy control sample. Vertical scatter plots were created using GraphPad Prism (Version 5.01), showing the results of the fold change ratio and the mean.

$$\Delta\mathbf{Ct} = \mathrm{Ct}_{\mathrm{GOI}} - \mathrm{Ct}_{\mathrm{Ref}}$$

$$\Delta\Delta\mathbf{Ct} = \Delta\mathrm{Ct}_{\mathrm{GOI\ treated}} - \Delta\mathrm{Ct}_{\mathrm{GOI\ control}}$$

$$\mathbf{Fold\ Change\ Ratio} = 2^{-\Delta\Delta\mathrm{Ct}}$$

**Figure 12: Relative quantification of mRNA expression using the ΔΔCt method.** Gene of interest is indicated as GOI and the reference gene as Ref.

# 3 Results

## 3.1 Tissue Micro Array analysis of Eukaryotic Initiation Factors in Colorectal Cancer

### 3.1.1 Colorectal Cancer Tissue Micro Array Panel

Formalin fixed paraffin embedded samples of CRC, liver metastases from CRC and respectively healthy control tissue from a total of 44 patients were collected and used to generate 2 TMAs. The CRC TMA was composed of 346 tissue spots including carcinoma and healthy tissue of 16 patients suffering from colon cancer (50% female; 50% male) and 11 patients with rectum cancer (27% female; 73% male). Several relevant tumor sides of the already mentioned patients were excised and assembled on the TMA. In addition a Liver-Metastases TMA (LM TMA) was generated. This included liver metastases tissue from 11 colon (27% female; 73% male) and 6 rectum cancer patients (100% male) with respectively healthy liver control tissue. Multiple relevant metastases tissue sides of these patients were used to generate the LM TMA with a total of 185 spots.

The TIS score, integrating density and intensity of the staining, was calculated in percent.

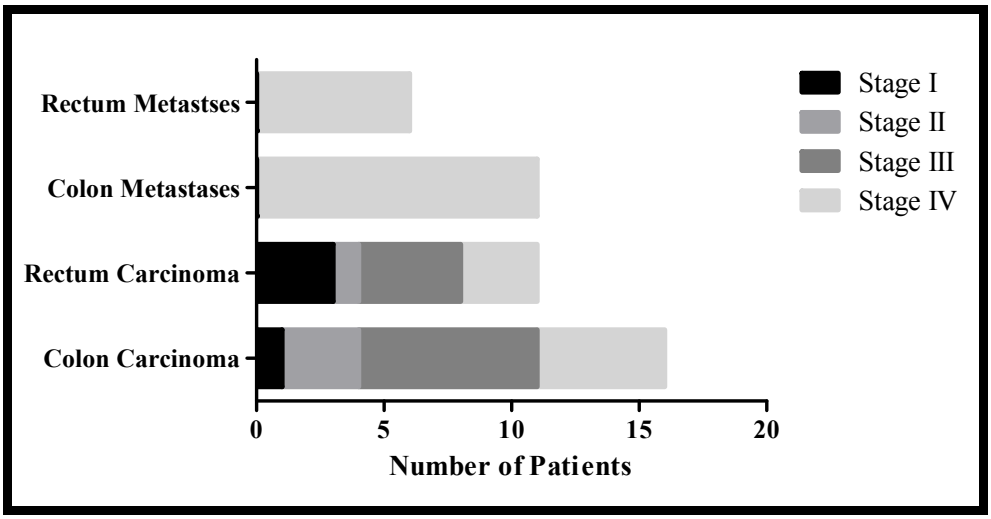


**Figure 13: Frequency of Tumor Location and TNM Stage.** The number of patients according to the tumor location was plotted against the related TNM Stage.

### 3.1.2 Immunohistochemistry staining of Liver Metastases from Colorectal Cancer

IHC was performed on the LM TMA representing different eIF subunits. Density of the IHC staining was predominantly evaluated as 100%. In comparison to healthy liver tissue, several eIFs were highly upregulated in liver metastases tissue from CRC.

IHC staining for eIF1 revealed no staining in approximately 100% of healthy liver tissue samples, whereas liver metastases samples from colon and rectum cancer displayed an increased strong to moderate staining intensity. The same was observed for IHC staining with eIF2α, eIF3H, eIF3B and eIF4G. IHC staining for eIF4E displayed a high to moderate staining intensity in 63% of liver metastases tissues from colon, whereas the intensity in metastases from rectum cancer was 90%. The same tendency was observed for eIF6 and eIF3A. eIF3M revealed no staining in healthy liver and metastases from colon and rectum cancer.

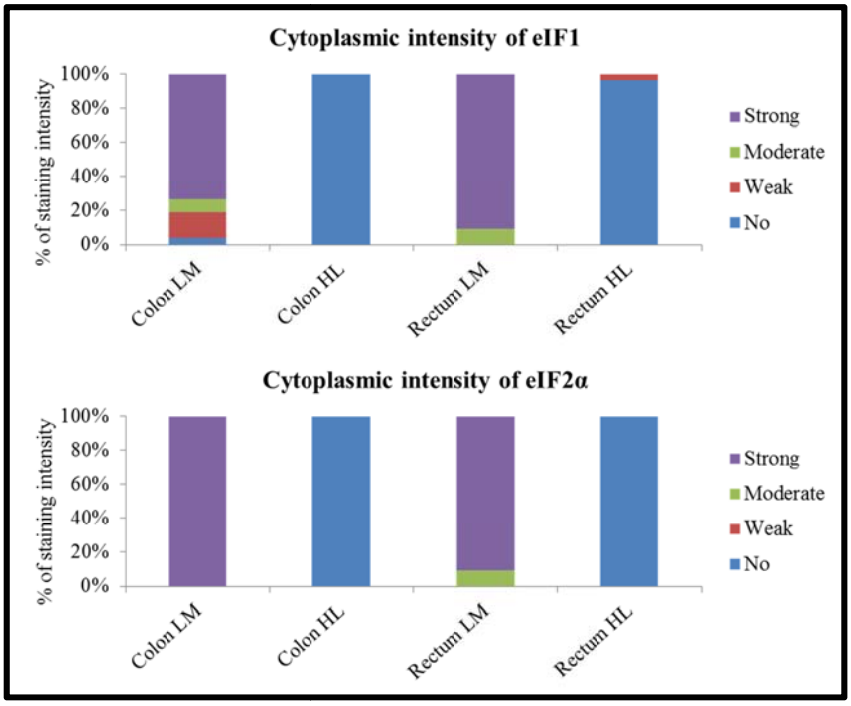


**Figure 14: Immunohistochemical Staining for eIF1 and eIF2α in Liver Metastases from Colorectal Cancer.**

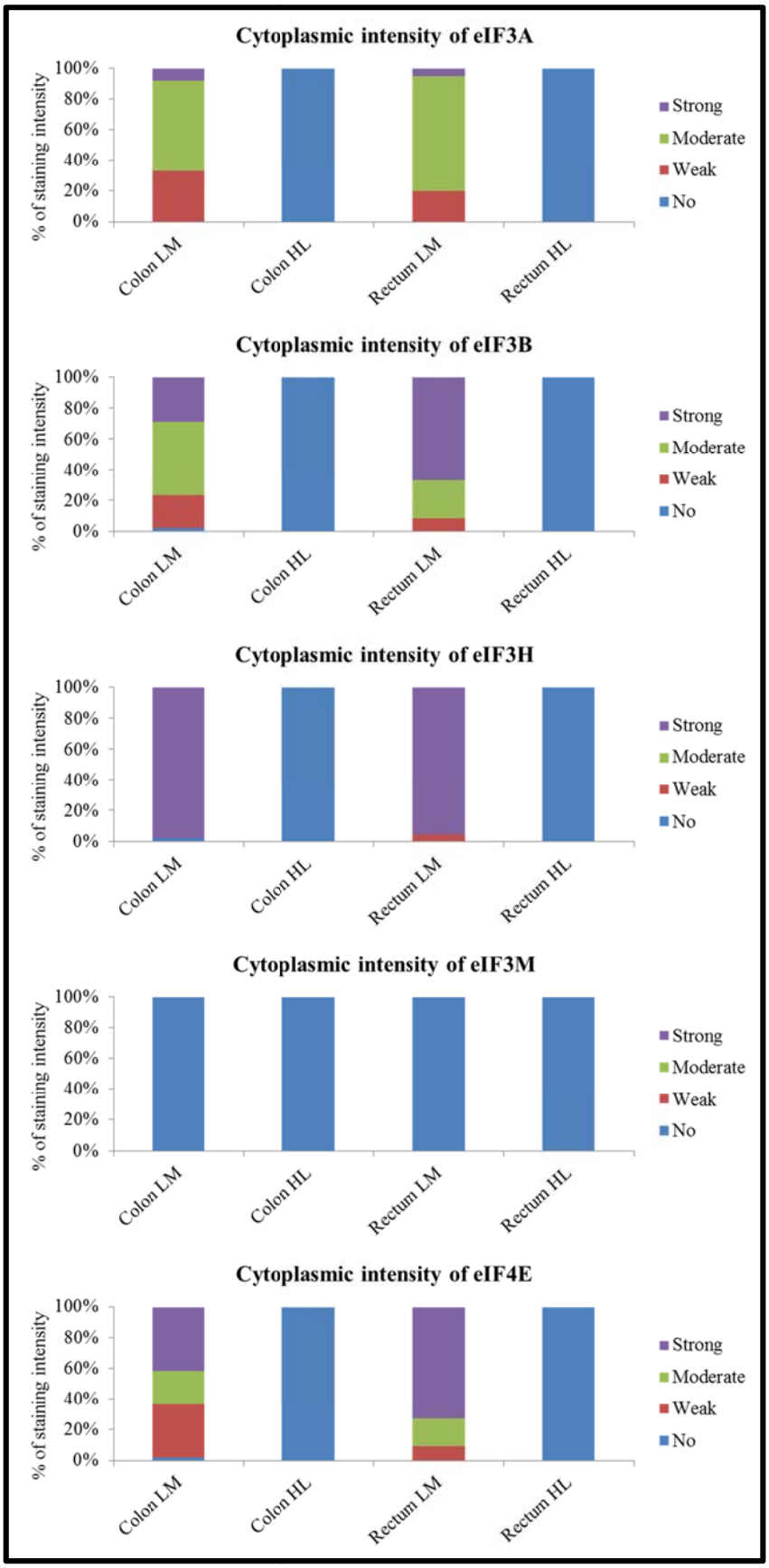


**Figure 15: Immunohistochemical Staining for eIF3A, eIF3B, eIF3H, eIF3M and eIF4E in Liver Metastases from Colorectal Cancer.**

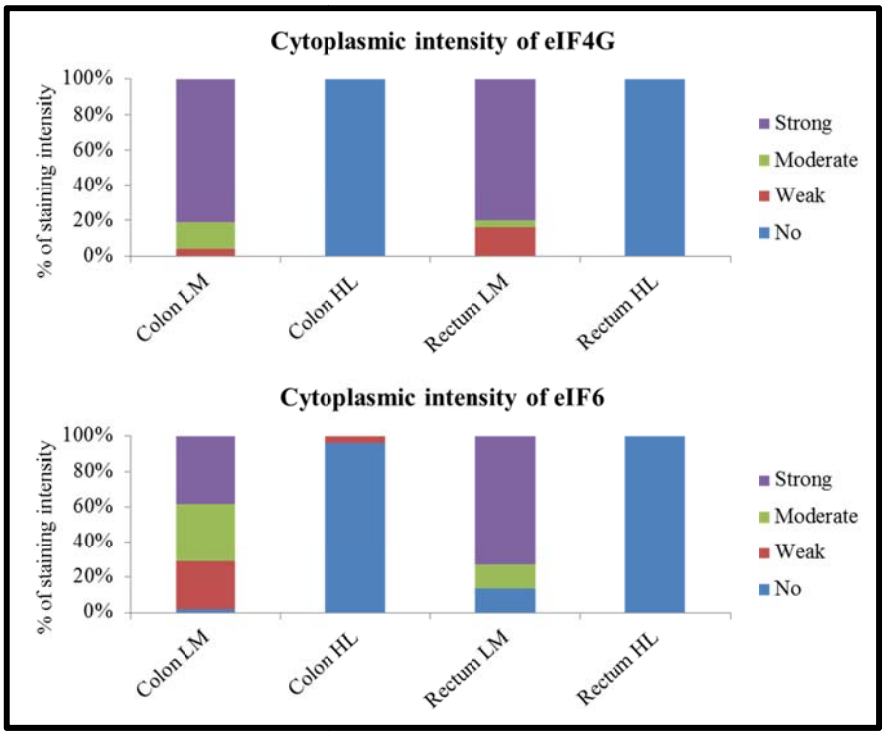


**Figure 16: Immunohistochemical Staining for eIF4G and eIF6 in Liver Metastases from Colorectal Cancer.**

### 3.1.3 Immunohistochemistry staining of Colorectal Cancer

IHC was performed on the CRC TMA representing different eIF subunits. Density of the IHC staining was predominantly evaluated as 100%.

Immunohistochemistry of the analyzed eIF subunits did not show significant differences comparing CRC tissue and respectively healthy control tissue. The observed staining intensities displayed an irregular expression pattern.

IHC staining for eIF2α and eIF3H revealed strong staining in approximately 100% of CRC tissue samples and healthy control samples. The staining for eIF3A, eIF3B, eIF1, eIF4E, eIF4G and eIF6 displayed strong to weak staining intensities with irregular expression pattern. eIF3M revealed no staining in CRC tissue and respectively healthy control tissue.

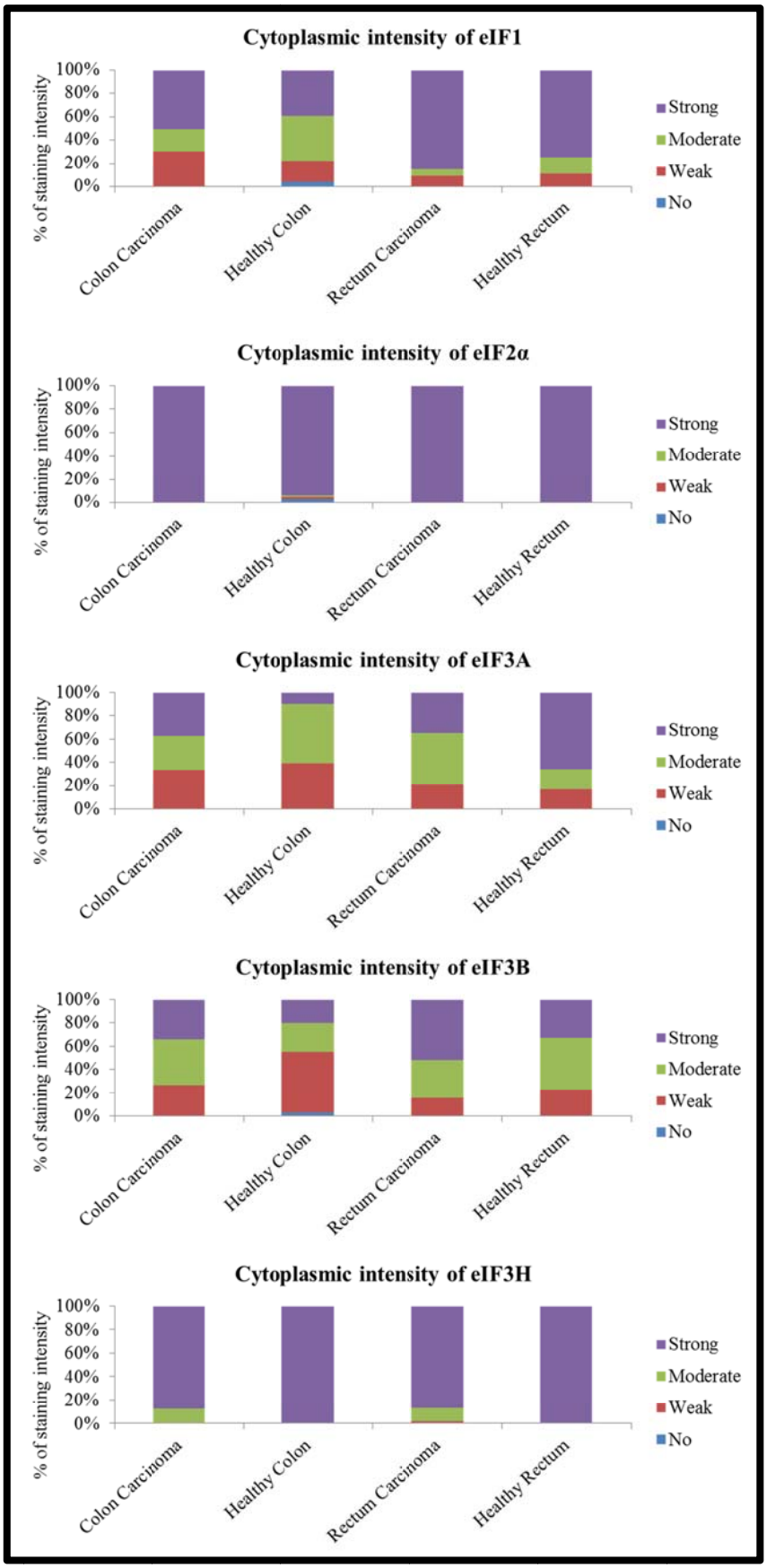


**Figure 17: Immunohistochemical Staining for eIF1, eIF2α, eIF3A, eIF3B and eIF3H in Colorectal Cancer Tissue.**

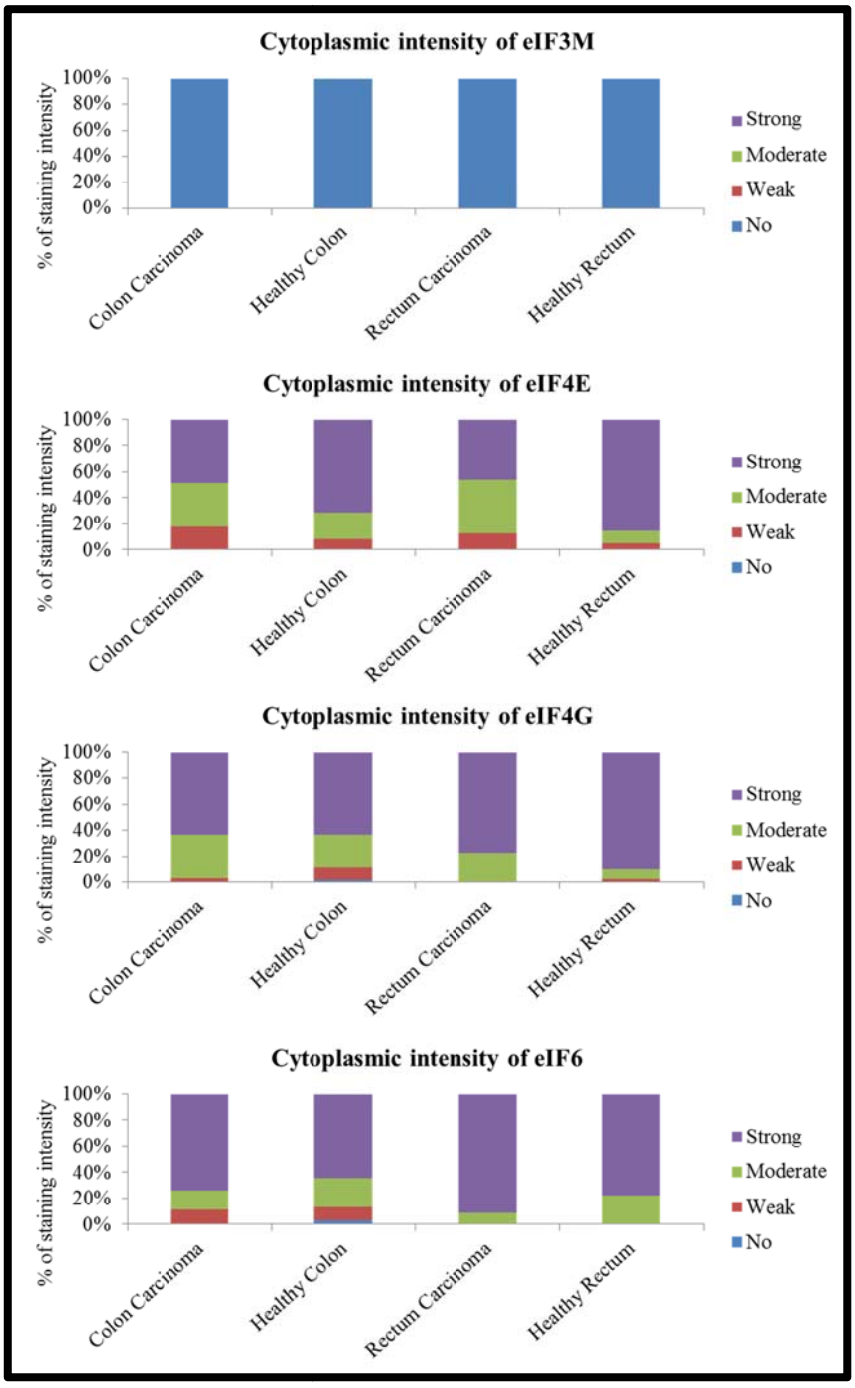


**Figure 18: Immunohistochemical Staining for eIF3M, eIF4E, eIF4G and eIF6 in Colorectal Cancer Tissue.**

## 3.2 Western Blot analysis of Eukaryotic Initiation Factors in Colorectal Cancer

Protein expression in CRC was analyzed by comparing colon and rectum primary carcinoma samples and respectively healthy control tissue using Western Blot and ImageJ analysis. Statistical evaluation was done using the unpaired two tailed t-test. The level of statistical significance was set at $p < 0.05$. Due to the low n number, further samples have to be analyzed. Several eIF subunits and mTOR components of 5 colon carcinoma samples and 5 rectum carcinoma samples were analyzed and normalized to particular healthy control tissue. Actin was used as internal housekeeping protein.

### 3.2.1 Protein expression analysis of mTOR components

Previous publications already displayed PI3K/AKT/mTOR signaling as an upstream pathway of cap dependent translation initiation. To get a broader overview of translation initiation in CRC, in addition to protein analysis of eIF subunits, upstream targets like PTEN, AKT, mTOR and 4E-BP1 were analyzed. Activated proteins were detected based on their specific phosphorylation sides by Western Blot.

#### *3.2.1.1 Protein expression of mTOR, PTEN and 4EBP1 is significantly upregulated in Rectum Cancer*

Protein expression of mTOR, PTEN and 4E-BP1 was significantly upregulated in rectal carcinoma samples compared to healthy control tissue. 4E-BP1 displayed, with an average increase of 3.5 times the highest expression, followed by mTOR with 3 times and PTEN with a mean expression of 2.5 times higher than the controls. In colon cancer mTOR, PTEN and 4E-BP1 revealed no significant changes in comparison to healthy control tissue. Compared to colon cancer, statistical analysis revealed a significant upregulation of PTEN and 4E-BP1 in rectum cancer ($p < 0.05$).

Compared to healthy control tissue, colon and rectum cancer tissues revealed no obvious changes in their phosphorylation status concerning phospho mTOR Ser2448, phospho PTEN Ser380 and phospho 4EBP1 Ser65.

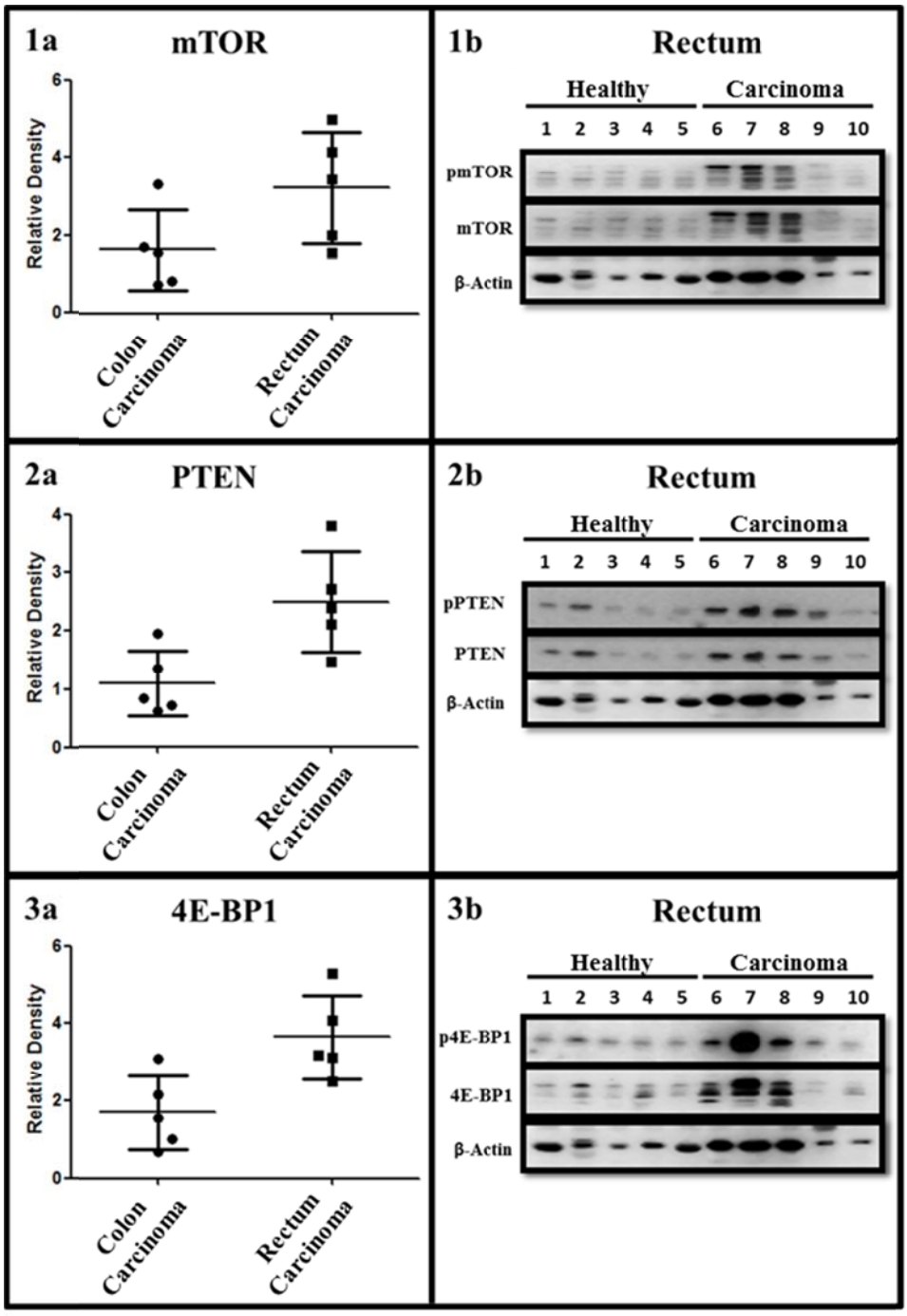


**Figure 19: Protein expression of mTOR, PTEN and 4E-BP1 in colon and rectum cancer.** [1-3] Protein expression in CRC tissue normalized to respectively healthy control tissue. [1] Protein expression of mTOR reveals no significant changes between colon and rectum cancer. In contrast to healthy rectum tissue, mTOR expression is upregulated in rectum cancer tissue ($p < 0.05$). [2] Compared to colon cancer, expression of PTEN is upregulated in rectum cancer ($p < 0.05$). In contrast to healthy rectum tissue, PTEN expression is upregulated in rectum cancer tissue ($p < 0.05$). [3] Compared to colon cancer, expression of 4E-BP1 is upregulated in rectum cancer ($p < 0.05$). In contrast to healthy rectum tissue, 4E-BP1 expression is upregulated in rectum cancer tissue ($p < 0.05$).

*3.2.1.2 Protein expression of AKT is significantly upregulated in Colon Cancer*

Protein expression of AKT was significantly upregulated by a factor of 1.7 in colon cancer samples compared to healthy colon control tissue ($p < 0.05$). In addition Western Blot data revealed a higher phosphorylation status of AKT Ser478 in healthy colon tissue referred to total AKT. Phosphorylation of AKT Ser478 in colon cancer tissue was reduced to about 40%. The analysis revealed no significant changes of AKT expression in rectum cancer tissue.

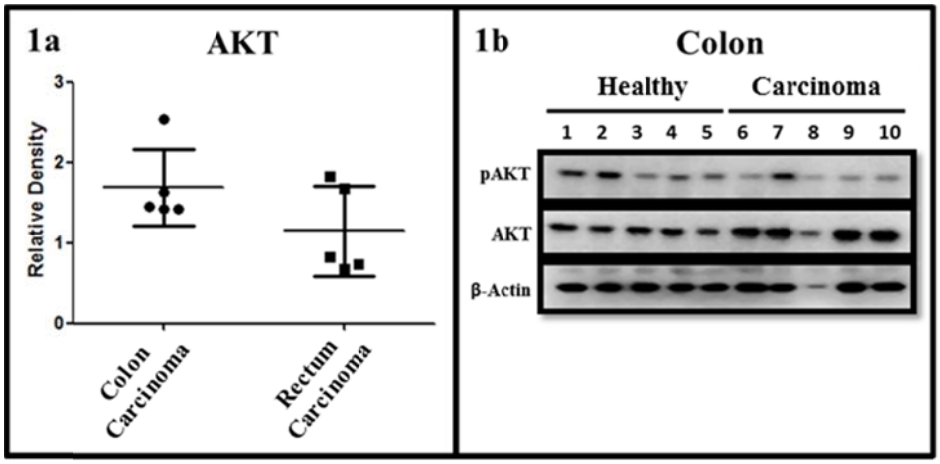


**Figure 20: Protein expression of AKT in colon and rectum cancer.** [1] Protein expression of AKT in CRC tissue normalized to respectively healthy control tissue reveals an AKT upregulation in colon cancer ($p < 0.05$) compared to rectum cancer. In contrast to healthy colon tissue, AKT is upregulated in colon cancer tissue ($p < 0.05$). Phosphorylation status of AKT Ser478 was reduced to about 40% in colon cancer tissue

### 3.2.2 Protein expression analysis of eIF subunits

*3.2.2.1 Protein expression of eIF2α, eIF3A and eIF3D is significantly upregulated in Colon Cancer*

Compared to the healthy colon control tissue, protein expression of eIF2α, eIF3A and eIF3D was significantly upregulated in colon cancer samples. eIF3A showed a highly upregulation of 40 times in colon cancer ($p < 0,05$) compared to healthy control tissue. In addition protein expression of eIF3A displayed a high tendency to be increased in rectal cancer by a factor of 6. The p-value for this calculation was 0.051. eIF2α was 4.5 times upregulated in colon cancer ($p < 0.05$) whereas in rectum cancer no significant changes were visible. eIF3D showed a significant upregulation with a mean of 2.2 in

colon cancer whereas no obvious changes in rectal cancer tissue could be detected. Statistical analysis revealed a significant upregulation of eIF2α and eIF3A in colon cancer compared to rectum cancer ($p < 0.05$).

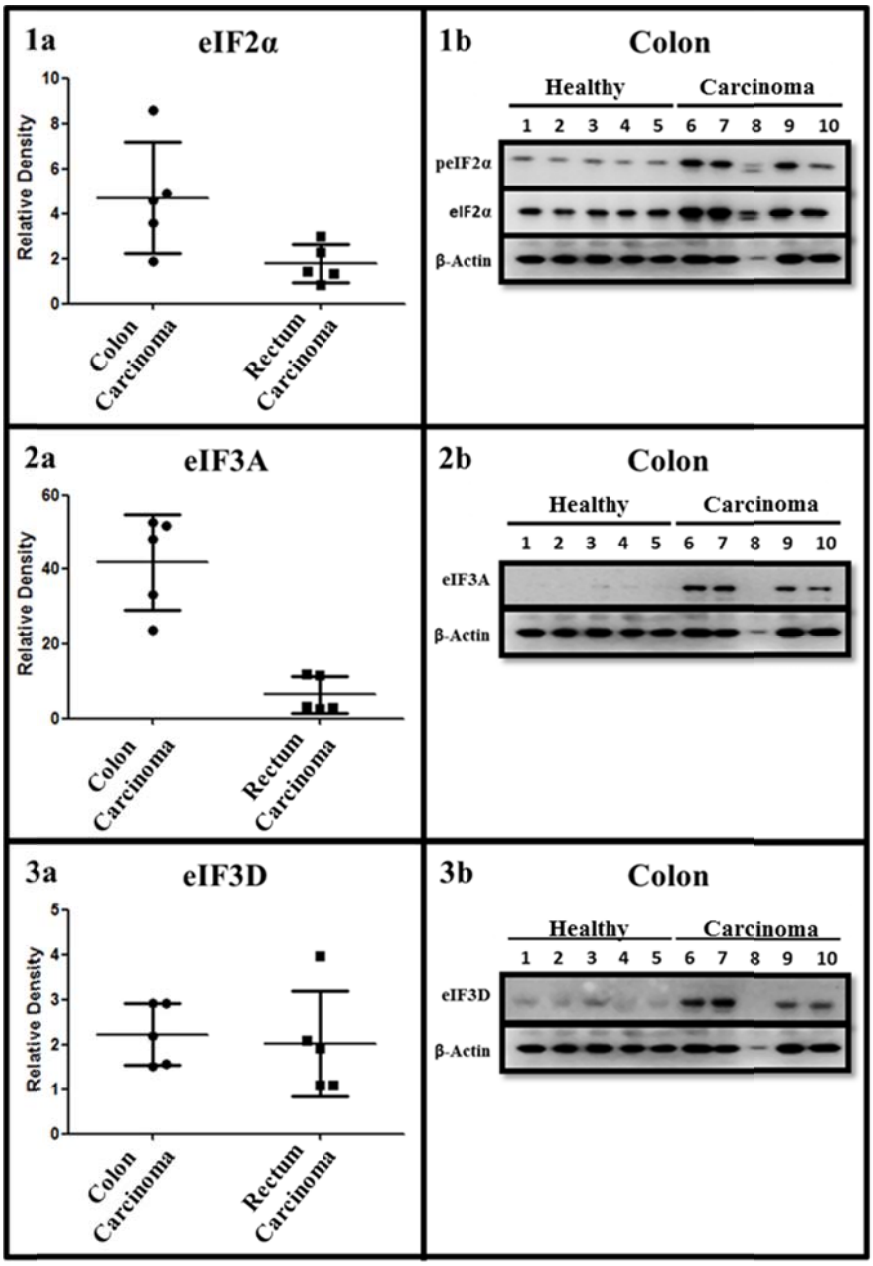


**Figure 21: Protein expression of eIF2α, eIF3A and eIF3D in colon and rectum cancer.** [1-3] Protein expression in CRC tissue normalized to respectively healthy control tissue. [1] Compared to rectum cancer, expression of eIF2α is increased in colon cancer ($p < 0.05$). In contrast to healthy colon tissue, eIF2α expression is upregulated in colon cancer tissue ($p < 0.05$). [2] Compared to rectum cancer, expression of eIF3A is upregulated in colon cancer ($p < 0.05$). In contrast to healthy colon tissue, eIF3A expression is upregulated in colon cancer tissue ($p < 0.05$). [3] Protein expression of eIF3D reveals no significant changes between colon and rectum cancer. In contrast to healthy colon tissue, eIF3D is upregulated in colon cancer tissue ($p < 0.05$).

### *3.2.2.2 Protein expression of eIF3θ is significantly downregulated in Colon Cancer*

ImageJ analysis revealed a significant 40% reduction for eIF3θ expression in colon carcinoma. The expression of eIF3θ in rectal cancer tissue displayed variable pattern with no significance being present.

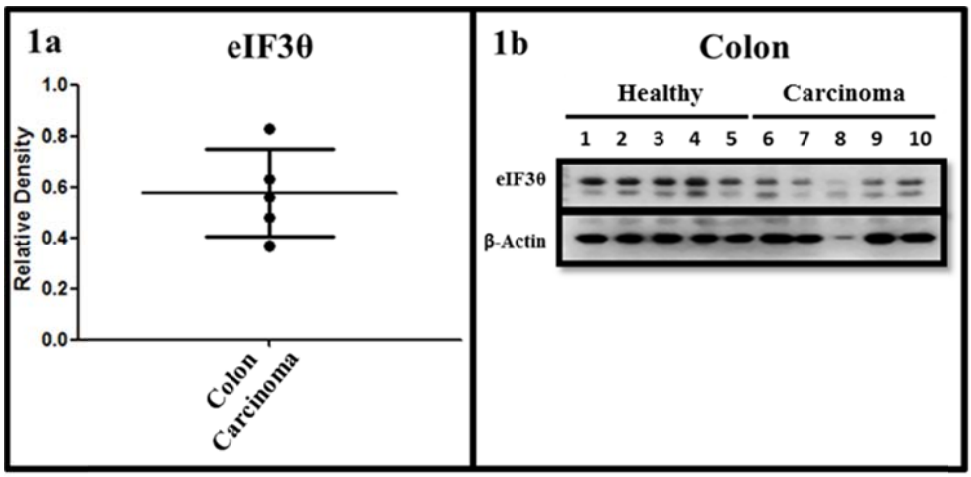


**Figure 22: Protein expression of eIF3θ in colon cancer.** [1] Protein expression of eIF3θ in colon cancer normalized to healthy colon tissue. In contrast to healthy colon tissue, eIF3θ is downregulated in colon cancer tissue ($p < 0.05$).

### *3.2.2.3 Protein expression of eIF3I and eIF4E is significantly upregulated in Rectum Cancer*

Compared to healthy rectum control tissue, protein expression of eIF3I and eIF4E was significantly upregulated in rectum cancer samples. eIF3I revealed a significant 2 fold upregulation in rectum cancer ($p < 0,05$). Protein expression of eIF3I displayed a tendency to be increased in colon cancer by a factor of 3 ($p=0.07$). Protein expression of eIF4E was 5.5 times upregulated in rectum cancer ($p < 0.05$) whereas in colon cancer no significant changes were visible. Statistical analysis revealed a significant upregulation of eIF4E in rectum cancer compared to colon cancer ($p < 0.05$).

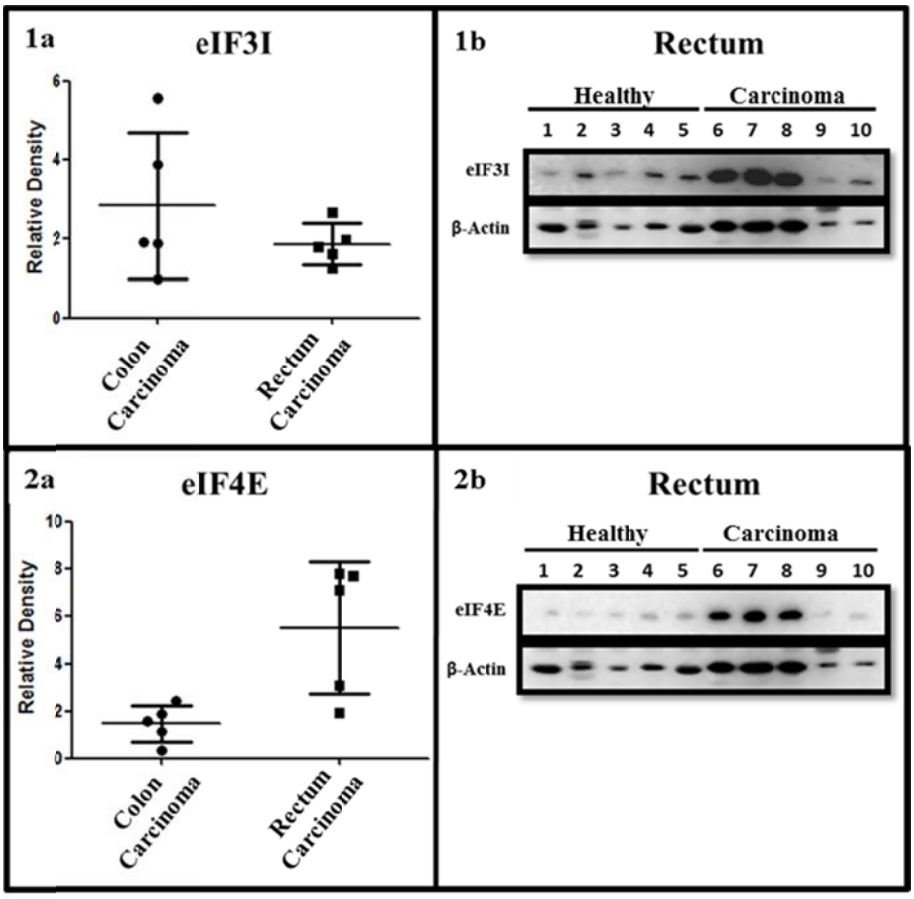


**Figure 23: Protein expression of eIF3I and eIF4E in colon and rectum cancer.** [1-3] Protein expression in CRC tissue normalized to respectively healthy control tissue. [1] Protein expression of eIF3I reveals no significant changes between colon and rectum cancer. In contrast to healthy rectum tissue, eIF3I expression is upregulated in rectum cancer tissue ($p < 0.05$). [2] Compared to colon cancer, expression of eIF4E is upregulated in rectum cancer ($p < 0.05$). In contrast to healthy rectum tissue, eIF4E expression is upregulated in rectum cancer tissue ($p < 0.05$).

### *3.2.2.4 Protein expression of eIF3B, eIF3M, eIF4B, eIF4G and eIF6 is significantly upregulated in Colon and Rectum Cancer*

Compared to respectively healthy control tissue, protein expression of eIF3B, eIF3M, eIF4B, eIF4G and eIF6 was significantly increased in colon and rectum cancer samples. In colon cancer tissue eIF4B showed the highest upregulation by factor 20 ($p < 0.05$), followed by eIF4G being about 13 fold increased ($p < 0.05$). eIF3M revealed a significant 2 fold upregulation and eIF3B was increased by a factor of 3 ($p < 0.05$). ImageJ analysis of eIF6 protein pattern revealed a significant 4 fold upregulation in colon cancer ($p < 0.05$). The same could be detected in rectal cancer tissue. In this case eIF4G showed the highest increase by 16 fold overexpression, followed by eIF4B with 6 fold overexpression, eIF6 with 5 fold overexpression and eIF3B being increased by a

factor of 3. eIF3M expression was 3 times increased in rectal cancer tissue. The p-value for these calculations was smaller than 0.05 and set as significant. Statistical analysis comparing colon and rectum cancer samples revealed a significant upregulation of eIF4B in colon cancer compared to rectum cancer ($p < 0.05$). In addition to the already represented eIFs, protein levels of eIF5, eIF3K, eIF3J, eIF3C and eIF3H were analyzed. These eIF subunits displayed no significant expression differences in colon or rectum cancer tissue compared to respectively healthy control tissue.

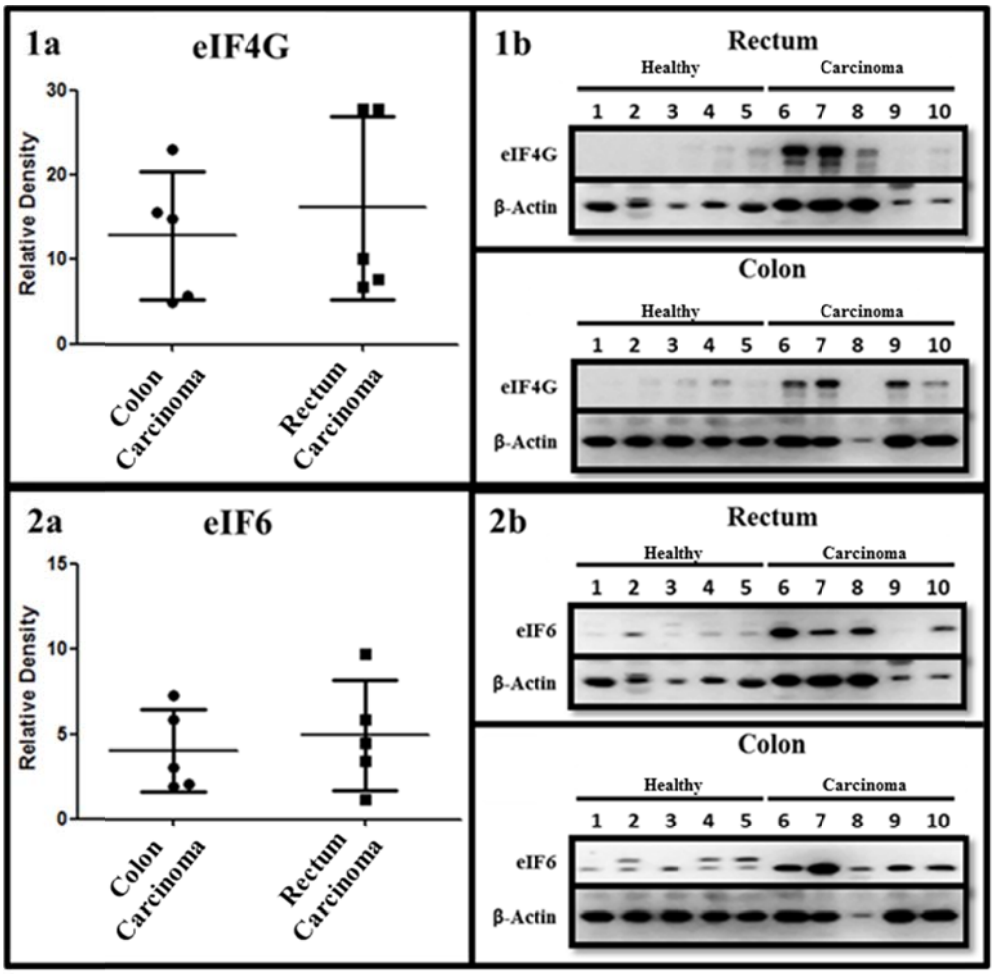


**Figure 24: Protein expression of eIF4G and eIF6 in colon and rectum cancer.** [1-3] Protein expression in CRC tissue normalized to respectively healthy control tissue. [1] Protein expression of eIF4G reveals no significant changes between colon and rectum cancer. In contrast to respectively healthy control tissue, eIF4G expression is upregulated in colon and rectum cancer tissue ($p < 0.05$). [2] Protein expression of eIF6 reveals no significant changes between colon and rectum cancer. In contrast to respectively healthy control tissue, eIF6 expression is upregulated in colon and rectum cancer tissue ($p < 0.05$).

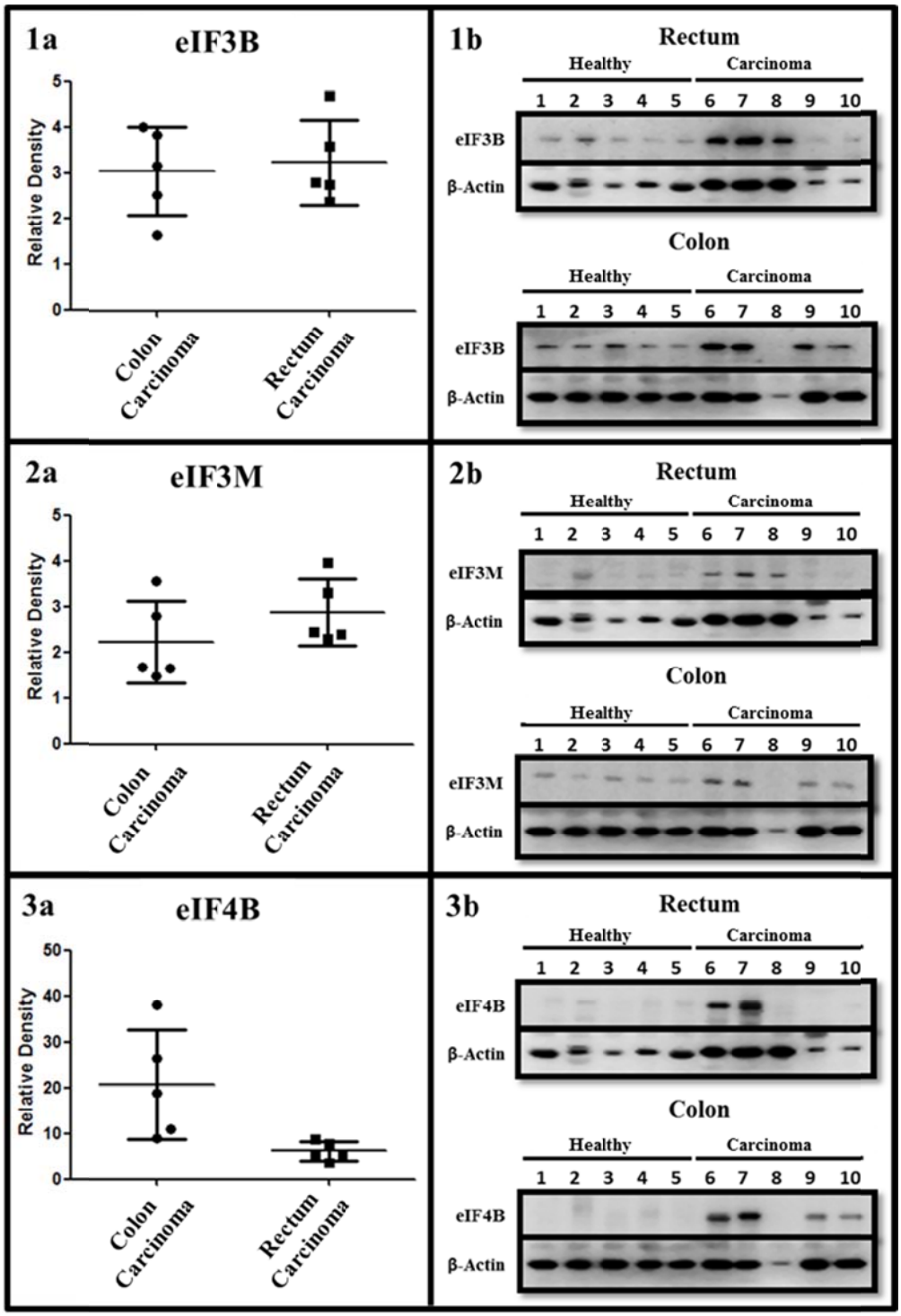


**Figure 25: Protein expression of eIF3B, eIF3M and eIF4B in colon and rectum cancer.** [1-3] Protein expression in CRC tissue normalized to respectively healthy control tissue. [1] Protein expression of eIF3B reveals no significant changes between colon and rectum cancer. In contrast to respectively healthy control tissue, eIF3B expression is upregulated in colon and rectum cancer tissue ($p < 0.05$). [2] Protein expression of eIF3M reveals no significant changes between colon and rectum cancer. In contrast to respectively healthy control tissue, eIF6 expression is upregulated in colon and rectum cancer tissue ($p < 0.05$). [3] Compared to rectum cancer, expression of eIF4B is upregulated in colon cancer ($p < 0.05$). In contrast to respectively healthy control tissue, eIF4B expression is upregulated in colon and rectum cancer tissue ($p < 0.05$).

## 3.3 Real-Time Analysis of Eukaryotic Initiation Factors in Colorectal Cancer

### 3.3.1 mRNA expression analysis of mTOR components

Real-Time PCR of mTOR and PTEN did not display significant differences between CRC tissue and respectively healthy control. In addition no significant changes were visible in statistical analysis of colon versus rectum cancer.

### 3.3.2 mRNA analysis of eIF subunits

#### *3.3.2.1 mRNA expression of eIF3C, eIF3M, eIF3H and eIF6 is significantly upregulated in Colon Cancer*

Compared to healthy colon control tissue, mRNA expression of eIF3C, eIF3M, eIF3H and eIF6 was significantly upregulated in colon cancer samples. Real-time analysis of eIF3C revealed a high upregulation of 30 times ($p < 0.05$). A 12 fold increase was observed for eIF6 ($p < 0.05$). eIF3M also displayed a high upregulation of 30 times in colon cancer ($p < 0.05$). mRNA expression of eIF3H was 25 times upregulated ($p < 0.05$). No significant changes in mRNA expression of eIF3C, eIF3M, eIF3H and eIF6 could be observed comparing rectum cancer and healthy rectum tissue. Statistical analysis revealed a trend in upregulation of eIF3M ($p = 0.06$) and eIF3H ($p = 0.06$) in colon cancer compared to rectum cancer ($p < 0.05$).

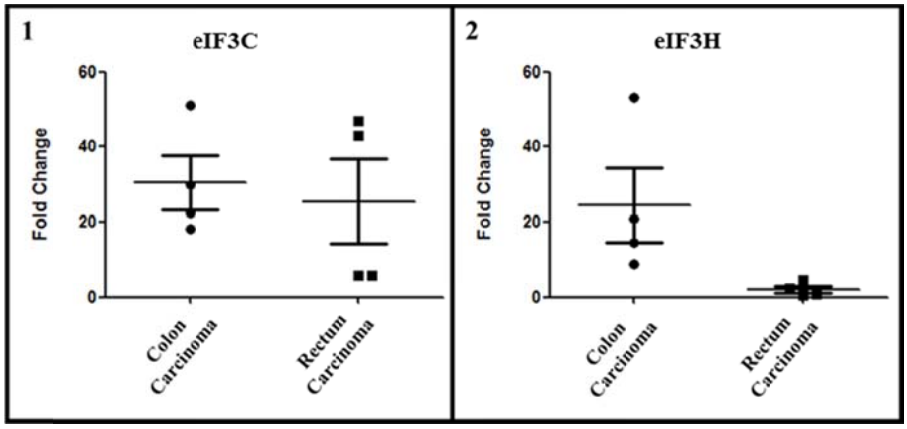


**Figure 26: mRNA expression of eIF3C and eIF3H in colon and rectum cancer.** [1-2] Normalized mRNA expression for eIF3C and eIF3H displays a significant increase in colon cancer tissue compared to healthy control.

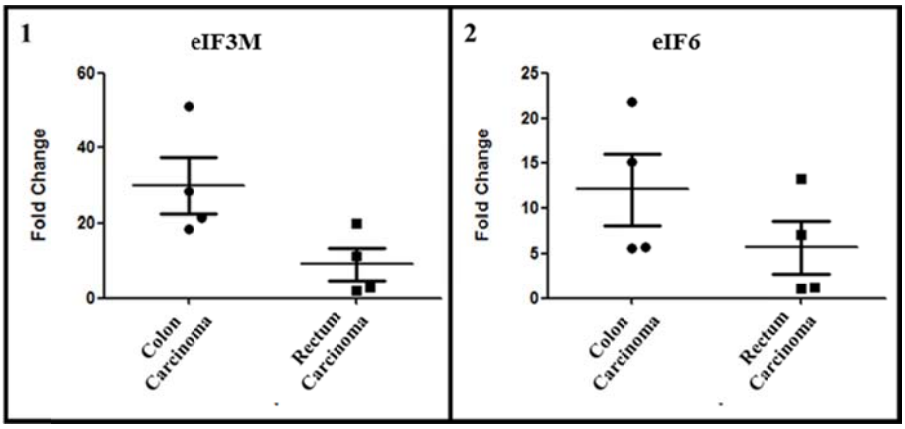


**Figure 27: mRNA expression of eIF3M and eIF6 in colon and rectum cancer.** [1-2] Normalized mRNA expression for eIF3M and eIF6 displays a significant increase in colon cancer tissue compared to healthy control.

### *3.3.2.2 mRNA expression of eIF2α, eIF3A, eIF3B and eIF4B is significantly upregulated in Rectum Cancer*

In comparison to healthy rectum tissue, mRNA expression of eIF2α, eIF3A, eIF3B and eIF4B was significantly upregulated in rectum cancer samples. Therefore eIF3B displayed the highest upregulation by factor 40 ($p < 0.05$), followed by eIF3A being about 28 fold increased ($p < 0.05$). eIF2α revealed a significant 20 fold upregulation and eIF4B was increased by a factor of 3 ($p < 0.05$). No significant changes in mRNA expression of eIF2α, eIF3A, eIF3B and eIF4B could be observed comparing colon cancer and healthy colon tissue. Compared to colon cancer statistical analysis revealed a significant upregulation of eIF3B in rectum cancer ($p < 0.05$).

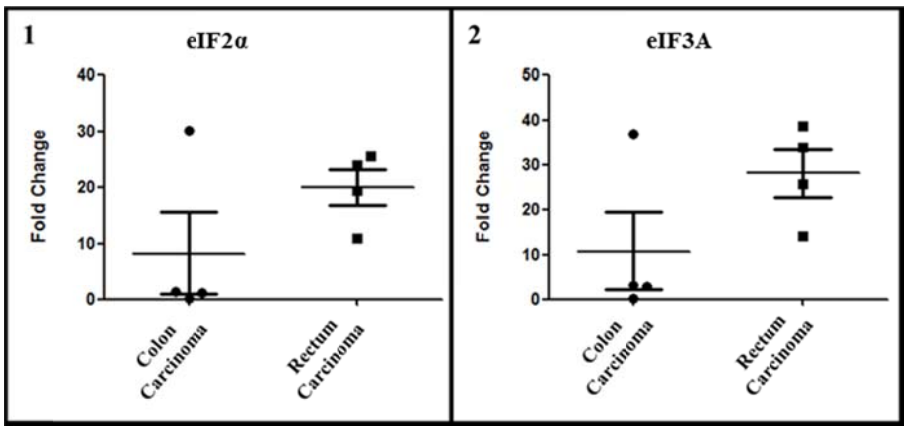


**Figure 28: mRNA expression of eIF2α and eIF3A in colon and rectum cancer.** [1-2] Normalized mRNA expression for eIF2α and eIF3A displays a significant increase in rectum cancer tissue compared to healthy control.

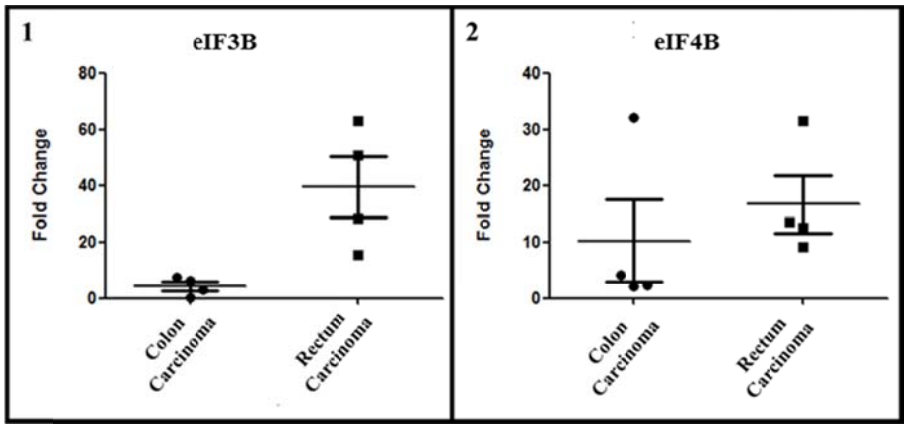


**Figure 29: mRNA expression of eIF3B and eIF4B in colon and rectum cancer.** [1-2] Normalized mRNA expression for eIF3B and eIF4B displays a significant increase in rectum cancer tissue compared to healthy control.

### *3.3.2.3 mRNA expression of eIF1 is significantly upregulated in Colon and Rectum Cancer*

Compared to respectively healthy control tissue, mRNA expression of eIF1 was significantly upregulated in colon and rectum cancer samples.

In colon cancer eIF1 displayed a 25 fold upregulation in comparison to healthy colon tissue. The same was visible for rectum cancer, displaying an upregulation of eIF1 by factor 30 compared to healthy rectum tissue. The p-value for this calculation was smaller than 0.05 and therefore set as significant. No significant eIF1 expression differences could be observed comparing colon and rectum cancer samples.

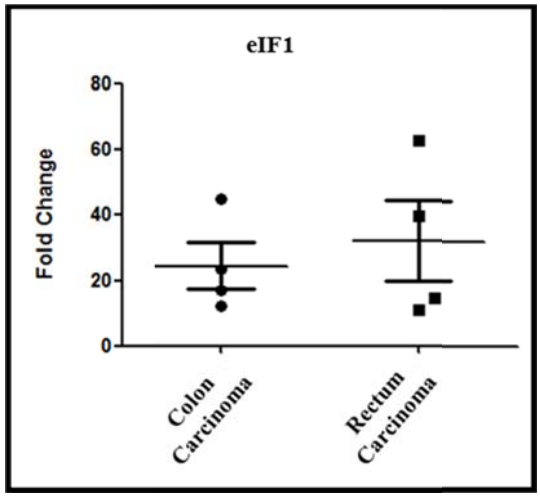


**Figure 30: mRNA expression of eIF1 in colon and rectum cancer.** Normalized mRNA expression of eIF1 displays a significant increase in colon and rectum cancer tissue compared to respectively healthy control.

## 3.4 Analysis of Colorectal Cancer patient derived Xenograft Models

Changes in protein expression of mTOR, PTEN and specific eIF subunits were analyzed in patient derived xenograft (PDX) models using respectively healthy control tissue for normalization. Therefore PDX models of 5 primary carcinoma samples and 2 liver metastases samples of patients suffering from rectum cancer, as well as 4 primary carcinoma samples and 1 liver metastasis sample of patients suffering from colon cancer were generated by EPO Berlin-Buch GmbH (Berlin, Germany). Xenotransplanted carcinomas and metastases were treated with different standard and novel chemotherapeutic drugs (see Table 2). The tumor volume was measured regularly and used to generate chemosensitivity growth curves. After a time period of 30-40 days the tumors were excised and analyzed on protein level by Western Blot. Chemosensitivity data were kindly provided by EPO Berlin-Buch GmbH. Tumor volume of treatment in comparison to control (T/C) was calculated in percent. According to the Oncotrack guideline a T/C smaller than 50% was set as biological meaningful.

### 3.4.1 Chemosensitivity of patient derived Xenograft Models in Colon Cancer

The PDX panel representing colon cancer consisted of 1 colon metastasis (CM) model and 4 colon primary carcinoma (CPC) models. The test for sensitivity to specific chemotherapeutic drugs revealed Irinotecan (mean T/C=21), 5-FU (mean T/C=35) and Cetuximab (mean T/C=42) as most efficient drugs to enhance growth of colon primary carcinoma. In colon primary carcinoma PDX models the tumor growth under treatment with IGF 1/2 mAB (mean T/C=191), AZ1 (mean T/C=142) and Volitinib (mean T/C=118) was even higher than untreated control. Treatment of the colon metastasis PDX model displayed a biological meaningful reduction of tumor growth under treatment with Cetuximab (T/C=9), Oxaliplatin (T/C=48) and Irinotecan (T/C=34). Tumor growth under treatment with IGF 1/2 mAB (T/C=251), 5-FU (T/C=110), Afatinib (T/C=111), Nintedanib (T/C=123) and Volitinib (T/C=161) was even higher than untreated control.

| Drug | CPC1 | CPC2 | CPC3 | CPC4 | CM1 |
|---|---|---|---|---|---|
| | T/C | | | | |
| Oxaliplatin | 70 | 98 | 62 | 89 | 48 |
| Irinotecan | 28 | 16 | 10 | 30 | 34 |
| 5-FU | 56 | 50 | 18 | 15 | 110 |
| Cetuximab | 60 | 26 | - | 40 | 9 |
| AZD8931 | 58 | 35 | 71 | 67 | 63 |
| AZD6244 | 25 | 35 | 45 | 70 | 58 |
| Afatinib | 84 | 25 | 64 | 89 | 111 |
| Avastin | 37 | 86 | 83 | 103 | 70 |
| Regorafenib | 44 | 92 | 82 | 52 | 74 |
| Nintedanib | 50 | 77 | 58 | 53 | 123 |
| mTOR FR | 80 | 96 | 72 | 24 | 93 |
| IGF 1/2 mAB | 153 | 363 | 149 | 97 | 251 |
| AZ1 | 101 | 260 | 125 | 81 | - |
| Volitinib | - | 198 | 84 | 71 | 161 |

**Table 16: Chemosensitivity testing of PDX models for colon primary carcinomas and colon metastasis.** Tumor volume of treatment in comparison to control (T/C) was calculated in percent. CPC=Colon Primary Carcinoma PDX Model / CM=Colon Metastasis PDX Model.

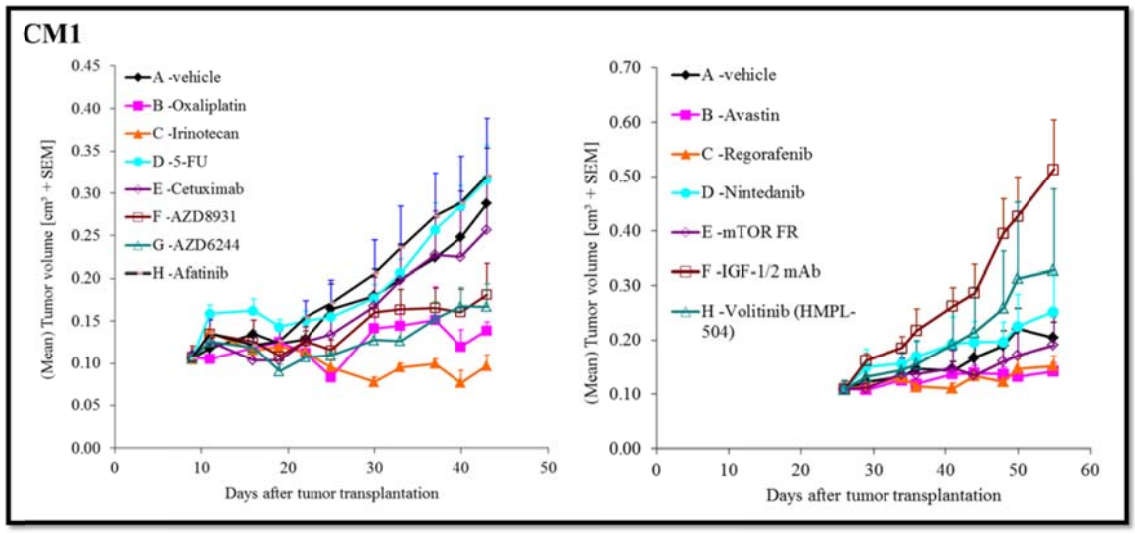


**Figure 31: Growth curve of the colon metastasis PDX model CM1 under chemotherapeutic treatment.** Treatment of CM1 displays a biological meaningful reduction of tumor growth under treatment with Cetuximab, Oxaliplatin and Irinotecan.

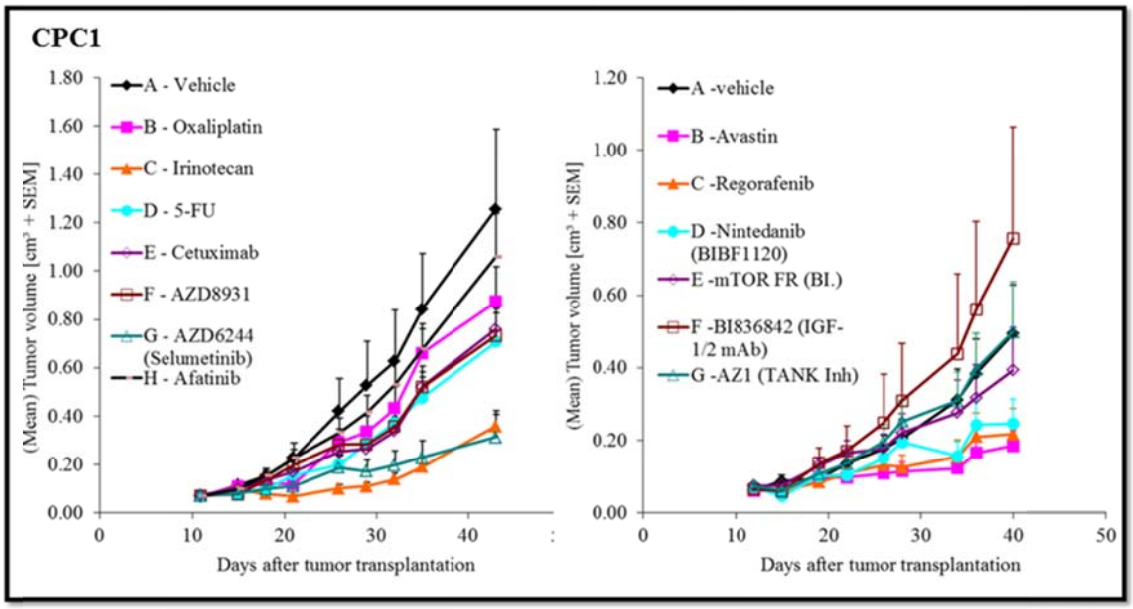


**Figure 32: Growth curve of the colon primary carcinoma PDX model CPC1 under chemotherapeutic treatment.** Treatment of CPC1 displays a biological meaningful reduction of tumor growth under treatment with Irinotecan, AZD6244, Avastin and Regorafenib.

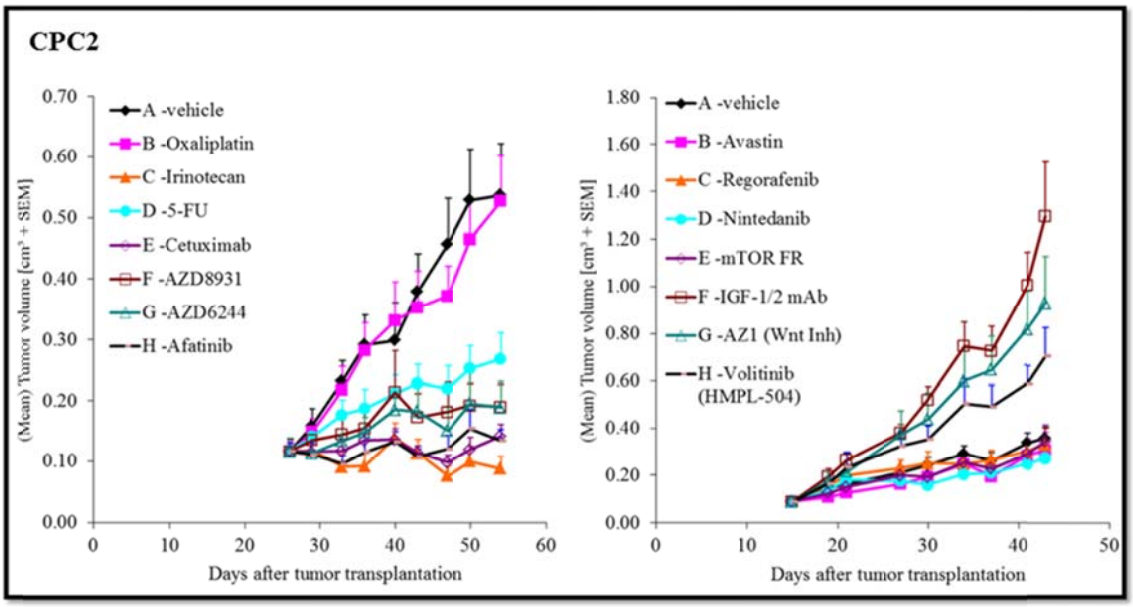


**Figure 33: Growth curve of the colon primary carcinoma PDX model CPC2 under chemotherapeutic treatment.** Treatment of CPC2 displays a biological meaningful reduction of tumor growth under treatment with Irinotecan, Cetuximab, AZD8931, AZD6244 and Afatinib.

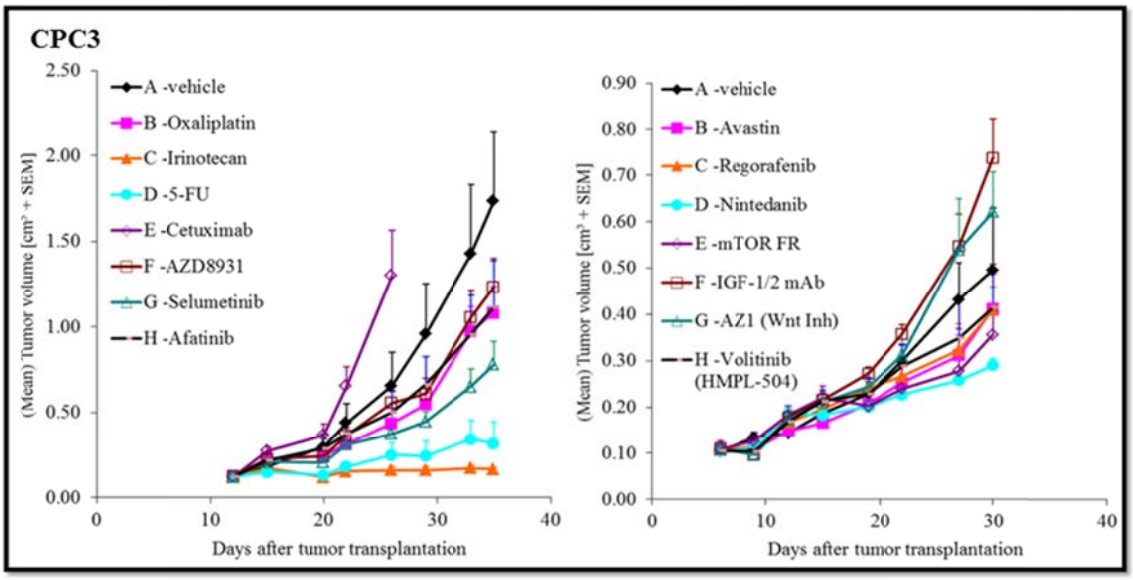


**Figure 34: Growth curve of the colon primary carcinoma PDX model CPC3 under chemotherapeutic treatment.** Treatment of CPC3 displays a biological meaningful reduction of tumor growth under treatment with Irinotecan, 5-FU and AZD6244 (Selumetinib).

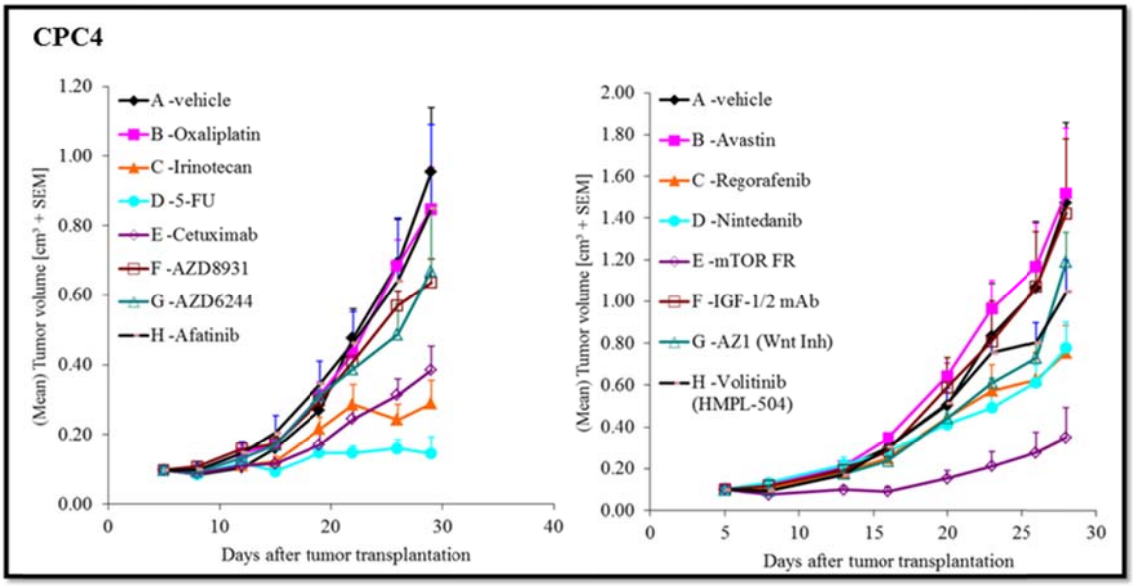


**Figure 35: Growth curve of the colon primary carcinoma PDX model CPC4 under chemotherapeutic treatment.** Treatment of CPC4 displays a biological meaningful reduction of tumor growth under treatment with Irinotecan, 5-FU, Cetuximab, Regorafenib, Nintedanib and mTOR FR.

### 3.4.2 Chemosensitivity of Patient derived Xenograft Models in Rectum Cancer

The PDX panel representing rectum cancer consisted of 2 rectum metastases (RM) and 4 rectum primary carcinoma (RPC) PDX models. The test for sensitivity to specific chemotherapeutic drugs displayed Irinotecan (mean T/C=16), Avastin (mean T/C=34), Regorafenib (T/C=34) and mTOR FR (mean T/C=36) as most efficient drugs to enhance growth of rectum primary carcinomas. Nintedanib (T/C=36), Oxaliplatin (T/C=45), 5-FU (T/C=46) and AZD6244 (T/C=40) also showed a biological meaningful growth reduction. In rectum primary carcinoma PDX models the tumor growth under treatment with IGF 1/2 mAB (mean T/C=126) and AZ1 (mean T/C=123) was even higher than untreated control. Treatment of rectum metastases PDX models revealed the highest tumor growth reduction under treatment with Irinotecan (mean T/C=9), 5-FU (mean T/C=21), Cetuximab (mean T/C=26) and mTOR FR (mean T/C=31). In addition a biological meaningful reduction of tumor growth was observed under treatment with Oxaliplatin (mean T/C=36), Afatinib (mean T/C=41), Nintedanib (mean T/C=45) and Avastin (mean T/C=37).

| Drug | RPC1 | RPC2 | RPC3 | RPC4 | RM1 | RM2 |
|---|---|---|---|---|---|---|
| | T/C | | | | | |
| Oxaliplatin | 30 | 34 | 50 | 64 | 46 | 26 |
| Irinotecan | 4 | 32 | 22 | 8 | 5 | 13 |
| 5-FU | 45 | 72 | 30 | 38 | 24 | 19 |
| Cetuximab | 76 | 89 | 122 | 19 | 10 | 42 |
| AZD8931 | 82 | 62 | 49 | 78 | 39 | 75 |
| AZD6244 | 32 | 36 | 36 | 55 | 38 | 62 |
| Afatinib | 49 | 78 | 58 | 75 | 38 | 44 |
| Avastin | 33 | 26 | 41 | 37 | 36 | 38 |
| Regorafenib | 39 | 21 | 52 | 26 | 41 | 75 |
| Nintedanib | 43 | 20 | 47 | 32 | 33 | 58 |
| mTOR FR | 13 | 13 | 62 | 33 | 38 | 24 |
| IGF 1/2 mAB | 190 | 73 | 130 | 111 | 87 | 83 |
| AZ1 | 80 | 70 | 221 | 119 | 75 | - |
| Volitinib | - | - | - | 93 | - | 73 |

**Table 17: Chemosensitivity testing of PDX models for rectum primary carcinomas and rectum metastases.** Tumor volume of treatment in comparison to control (T/C) was calculated in percent. RPC=Rectum Primary Carcinoma PDX Model / RM=Rectum Metastases PDX Model.

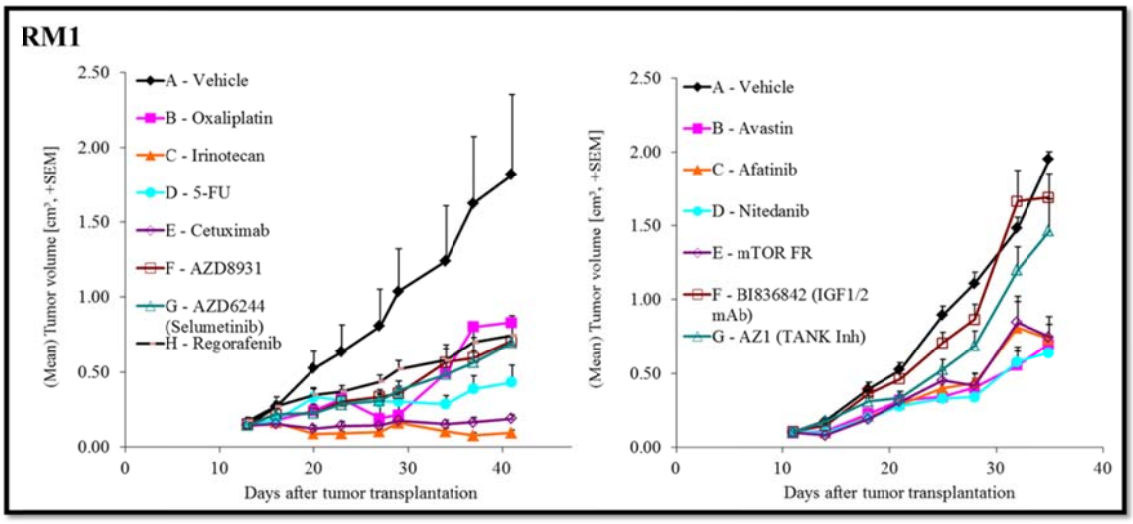


**Figure 36: Growth curve of the rectum metastasis PDX model RM1 under chemotherapeutic treatment.** Treatment of RM1 displays a biological meaningful reduction of tumor growth under treatment with all mentioned drugs except IGF 1/2 mAB and AZ1.

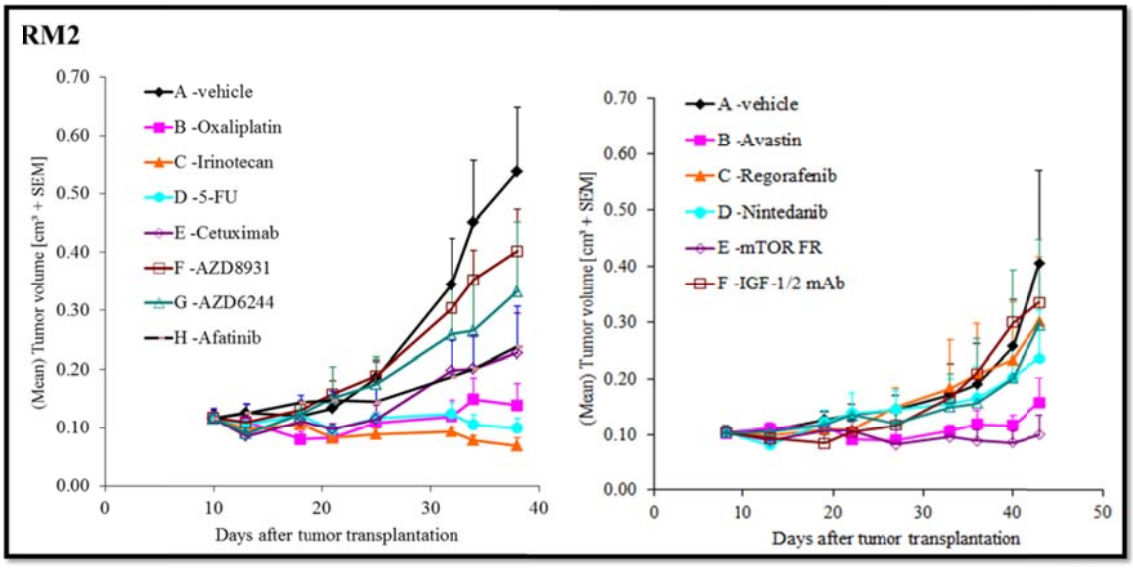


**Figure 37: Growth curve of the rectum metastasis PDX model RM2 under chemotherapeutic treatment.** Treatment of RM2 displays a biological meaningful reduction of tumor growth under treatment with Oxaliplatin, Irinotecan, 5-FU, Cetuximab, Afatinib, Avastin and mTOR FR.

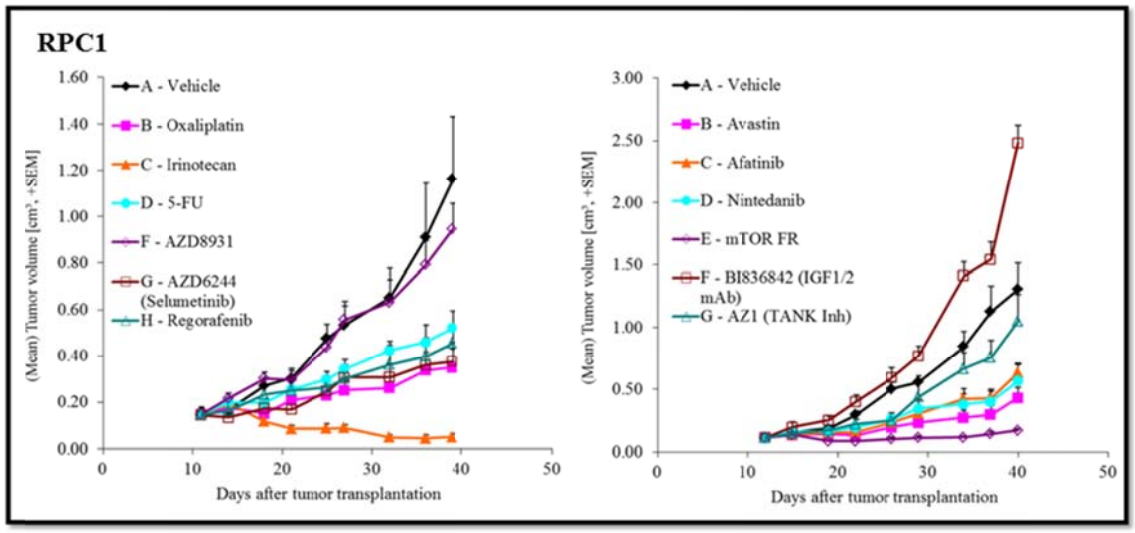


**Figure 38: Growth curve of the rectum primary carcinoma PDX model RPC1 under chemotherapeutic treatment.** Treatment of RPC1 displays a biological meaningful reduction of tumor growth under treatment with Oxaliplatin, Irinotecan, 5-FU, AZD6244, Avastin, Regorafenib and mTOR FR.

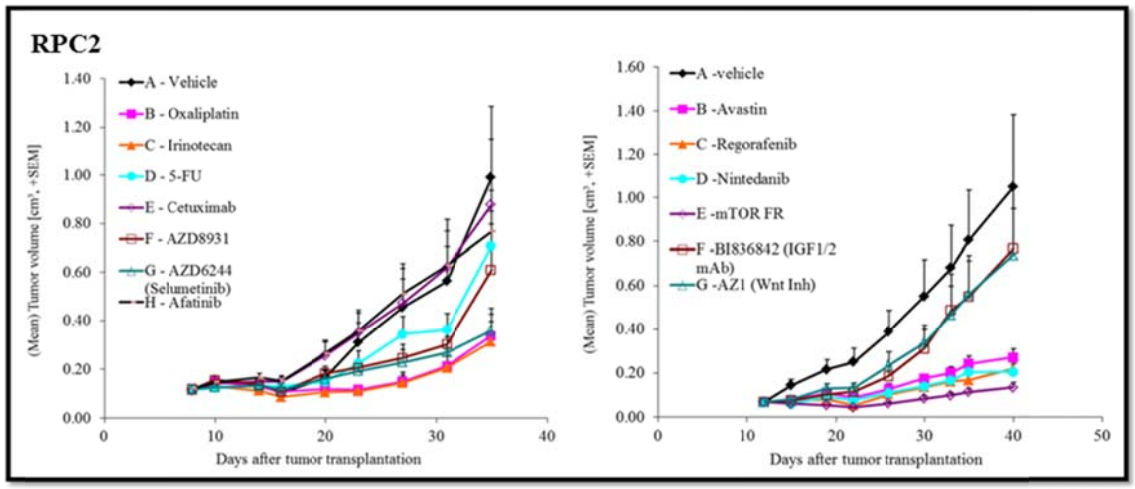


**Figure 39: Growth curve of the rectum primary carcinoma PDX model RPC2 under chemotherapeutic treatment.** Treatment of RPC2 displays a biological meaningful reduction of tumor growth under treatment with Oxaliplatin, Irinotecan, AZD6244, Avastin, Regorafenib, Nintedanib and mTOR FR.

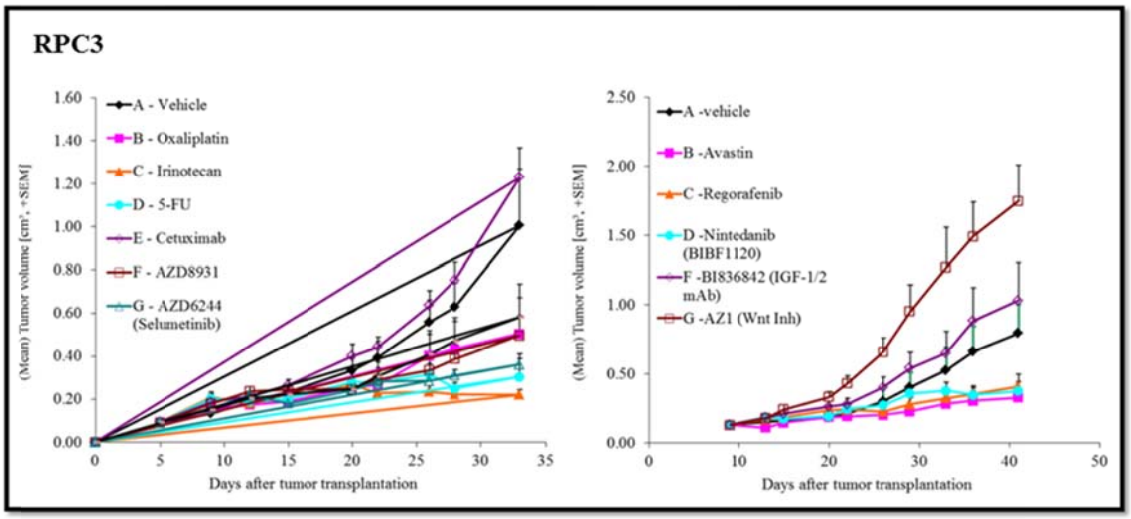


**Figure 40: Growth curve of the rectum primary carcinoma PDX model RPC3 under chemotherapeutic treatment.** Treatment of RPC3 displays a biological meaningful reduction of tumor growth under treatment with Irinotecan, 5-FU, AZD6244 and Avastin.

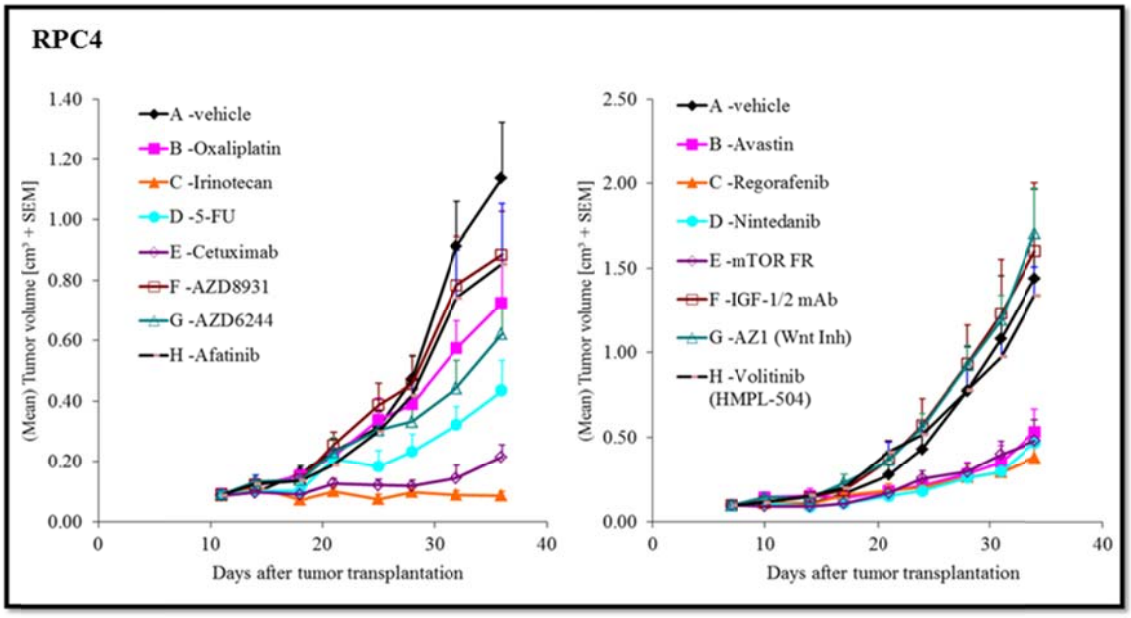


**Figure 41: Growth curve of the rectum primary carcinoma PDX model RPC4 under chemotherapeutic treatment.** Treatment of RPC4 displays a biological meaningful reduction of tumor growth under treatment with Irinotecan, Cetuximab, Avastin, Regorafenib, Nintedanib and mTOR FR.

### 3.4.3 Western Blot analysis of Eukaryotic Initiation Factors in Colorectal cancer patient derived Xenograft Models

Changes in protein expression of different eIF subunits and mTOR components in treated PDX models of colorectal primary carcinoma tissue and liver metastases tissue from colorectal cancer were analyzed using the western blot technique and ImageJ evaluation. Therefore primary carcinoma PDX models and metastases PDX models were treated with different chemotherapeutic drugs (see Table 2). During relative quantification, obtained protein levels of PDX models were normalized to respectively healthy control tissue. Actin was used as internal housekeeping protein. Statistical analysis was done using the Kruskal-Wallis test, which is used to compare more than two data sets. The level of statistical significance was set at $P < 0.05$.

#### *3.4.3.1 Protein expression of Eukaryotic Initiation Factors in Colon Cancer patient derived Xenograft Models*

To display protein expression of different eIF subunits during chemotherapeutic treatment, 4 colon primary carcinoma PDX models and 1 colon metastasis PDX model were generated. In comparison to untreated control, mTOR showed a trend to be upregulated under treatment with Oxaliplatin and Cetuximab in colon primary carcinoma PDX models. A partly downregulation was visible in the AZ1 treated CPC PDX model. Protein expression of mTOR in the colon metastasis (CM) PDX model revealed a tendency to be upregulated under Afatinib treatment. According to untreated control, mTOR, eIF2α, eIF3J, eIF4B and eIF5 showed a tendency to be increased in the Afatinib treated CM PDX model. In addition PTEN seemed to be decreased in the Avastin treated CM PDX model. Protein expression of PTEN, eIF2α, eIF3A, eIF3J, eIF3B, eIF4B, eIF4G and eIF5 was heterogeneous and displayed no visible changes comparing untreated and treated colon cancer tissue. Statistical analysis using the Kruskal-Wallis test revealed that the observed tendencies were not statistically significant.

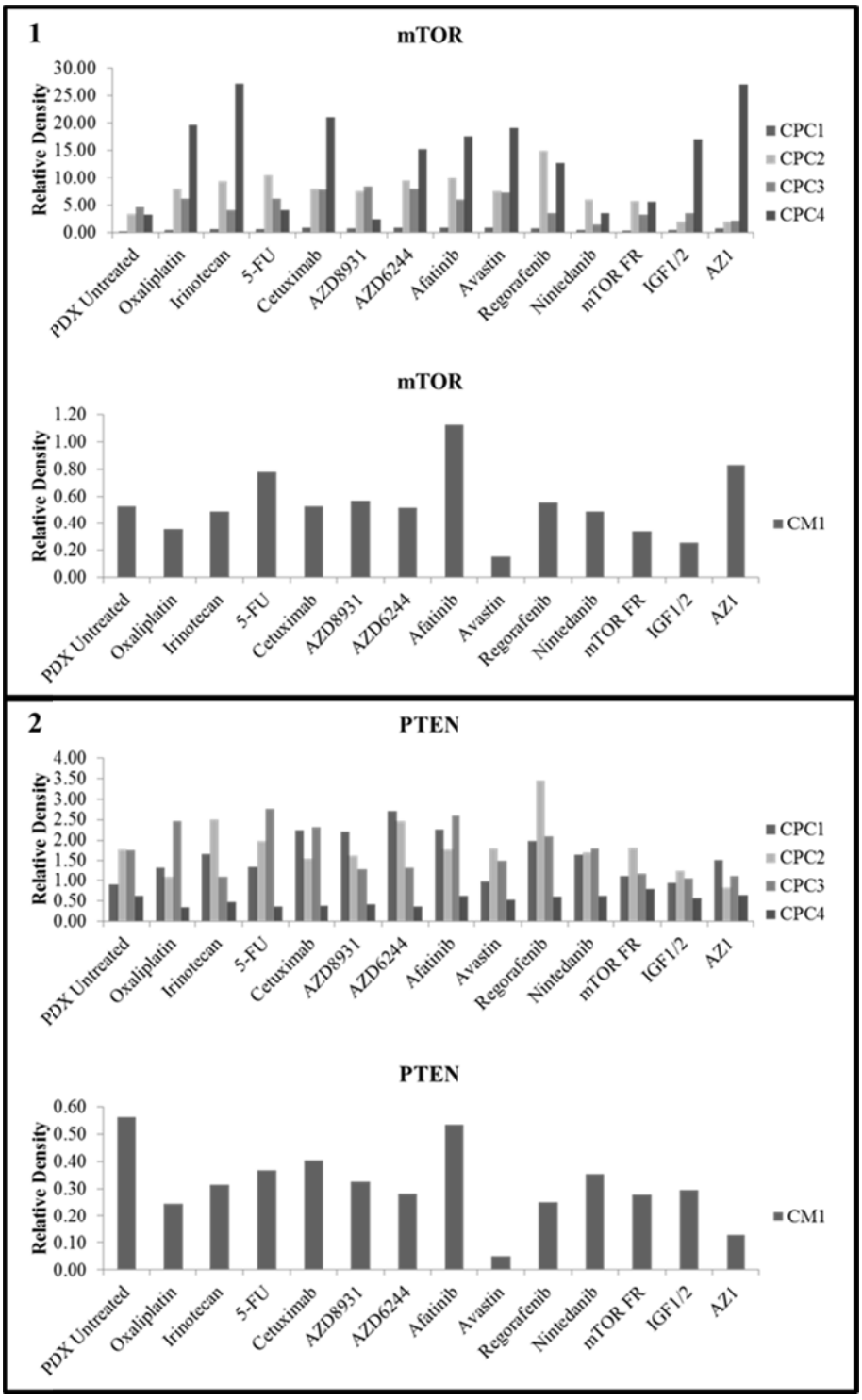


**Figure 42: Protein expression of mTOR and PTEN in untreated and treated colon cancer and colon metastases PDX models.** Statistical analysis reveals no statistically significant differences in protein expression.

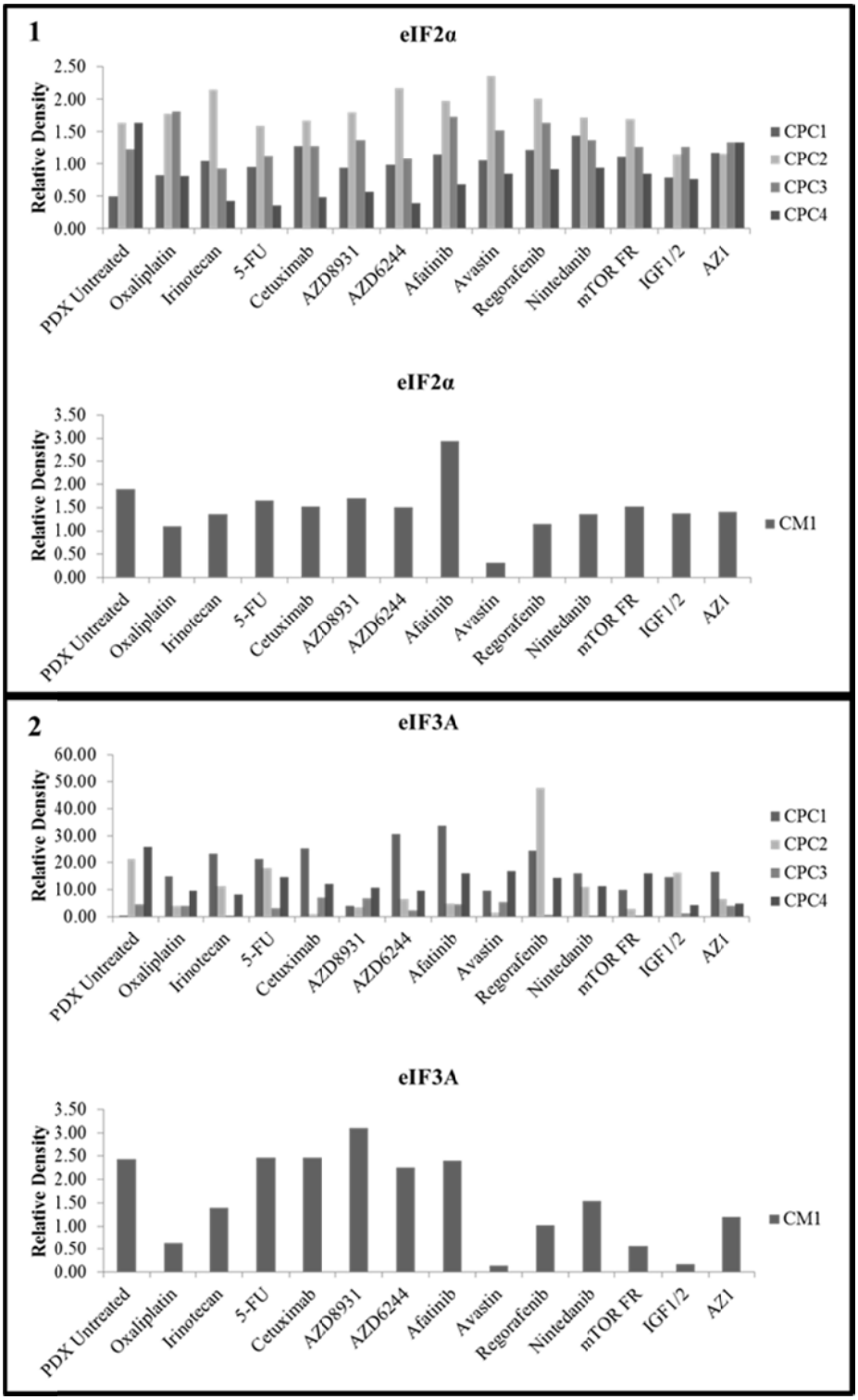


**Figure 43: Protein expression of eIF2α and eIF3A in untreated and treated colon cancer and colon metastases PDX models.** Statistical analysis reveals no statistically significant differences in protein expression.

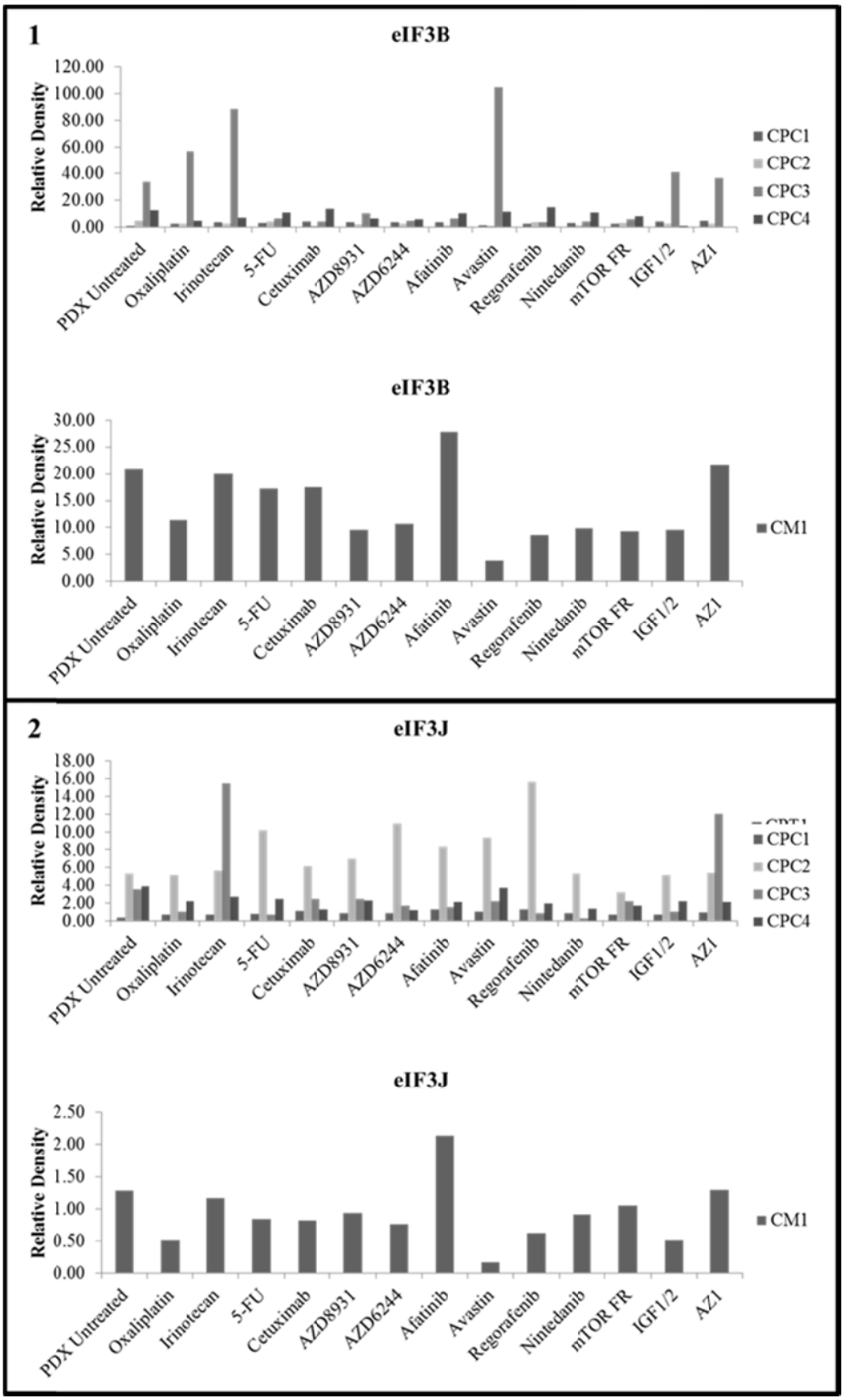


**Figure 44: Protein expression of eIF3B and eIF3J in untreated and treated colon cancer and colon metastases PDX models.** Statistical analysis reveals no statistically significant differences in protein expression.

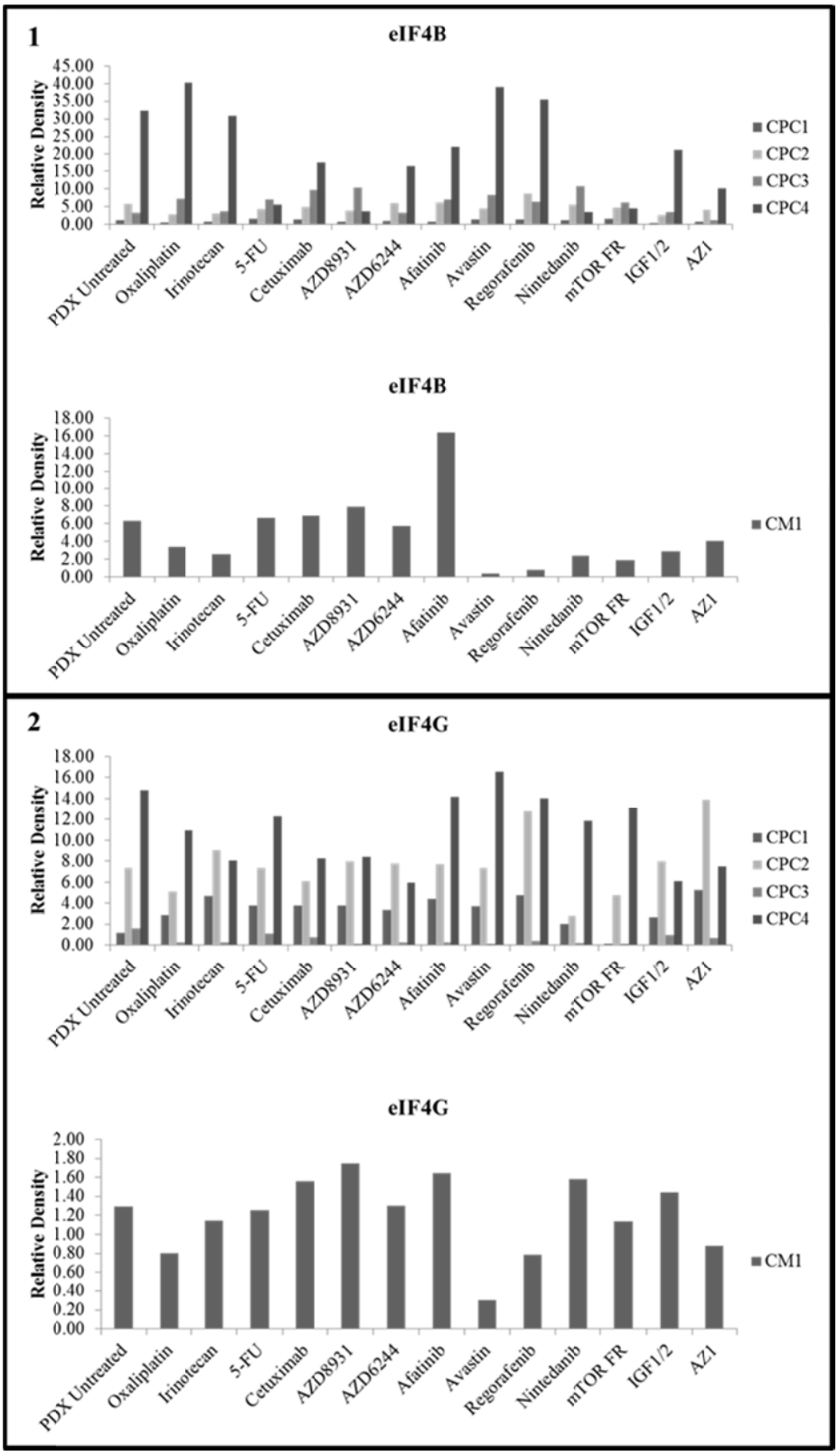


**Figure 45: Protein expression of eIF4B and eIF4G in untreated and treated colon cancer and colon metastases PDX models.** Statistical analysis reveals no statistically significant differences in protein expression.

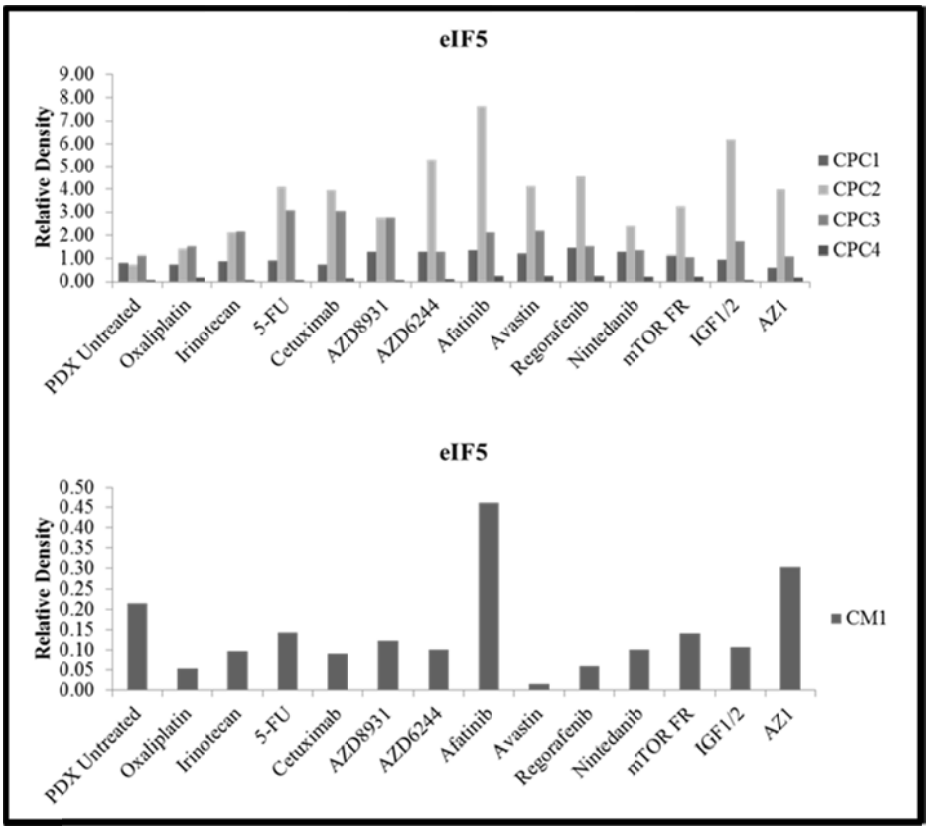


**Figure 46: Protein expression of eIF5 in untreated and treated colon cancer and colon metastases PDX models.** Statistical analysis reveals no statistically significant differences in protein expression.

### *3.4.3.2 Protein expression of Eukaryotic Initiation Factors in Rectum Cancer patient derived Xenograft Models*

To analyze protein expression of different eIF subunits under chemotherapeutic treatment, 4 rectum primary carcinoma (RPC) PDX models and 2 rectum metastasis (RM) PDX model were generated. Protein expression of eIF3J showed a tendency to be downregulated in RM PDX models under treatment with Nintedanib, mTOR FR and IGF 1/2 mAB. In addition these models displayed a trend in downregulation of eIF3A under treatment with Irinotecan, 5-FU, Avastin, Regorafenib, Nintedanib and mTOR FR. Protein expression of eIF4G was increased in Oxaliplatin and Cetuximab treated RPC PDX.

Protein expression of PTEN, eIF2α, eIF3J, eIF3B, eIF4B and eIF5 was heterogeneous and displayed no visible changes comparing untreated and treated rectum cancer tissue. Statistical analysis using the Kruskal-Wallis test revealed that the observed tendencies were not statistically significant.

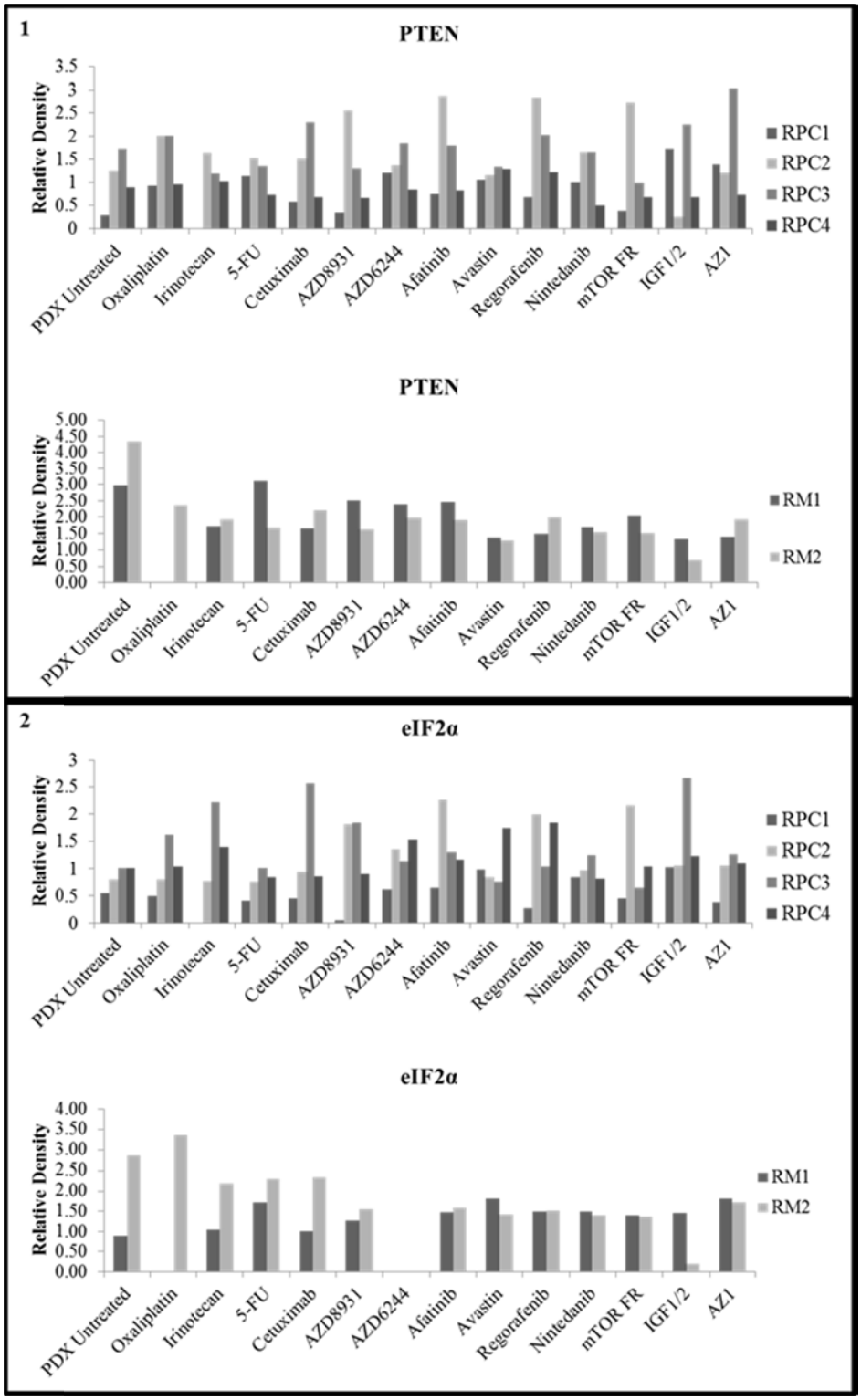


**Figure 47: Protein expression of PTEN and eIF2α in untreated and treated rectum cancer and rectum metastasis PDX models.** Statistical analysis reveals no statistically significant differences in protein expression.

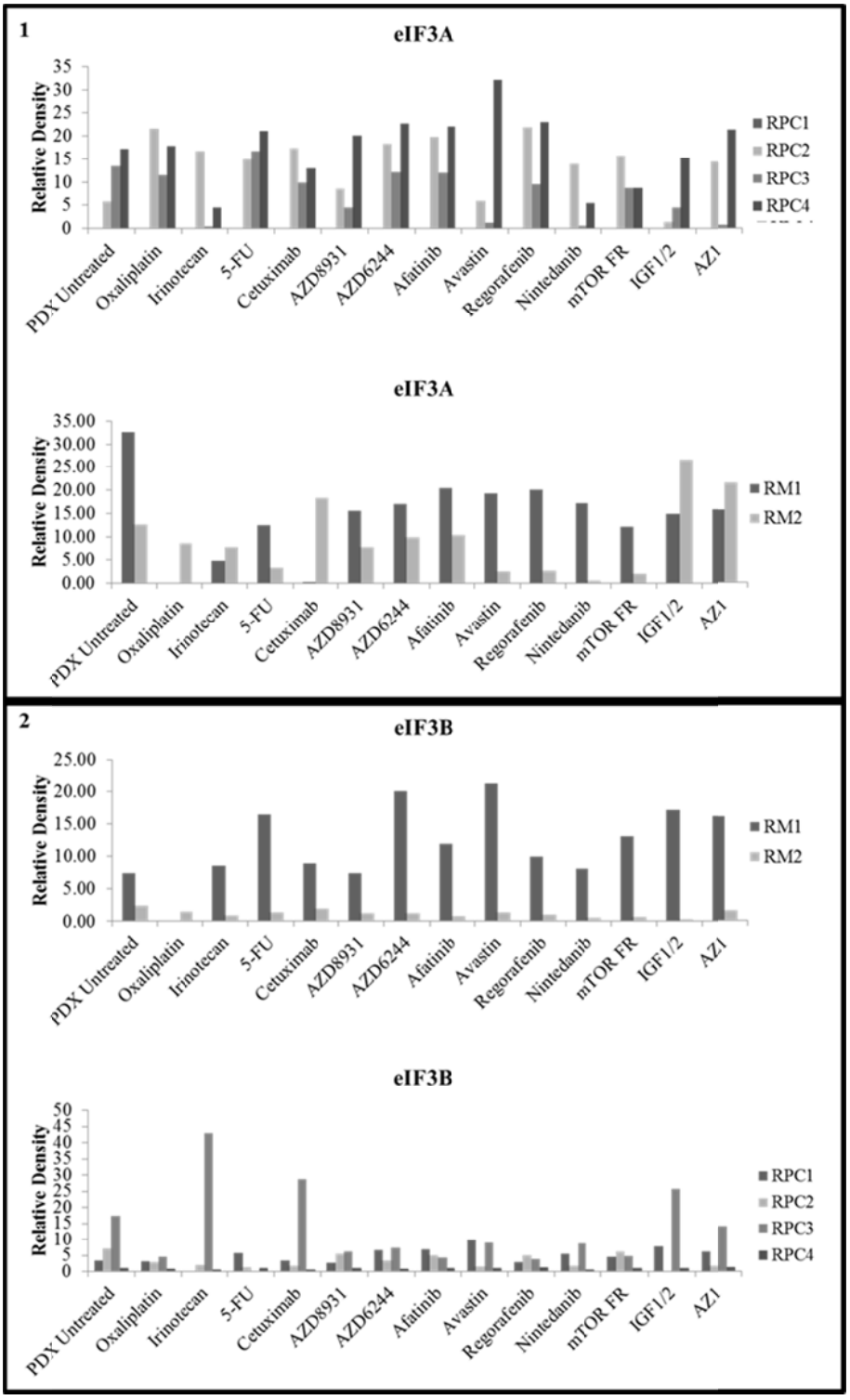


**Figure 48: Protein expression of eIF3A and eIF3B in untreated and treated rectum cancer and rectum metastasis PDX models.** Statistical analysis reveals no statistically significant differences in protein expression.

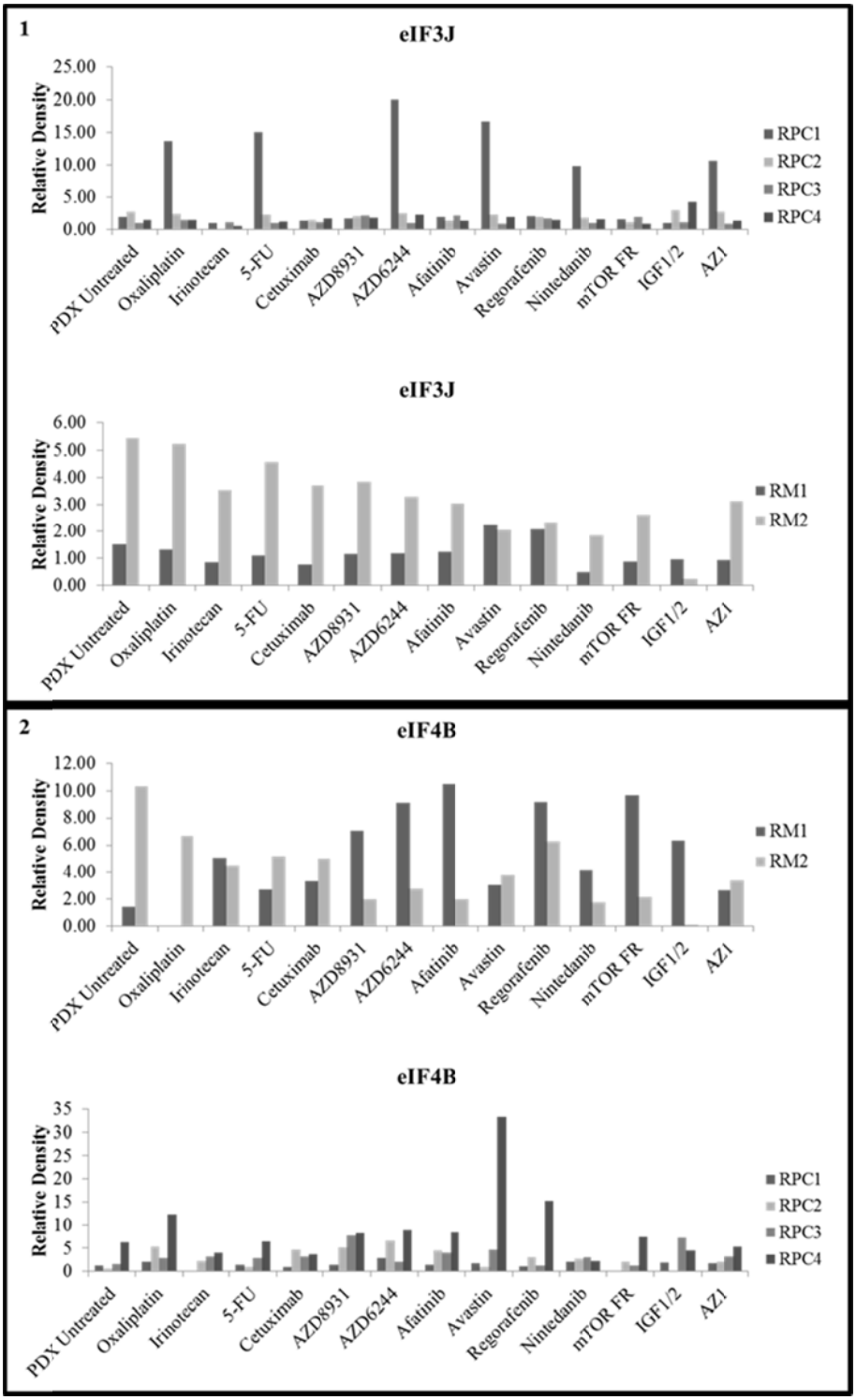


**Figure 49: Protein expression of eIf3J and eIF4B in untreated and treated rectum cancer and rectum metastasis PDX models.** Statistical analysis reveals no statistically significant differences in protein expression.

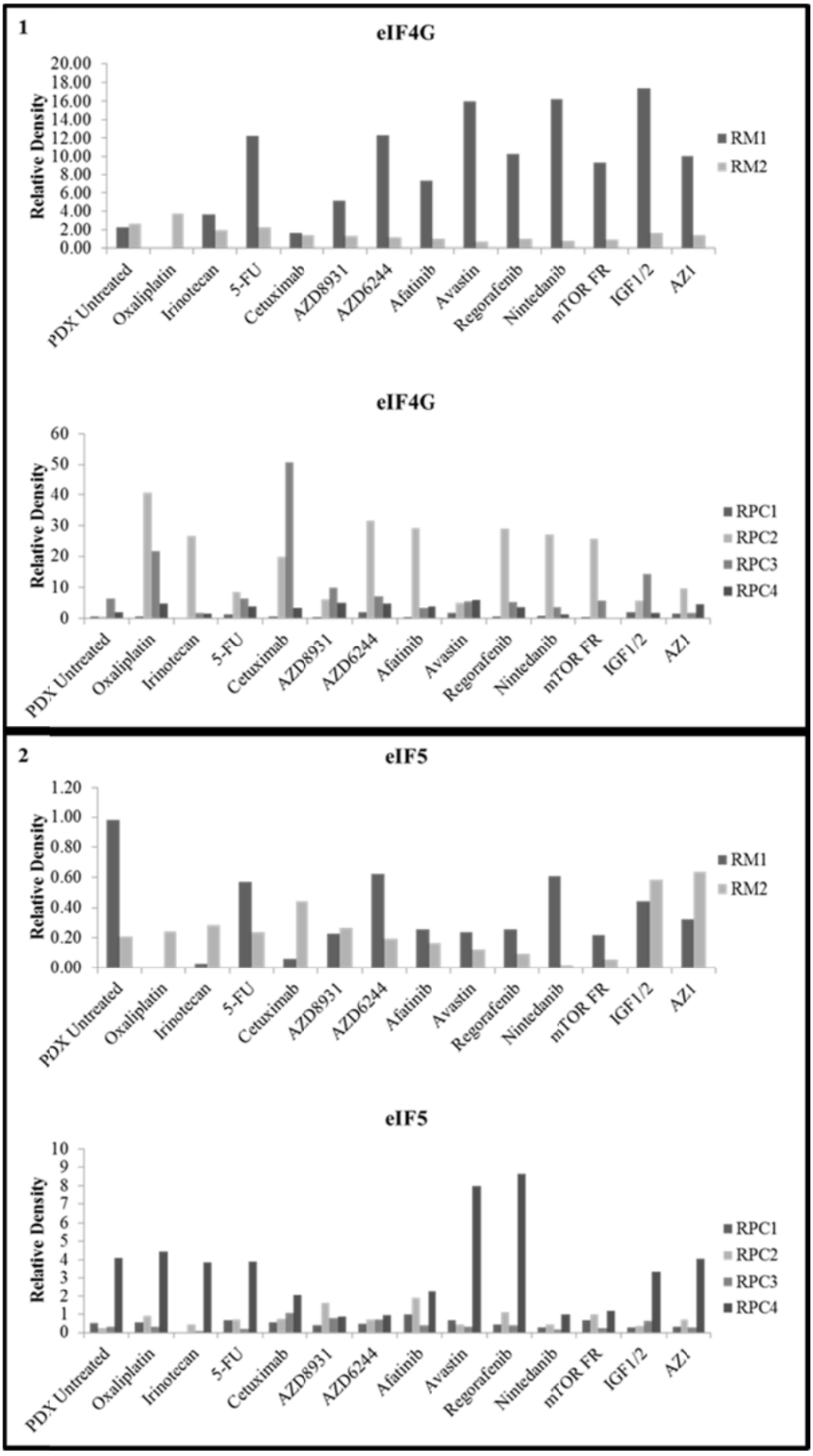


**Figure 50: Protein expression of eIF4G and eIF5 in untreated and treated rectum cancer and rectum metastasis PDX models.** Statistical analysis reveals no statistically significant differences in protein expression.

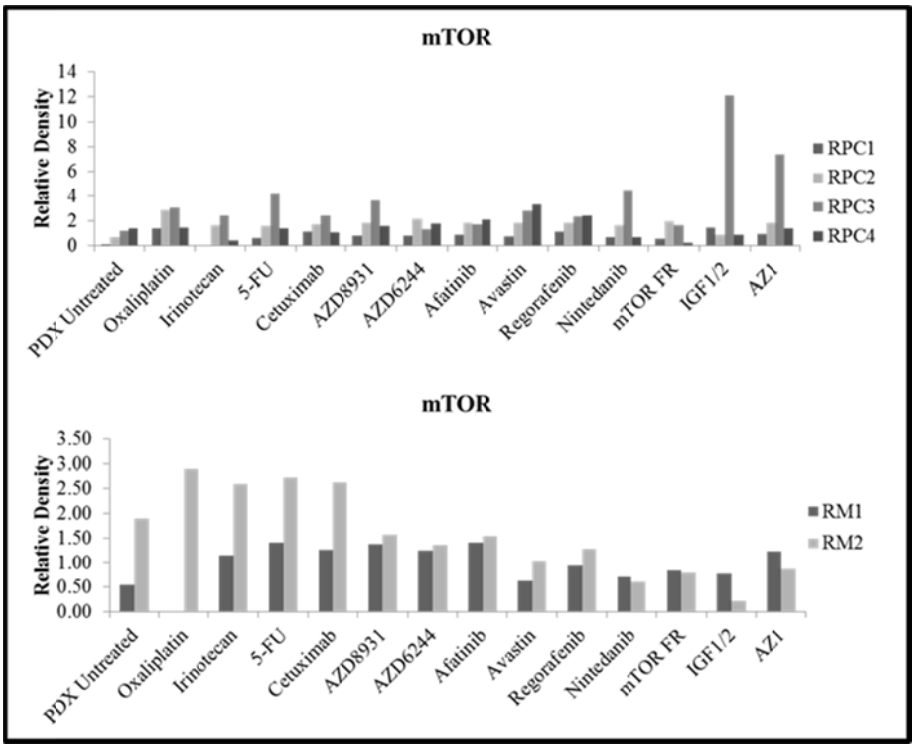


**Figure 51: Protein expression of mTOR in untreated and treated rectum cancer and rectum metastasis PDX models.** Statistical analysis reveals no statistically significant differences in protein expression.

# 4 Discussion

With almost 1.4 million new cases per year worldwide, CRC is the third most commonly diagnosed cancer type [1]. Altered translation initiation and abnormal gene expression increase the risk of cancer development. Previous studies displayed, that deregulation along the eIF cascade is associated with malignant transformation and progression of cancer [47] [48]. More detailed research in CRC is necessary to find novel biomarkers and therapeutic targets. The aim of this project was to analyze the contribution of various eIFs and their relating upstream mTOR targets in CRC, to find a link between translation initiation and carcinogenesis. Analysis was done on protein level using Tissue Micro Arrays (TMA) and Western Blot. In addition mRNA analysis was performed with Real-Time PCR to show variations on mRNA level.

Whereas TMA data revealed no significant differences comparing CRC and respectively healthy control tissue, significant changes in protein expression of various eIF subunits and mTOR components could be detected by Western Blot analysis.
A constitutive activation of mTOR signaling is shown to be a hallmark of cancer [61] and is associated to cell growth and cell cycle progression. mTOR is a downstream target of AKT, which is highly overexpressed in CRC [62]. AKT can be inhibited by the phosphatase and tensin homolog (PTEN), which acts as tumor suppressor. The loss of PTEN in mice results in formation of different cancer types. Active AKT phosphorylates and inhibits the TSC1/2 complex leading to activation of Rheb which activates mTOR. Active mTOR further phosphorylates its downstream targets S6K and 4E-BP1 [42]. Due to phosphorylation, 4E-BP1 dissociates from eIF4E and cap depended translation initiation is performed [44]. Inhibition of mTOR expression by knock down experiments results in considerably decreased *in vitro* and *in vivo* cell growth in CRC [63].
In this study the gathered data revealed that protein expression pattern of pmTOR/mTOR, pPTEN/PTEN, p4EBP1/4EBP1 are significantly upregulated in rectum carcinoma samples compared to healthy rectum tissue. Increased levels of activated mTOR and 4E-BP1 might indicate the promotion of cap dependent translation and the involvement of the mTOR pathway to CRC carcinogenesis. Increased protein expression of mTOR and 4E-BP1 might also indicate, that the observed PTEN

upregulation of 2.5 times did not block their phosphorylation significantly. Protein expression of pAKT/AKT was significantly upregulated in Colon Cancer indicating increased activation of mTOR signaling and its downstream located eIF pathway. Comparing colon and rectum cancer, PTEN was significantly increased in rectum carcinoma samples, which might indicate an increased inhibition of the mTOR pathway.

Previous studies already demonstrated an involvement of eIFs in cancer development and progression [48]. The downstream target of already mentioned 4E-BP1 is eIF4E, which is one of the best studied eIF subunits. eIF4E overexpression has been detected in colon cancer and is linked to changes in cellular morphology, enhanced proliferation, tumorigenesis and formation of metastases. eIF1 functions with eIF1A and eIF3 in the formation of a stable 40S preinitiation complex . Previous studies also revealed that expression of eIF2α in normal cells is increased transiently, whereas constitutive overexpression supports tumor initiation and progression of CRC [47]. The multisubunit translation initiation factor eIF3 plays a central role in protein synthesis. Elevated levels of eIF3A have been observed in colon cancer cell lines [64]. eIF3B overexpression was detected in colon cancer cell line SW1116, where specific eIF3B knockdown inhibits proliferation [65]. eIF3C was found to be an oncogene and was shown to be significantly increased in cancer cells. An amplification of the EIF3C gene was found in head and neck squamous cell carcinomas. Knockdown experiments revealed that suppression of eIF3c expression significantly reduced cell proliferation and colony formation of RKO colon cancer cells [66]. Increased expression of eIFD was shown to bear a predictive value for establishing resistance against combined treatment with cisplatin and flurouracil in gastric cancer patients. In addition a knockdown of eI3D is associated with apoptotic response and inhibited cell proliferation in patients with non-small cell lung cancer [67] [68]. Previous studies displayed a variant of eIF3H to be associated with colorectal cancer risk, whereas EIF3H may act as susceptibility gene for colorectal carcinoma [33]. eIF3I, which is also known as transforming growth factor β (TGF β) receptor, was found to be enhanced in hepatocellular carcinoma, repressing TGF β activity. In addiation eIF3I overexpression was shown to promote colon oncogenesis [33][69]. eIF3M is one of the most uncharacterized noncore eIF subunits and is highly expressed in human colon cancer cell lines and colon cancer carcinomas. It is proposed to mediate regulation of genes being important in CRC tumorigenesis. Specific knockdown of eIF3M in human colon cancer cell line HCT116 displayed

decreased cell proliferation, impeded cell cycle progression and increased cell death [47]. eIF4b is reported to modulate, in addition with eIF4g, the helicase activity of eIF4a and establishes bridges between mRNA and the 40S ribosomal subunit. Phosphorylation of eIF4B strengthens its interaction with eIF3A. During knockdown experiments of eIF4B in cancer cells attenuated proliferation and increased stress-driven apoptosis was observed [70]. eIF6 is required for ribosome biogenesis and regulation of ribosome subunit association activity in the cytoplasm. Overexpression of eIF6 was detected in head, neck and colorectal carcinomas in association with disease progression [48].

The here in this study obtained protein data revealed a significant upregulation of various eIF subunits in CRC tissue. Protein expression of eIF2α, eIF3A and eIF3D was significantly upregulated, whereas eIF3θ was decreased in colon cancer compared to healhy colon control. In accordance with previous studies, these data may indicate an increased level of tumor initiation and progression of colon cancer. In comparison to healthy rectum tissue eIF3I and eIF4E were significantly increased in rectum cancer. Like other studies already displayed, eIF3I overexpression might indicate the promotion of colon oncogenesis. In difference to previous studies eIF4E was only significantly overexpressed in rectum carcinoma, whereas the overexpression of eIF4E might be linked to changes in cellular morphology, enhanced proliferation, tumorigenesis and formation of metastases. A significant overexpression of eIF3B, eIF3M, eIF4B and eIF6 was visible in colon as well as in rectum cancer. Upregulation of these eIF subunits might explain increased proliferation in CRC. In addition various eIF subunits were analyzed on mRNA level by Real-Time PCR. Obtained data revealed a significant upregulation of eIF3C, eIF3M, eIF3H and eIF6 mRNA in colon cancer compared to healthy colon tissue. In comparison to healthy rectum tissue mRNA of eIF2α, eIF3A, eIF3B and eIF4B was significantly overexpressed in rectum cancer.

Previous studies already reported the presence of molecular differences between colorectal cancer formed in the proximal and distal colon [23]. I was able to show significant changes in eIF expression between colon and rectum cancer. Comparing colon and rectum cancer eIF2α, eIF3A and eIF4B were significantly increased in colon carcinoma tissue, whereas eIF4E displayed a significant overexpression in rectum carcinoma samples.

In addition to primary carcinoma analysis, chemosensitivity of various treated colon and rectum cancer PDX models was tested. The test for sensitivity to specific chemotherapeutic drugs revealed the standard CRC chemotherapeutic drugs Irinotecan, 5-FU, Oxaliplatin and Cetuximab as most efficient drugs to enhance growth of colon and rectum carcinomas. Treatment with novel drugs like IGF 1/2 mAB, AZ1 and Volitinib did not display a biological meaningful reduction of tumor growth and even revealed a higher tumor growth as untreated control in various CRC PDX models.
In addition to chemosensitivity testing CRC PDX models were analyzed on protein level. No significant changes in eIF expression pattern could be observed comparing CRC and respectively healthy control tissues.

This study was a preliminary trial to characterize the expression of eIF subunits in relation to the mTOR signaling pathway in CRC and assesses their possible use in biomarker identification and targeted therapy. For being able to display serious results and interpretations in order to reduce standard deviation, a larger cohort of samples has to be analyzed. To assess eIFs as possible biomarkers and therapeutic targets, further experiments are required. Cell culture experiments with different colon and rectum cell lines will be necessary to compare expression pattern of eIFs with primary carcinoma samples. In addition cell lines have to be treated with specific mTOR inhibitors and chemotherapeutic drugs, to display the attitude of eIFs under various treatment conditions. As a next step, knock down experiments using specific eIF constructs have to be done, to show the impact of these subunits on cell proliferation and cancer progression. Those *in vitro* experiments may afterwards be transferred to *in vivo* models using mice and rats to offer the opportunity to find new biomarkers and therapeutic targets.

# 5 Abbreviations

| | |
|---|---|
| TMA | tissue micro array |
| CRC | colorectal cancer |
| °C | degree Celsius |
| IHC | Immunohistochemistry |
| Min | minutes |
| AD | Aqua Destillata |
| H | hour |
| V | Volt |
| Sec | seconds |
| AB | antibody |
| mA | milli ampere |
| POI | protein of interest |
| HKG | housekeeping gene |
| mRNA | messenger ribonucleic acid |
| qRT-PCR | quantitative real-time polymerase chain reaction |
| HE | Haemotoxylin/Eosin |
| RT | room temperature |
| Ct | cycle threshold |
| TNM | Tumor, Node, Metastasis |
| AJCC | American Joint Committee on Cancer |
| CIN | chromosomal instability |
| MSI | microsatellite instability |
| CIMP | CpG Island Methylator Phenotype |
| 5-FU | 5-Fluorouracil |
| IFL | Irinotecan |
| LV | Leucovorin |
| eIF | Initiation Factor |
| 4E-BP | eIF4E binding protein |
| mTOR | mammalian target of rapamycin |
| PI3K | phosphatidylinositol-3-kinases |
| PTEN | Phosphatase and tensin homolog |
| S6K | S6 kinase |
| Wt | wild type |
| APC | adenomatous polyposis coli |
| i.e. | id est |
| GI | gastro intestinal |
| AJCC | American Joint Committee on Cancer |
| FFPE | Formalin fixed paraffin embedded |
| PDX | Patient derived Xenograft |
| T/C | Median tumor volume of treatment in comparison to control |
| RTK | receptor tyrosine kinase |
| CPT | Colon Primary Tumor |
| CM | Colon Metastasis |
| TIS | Total Immunostaining Score |
| LM TMA | Liver Metastases Tissue Micro Array |

# 6 List of Tables

# 7 List of Figures

# 8 References


[1] WHO, “World cancer factsheet,” 2014.

[2] S. Hamilton, B. Vogelstein, S. Kudo, E. Riboli, S. Nakamura, and P. Hainout, “Tumours of the Colon and Rectum,” *Pathol. Genet. Tumours Dig. Syst.*, pp. 103–129., 2000.

[3] T. F. Imperiale, R. Juluri, E. a. Sherer, E. a. Glowinski, C. S. Johnson, and M. S. Morelli, “A risk index for advanced neoplasia on the second surveillance colonoscopy in patients with previous adenomatous polyps,” *Gastrointest. Endosc.*, vol. 80, no. 3, pp. 471–478, 2014.

[4] G. H. Lee, G. Malietzis, a. Askari, D. Bernardo, H. O. Al-Hassi, and S. K. Clark, “Is right-sided colon cancer different to left-sided colorectal cancer? – A systematic review,” *Eur. J. Surg. Oncol.*, vol. 41, no. 3, pp. 300–308, 2015.

[5] L. B. Saltz and D. P. Kelsen, “Adjuvant treatment of colorectal cancer.,” *A Cancer J. Clin.*, vol. 57, no. 3, pp. 168–183, 2007.

[6] A. C. Society, “Colorectal Cancer Facts & Figures 2014-2016,” pp. 1–32, 2014.

[7] M. Hartmann, M. Pabst, R. Schmied, H. Caluba, and G. Dohr, *Zytologie, Histologie and Mikroskopische Anatomie*. 2005.

[8] B. Young, *Wheater’s Functional Histology*, 5th ed. Churchill Livingstone, 2006.

[9] S. Prasad, *Practical Histology for Medical Students*, 1st ed. Jaybee Brothers, 2007.

[10] “Histology of the large intestine.” [Online]. Available: http://www.kln.ac.lk/science/depts/zoology/index.php?option=com_content&view=article&id=46&Itemid=46.

[11] “Normal Colon Histology.” [Online]. Available: http://histology-world.com/photoalbum/displayimage.php?album=5&pid=1126.

[12] “Normal Rectum Histology.” [Online]. Available: http://histology-world.com/photoalbum/displayimage.php?album=5&pid=1147.

[13] N. Segnan, C. Senore, B. Andreoni, A. Arrigoni, L. Bisanti, A. Cardelli, G. Castiglione, C. Crosta, R. DiPlacido, A. Ferrari, R. Ferraris, F. Ferrero, M. Fracchia, S. Gasperoni, G. Malfitana and M. Dalmasso, “Randomized trial of different screening strategies for colorectal cancer: Patient response and detection rates,” *J. Natl. Cancer Inst.*, vol. 97, no. 5, pp. 347–357, 2005.

[14] M. Fleming, S. Ravula, S. F. Tatishchev, and H. L. Wang, “Colorectal carcinoma: Pathologic aspects.,” *J. Gastrointest. Oncol.*, vol. 3, no. 3, pp. 153–73, 2012.

[15] C. C. Compton and F. L. Greene, “The staging of colorectal cancer: 2004 and beyond.,” *CA. Cancer J. Clin.*, vol. 54, no. 6, pp. 295–308, 2004.

[16] E. Abdalla, R. Adam, A. Bilchik, and D. Jaeck, “Improving resectability of hepatic colorectal metastases: expert consensus statement,” *Ann Surg Oncol.*, vol. 13, pp. 1271–1280, 2006.

[17] M. Donadon, D. Ribero, G. Morris-Stiff, E. Abdalla, and J. Vauthey, “New paradigm in the management of liver-only metastases from colorectal cancer,” *Gastrointest Cancer Res.*, vol. 1, pp. 20–27, 2007.

[18] “TNM Classification for Colorectal Cancer.” [Online]. Available: http://www.hopkinscoloncancercenter.org/CMS/CMS_Page.aspx?CurrentUDV=59&CMS_Page_ID=EEA2CD91-3276-4123-BEEB-BAF1984D20C7.

[19] S. Al-Sohaily, A. Biankin, R. Leong, M. Kohonen-Corish, and J. Warusavitarne, “Molecular pathways in colorectal cancer.,” *J. Gastroenterol. Hepatol.*, vol. 27, no. 9, pp. 1423–31, 2012.

[20] E. Fearon and B. Vogelstein, “A genetic model for colorectal tumorigenesis,” *Cell*, vol. 61, pp. 759–767, 1990.

[21] M. Pino and D. Chung, “The chromosomal instability pathway in colon cancer,” *Gastroenterology*, vol. 138, pp. 2059–2072, 2010.

[22] J. Bogaert and H. Prenen, “Molecular genetics of colorectal cancer,” *Ann. Gastroenterol.*, vol. 27, no. 1, pp. 9–14, 2014.

[23] A. Goel and C. Boland, “Epigenetics of colorectal cancer,” *Gastroenterology*, vol. 143, pp. 1442–1460, 2012.

[24] O. K. . Glebov, L. M. . Rodriguez, K. . Nakahara, J. . Jenkins, J. . Cliatt, J. . Humbyrd, C.-J.a, DeNobile, P. . Soballe, and R. Simon, “Distinguishing right from left colon by the pattern of gene expression,” *Cancer Epidemiol. Biomarkers Prev.*, vol. 12, pp. 755–762, 2003.

[25] W. Schwenk, B. Böhm, and J. M. Müller, “Postoperative pain and fatigue after laparoscopic or conventional colorectal resections. A prospective randomized trial.,” *Surg. Endosc.*, vol. 12, no. 9, pp. 1131–1136, 1998.

[26] A. Manuscript, “Experience in hepatic resection for metastatic colorectal cancer: Analysis of clinical and pathologic risk factors,” *Surgery. Author Manuscr.*, vol. 116, pp. 703–711, 1994.

[27] J. Martenson, C. Willett, D. Sargent, J. Mailliard, and J. Donohue, “Phase III study of adjuvant chemotherapy and radiation therapy compared with chemotherapy alone in the surgical adjuvant treatment of colon cancer: results of intergroup protocol 0130,” *J. Clin. Oncol.*, vol. 22, pp. 3277–3283, 2004.

[28] E. Balch, A. De Meo, and J. Guillem, “Modern management of rectal cancer,” *World J Gastroenterol*, vol. 12, pp. 3185–3195, 2006.

[29] N. Baxter and J. Garcia-Aguilar, “Organ preservation for rectal cancer,” *J. Clin. Oncol.*, vol. 28, pp. 1014–1020, 2007.

[30] “Treatment Strategies for Rectal Cancer.” [Online]. Available: http://www.cancer.gov/cancertopics/pdq/treatment/rectal/HealthProfessional/page4/page4.

[31] “Chemotherapy regimens for CRC.” [Online]. Available: * http://www.cancer.gov/cancertopics/pdq/treatment/colon/HealthProfessional/page4.

[32] “Chemotherapeutic drugs for CRC treatment.” [Online]. Available: http://www.cancer.gov/cancertopics/treatment/drugs/colorectal.

[33] R. Spilka, C. Ernst, A. K. Mehta, and J. Haybaeck, “Eukaryotic translation initiation factors in cancer development and progression,” *Cancer Lett.*, vol. 340, no. 1, pp. 9–21, 2013.

[34] R. Spilka, K. Laimer, F. Bachmann, G. Spizzo, A. Vogetseder, M. Wieser, H. Müller, J. Haybaeck, and P. Obrist, “Overexpression of eIF3a in squamous cell carcinoma of the oral cavity and its putative relation to chemotherapy response,” *J. Oncol.*, vol. 2012, 2012.

[35] R. Jackson, C. Hellen, and T. Pestova, “The mechanism of eukaryotic translation initiation and principles of its regulation,” *Nat. Rev. Cell Biol.*, vol. 11, pp. 113–127, 2010.

[36] T. Pestova and V. Kolupaeva, “The roles of individual eukaryotic translation initiation factors in ribosomal scanning and initiation codon selection.,” *Genes Dev.*, vol. 16, no. 22, pp. 2906–2922, 2002.

[37] C. Betz and N. Hall, “Where is mTOR and what is it doing there?,” *J. Cell Biol.*, vol. 203, no. 4, pp. 563–574, 2013.

[38] H. Populo, M. Lopes, and P. Soares, “The mTOR signaling pathway in human cancer,” *Int. J. Mol. Sci.*, vol. 13, no. 2, pp. 1886–1918, 2012.

[39] R. Zoncu, A. Efeyan, and D. Sabatini, “No mTOR: from growthsignal integration to cancer, diabetes and ageing,” *Nat. Rev. Cell Biol.*, vol. 12, no. 1, pp. 21–35, 2011.

[40] D. Fingar, S. Salama, C. Tsou, E. Harlow, and J. Blenis, “Mammalian cell size is controlled by mTOR and its downstream targets S6K1 and 4EBP1/eIF4E,” *Genes Dev.*, vol. 16, no. 12, pp. 1472–1487, 2002.

[41] D. Kim, S. Sarbassov, and M. Ali, “mTOR interacts with raptor to form a nutrient-sensitive complex that signals to the cell growth machinery,” *Cell*, vol. 110, no. 2, pp. 163–175, 2002.

[42] M. Showkat, M. A. Beigh, and K. I. Andrabi, “mTOR Signaling in Protein Translation Regulation : Implications in Cancer Genesis and Therapeutic Interventions,” *Nat. Rev.*, vol. 14, pp. 261–278, 2015.

[43] A. Pause and A. Belsham, “Insulin-dependent stimulation of protein synthesis by phosphorylation of a regulator of 5’-cap function,” *Nature*, vol. 371, pp. 762–767, 1994.

[44] N. Hay and N. Sonenberg, “Upstream and downstream of mTOR,” *Genes Dev.*, vol. 18, no. 16, pp. 1926–1945, 2004.

[45] C. Gingras, B. Raught, and A. Gygi, “Hierarchical phosphorylation of the translation inhibitor 4E-BP1,” *Genes Dev.*, vol. 15, no. 21, pp. 2852–2864, 2001.

[46] “Regulation of the mTORC1 pathway.” [Online]. Available: http://www.biomedcentral.com/1741-7007/9/69/figure/F1.

[47] A. Parsyan, G. Hernández, and S. Meterissian, “Translation initiation in colorectal cancer,” *Cancer Metastasis Rev.*, vol. 31, no. 1–2, pp. 387–395, 2012.

[48] D. Silvera, S. Formenti, and R. Schneider, “Translation control in cancer,” *Nat. Rev.*, vol. 10, pp. 254–266, 2010.

[49] R. McLendon, A. Friedmann, and D. Bigner, “Comprehensive genomic characterization defines human glioblastoma genes and core pathways,” *Nat. Rev.*, vol. 455, no. 7216, pp. 1061–1068, 2008.

[50] G. Dalgliesh, K. Furge, C. Greenmann, and L. Chen, “Systematic sequencing of renal carcinoma reveals inactivation of histone modifying genes,” *Nature*, vol. 463, no. 7279, pp. 360–363, 2010.

[51] C. Robbin, W. Tembe, A. Baker, and S. Sinari, “Copy number and targeted mutational analysis reveals novel somatic events in metastatic prostate tumors.,” *Genome Res.*, vol. 21, no. 1, pp. 47–55, 2011.

[52] J. Samuels, Z. Wang, A. Bardelli, N. Silliman, and J. Ptak, “High frequency of mutations of the PIK3CA gene in human cancers,” *Science (80-. ).*, vol. 304, no. 5670, p. 554, 2004.

[53] B. M. Cracchiolo, D. S. Heller, P. M. J. Clement, E. C. Wolff, M. H. Park, and H. M. Hanauske-Abel, “Eukaryotic initiation factor 5A-1 (eIF5A-1) as a diagnostic marker for aberrant proliferation in intraepithelial neoplasia of the vulva,” *Gynecol. Oncol.*, vol. 94, no. 1, pp. 217–222, 2004.

[54] Z. Dong and Y. L. Zhang, “Initiation factor eIF3 and regulation of mRNA translation, cell growth, and cancer,” *Crit. Rev. Oncol. Hematol.*, vol. 59, no. 169–180, 2006.

[55] A. Benedetti and J. Graff, “eIF-4E expression and regulation and its role in malignancies and metastasis.,” *Oncogene*, vol. 23, pp. 3189–3199, 2004.

[56] I. Fichtner, J. Rolff, R. Soong, J. Hoffmann, S. Hammer, A. Sommer, M. Becker, and J. Merk, “Establishment of patient-derived non-small cell lung cancer xenografts as models for the identification of predictive biomarkers,” *Clin. Cancer Res.*, vol. 14, no. 20, pp. 6456–6468, 2008.

[57] J. Haybaeck, P. Guilhamon, L. M. Butcher, N. Presneau, G. a Wilson, A. Feber, D. S. Paul, M. Schütte, U. Keilholz, J. Hoffman, M. T. Ross, A. M. Flanagan, and S. Beck, “Assessment of patient-derived tumour xenografts (PDXs) as a discovery tool for cancer epigenomics,” *Genome Med.*, vol. 6, no. 12, pp. 1–10, 2014.

[58] A. S. Singh and A. K. S. Sau, “Tissue Microarray: A powerful and rapidly evolving tool for high-throughput analysis of clinical specimens,” *Int. J. Case Reports Images*, vol. 01, no. 01, p. 1, 2010.

[59] C. Moore, “Introduction to western blotting,” *MorphoSys UK*, p. 47, 2009.

[60] M. W. Pfaffl, J. Vandesompele, and M. Kubista, *Real-Time PCR: Current Technology and Applications.*, vol. 4. 2009.

[61] D. Hanahan and R. a. Weinberg, “Hallmarks of cancer: The next generation,” *Cell*, vol. 144, no. 5, pp. 646–674, 2011.

[62] S. Johnson, P. Gulhati, B. Rampy, and Y. Han, “Novel Expression Patterns of PI3K/Akt/mTOR Signaling Pathway Components in Colorectal Cancer,” *J. Am. Coll. Surg.*, vol. 210, no. 5, pp. 767–776, 2010.

[63] Y.-J. Zhang, D. Qiang, S. Dan-Feng, and X. Hua, “mTOR Signaling Pathway Is a Target for the Treatment of Colorectal Cancer,” *Ann. Surg. Oncol.*, vol. 16, no. 9, pp. 2617–2628, 2009.

[64] Z. Liu, Z. Dong, Z. Yang, Q. Chen, Y. Pan, Y. Yang, P. Cui, X. Zhang, and J. T. Zhang, “Role of eIF3a (eIF3 p170) in intestinal cell differentiation and its association with early development,” *Differentiation*, vol. 75, no. 7. pp. 652–661, 2007.

[65] Z. Wang, J. Chen, J. Sun, Z. Cui, and H. Wu, “RNA interference-mediated silencing of eukaryotic translation initiation factor 3, subunit B (EIF3B) gene expression inhibits proliferation of colon cancer cells,” *World J. Surg. Oncol.*, vol. 10, no. 1, p. 119, 2012.

[66] N. Song, Y. Wang, X. Gu, Z. Chen, and L. Shi, “Effect of siRNA-mediated knockdown of EIF3C gene on the survival of colon cancer cells,” *BJZUS*, vol. 1581, no. 6, pp. 1–8, 2013.

[67] L. Zhifeng, X. Liwen, and L. Qiang, “Knockdown of eIF3d inhibits cell proliferation through G2/M phase arrest in non-small cell lung cancer,” *Med. Oncol.*, vol. 32, pp. 183–191, 2015.

[68] H. K. Kim, I. J. Choi, C. G. Kim, H. S. Kim, A. Oshima, A. Michalowski, and J. E. Green, “A gene expression signature of acquired chemoresistance to cisplatin and fluorouracil combination chemotherapy in gastric cancer patients,” *PLoS One*, vol. 6, no. 2, 2011.

[69] Q. Jing, Z. Dong, and L. Jianguo, “EIF3i Promotes Colon Oncogenesis by Regulating COX-2 Protein Synthesis and β-Catenin Activation,” *Oncogene*, vol. 33, no. 32, pp. 4146–4163, 2014.

[70] D. Shahbazian, A. Parsyan, E. Petroulakis, J. Hershey, and N. Sonenberg, “eIF4B controls survival and proliferation and is regulated by proto-oncogenic signaling pathways,” *Cell Cycle*, vol. 9, no. 20, pp. 4106–4109, 2010.